
Final Report

March 2006

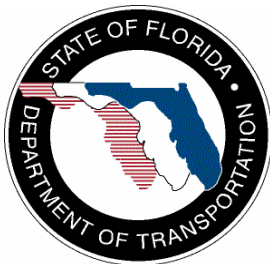
UF Project No. 00030907
Contract No. BD545, RPWO# 9

CRACK CONTROL IN TOPPINGS FOR PRECAST FLAT SLAB BRIDGE DECK CONSTRUCTION

Principal Investigator:	H. R. (Trey) Hamilton, P.E., Ph.D.
Co-Principal Investigator:	Ronald A. Cook, P.E., Ph.D.
Graduate Research Assistant:	Lazaro Alfonso
Project Manager:	Marcus Ansley, P.E.

Department of Civil & Coastal Engineering
College of Engineering
University of Florida
Gainesville, Florida 32611

Engineering and Industrial Experiment Station



DISCLAIMER

The opinions, findings, and conclusions expressed in this publication are those of the authors and not necessarily those of the State of Florida Department of Transportation.

1. Report No.		2. Government Accession No.		3. Recipient's Catalog No.	
4. Title and Subtitle Crack Control in Toppings for Precast Flat Slab Bridge Deck Construction				5. Report Date March 2006	
				6. Performing Organization Code	
7. Author(s) L. Alfonso, R. A. Cook, and H. R. Hamilton III				8. Performing Organization Report No. 00030907	
9. Performing Organization Name and Address University of Florida Department of Civil & Coastal Engineering P.O. Box 116580 Gainesville, FL 32611-6580				10. Work Unit No. (TRAIS)	
				11. Contract or Grant No. BD545, RPWO# 9	
12. Sponsoring Agency Name and Address Florida Department of Transportation 605 Suwannee Street, MS 30 Tallahassee, FL 32399				13. Type of Report and Period Covered Final Report	
				14. Sponsoring Agency Code	
15. Supplementary Notes					
16. Abstract <p>FDOT has experienced problems with reflective cracking in the topping of some precast flat slab bridges. The cracking usually occurs over the joint between the precast panels on which the topping is placed, hence the term reflective cracking. This research project evaluated techniques for improving crack control in these toppings. Four full-scale bridge superstructures were constructed to evaluate steel fibers, synthetic fibers, steel/synthetic fiber blend, carbon fiber reinforced composite (CFRP) grid, and shrinkage reducing admixture. Each superstructure was composed of three 4-ft. x 30-ft precast flat slabs with a 6 in. concrete topping. The toppings were visually monitored for 30 weeks for crack formation. Load tests were also performed on each of the specimens. Insufficient tensile stresses from drying shrinkage were generated in the toppings to induce cracking. One possible explanation is that the placement and curing were conducted in relatively ideal conditions which contributed to the lower shrinkage strains. Another is that the slabs were constructed in the very humid summer months in which ambient humidity was at 80% or above, providing improved curing conditions over that which might occur in the dryer winter months. Yet another is that these specimens were not as wide as is generally seen in the bridges where reflective cracking has been observed. It is suspected that a wider cross-section would lead to more lateral restraint in the center of the cross-section.</p> <p>Modulus of elasticity and tensile strength were unaffected by the crack control treatments used in this research. In both the restrained ring and load test the all steel fiber (STL) topping provided nearly an order of magnitude reduction in crack widths. The CFRP grid (GRD) topping reduced the crack widths in the load test by a factor of two. In the restrained ring test the blended fiber (BND) and all synthetic fiber (SYN) toppings reduced crack widths by a factor of four. In the load test, BND and SYN toppings reduced the crack widths by a factor of two. The topping with shrinkage reducing admixture (SRA) reduced crack widths in the restrained shrinkage test by a factor of seven.</p>					
17. Key Word Flat slab, fiber reinforced concrete, shrinkage-reducing admixture, carbon-fiber, shrinkage cracking, restrained ring			18. Distribution Statement No restrictions.		
19. Security Classif. (of this report) Unclassified		20. Security Classif. (of this page) Unclassified		21. No. of Pages 120	22. Price

ACKNOWLEDGMENTS

The authors acknowledge and thank the Florida Department of Transportation for providing the funding for this research project. This project was a collaborative effort between the University of Florida and the FDOT Structures Research Laboratory (Tallahassee). The authors thank the FDOT Structures Research Laboratory personnel (Marc Ansley, David Allen, Frank Cobb, Steve Eudy, Tony Johnston, Paul Tighe) for constructing the specimens and conducting materials testing. Material testing was also conducted by Richard Delorenzo at the FDOT State Materials Office. The authors also like to thank Dura-Stress Inc. Leesburg, FL and Charles Baker for constructing the flat slabs as well as Nycon, Inc.; W.R. Grace & Co.; and TechFab, LLC, for their contributions to this research.

The authors also thank Claire Lewinger and Eric Cannon for their contribution to the slab loading and crack width measurement and Dr. Jae Chung for his assistance with the finite element modeling.

EXECUTIVE SUMMARY

FDOT has experienced problems with reflective cracking in the topping of some precast flat slab bridges. The cracking usually occurs over the joint between the precast panels on which the topping is placed, hence the term reflective cracking. This research project evaluated techniques for improving crack control in these toppings. Selection was focused on their effectiveness, ease of implementation and application, and effect on the labor and construction cost of the bridge. Commercially available treatments for crack control were reviewed and several were selected for further testing including steel fibers, synthetic fibers, steel/synthetic fiber blend, carbon fiber reinforced composite (CFRP) grid, and shrinkage reducing admixture.

Four full-scale bridge superstructures were constructed to evaluate the crack control treatments. Each superstructure was composed of three 4-ft. x 30-ft precast flat slabs with a 6 in. concrete topping. The precast slabs were constructed off-site by a prestressed concrete manufacturer. The treatments were each incorporated into a standard FDOT approved concrete mixture and cast on-site by FDOT Structures Laboratory staff. Cylinder tests were conducted for compressive and tensile strength, and modulus of elasticity. The cracking performance of the treatments was evaluated using a restrained ring test. The toppings were visually monitored for 30 weeks for crack formation. Plastic shrinkage cracks were visible in the control topping as well as the toppings with the shrinkage reducing admixture (SRA) and CFRP grid (GRD). No further cracking, however, formed during the monitoring period.

In addition to the restrained ring test, and to provide a relative measure of the treatments under transverse tensile stress, load tests were performed on each of the specimens. The bearing pads were relocated so that the self-weight of the specimens caused flexural tensile stresses to form in the topping over the precast joints. Additional weight was needed to generate cracking in some of the specimens.

Based on observations during construction, the results of the materials tests, and the performance of the toppings, the following is concluded:

- Insufficient tensile stresses from drying shrinkage were generated in the toppings to induce cracking. One possible explanation is that the placement and curing were conducted in relatively ideal conditions which contributed to the lower shrinkage strains. Another is that the slabs were constructed in the very humid summer months in which ambient humidity was at 80% or above, providing improved curing conditions over that which might occur in the dryer winter months. This was supported by the fact that the restrained ring specimens did not crack until after the relative humidity dropped below 70 percent. Yet another is that these specimens were not as wide as is generally seen in the bridges where reflective cracking has been observed. It is suspected that a wider cross-section would lead to more lateral restraint in the center of the cross-section.
- Modulus of elasticity and tensile strength were unaffected by the crack control treatments used in this research.
- In both the restrained ring and load test the all steel fiber (STL) topping provided nearly an order of magnitude reduction in crack widths.
- The CFRP grid (GRD) topping reduced the crack widths in the load test by a factor of two.

- In the restrained ring test the blended fiber (BND) and all synthetic fiber (SYN) toppings reduced crack widths by a factor of four. In the load test, BND and SYN toppings reduced the crack widths by a factor of two.
- The topping with shrinkage reducing admixture (SRA) reduced crack widths in the restrained shrinkage test by a factor of seven.

As with any concrete construction, proper mixing, transporting, placement, and curing are crucial to a successful finished product. With reasonable care, we have shown that this system (for the width and configuration tested) can be constructed without reflective cracking even when additives are not used. As has been shown, however, added assurance can be attained with the use of additives. While the all steel fiber system (STL) was shown to be the most effective in reducing crack widths under load and in the restrained ring test, it was also rated as the most difficult to place, vibrate, and finish, followed by the all synthetic fibers (SYN) and blended fibers (BND). If the fiber is added directly to an FDOT approved mix, without accounting for the reduction in workability, then the temptation to add water at the job site is heightened by the reduction in workability. When fiber additives are being considered for use in toppings, it is recommended that trial mixes be prepared to ensure that adequate workability will be available without the addition of water. Indeed, fiber-reinforced concrete with fiber volumes such as those used for the steel (STL) and synthetic (SYN) fibers specimens should incorporate a high-range-water reducer to improve workability.

TABLE OF CONTENTS

1	INTRODUCTION.....	8
1.1	BACKGROUND.....	8
1.2	RESEARCH OBJECTIVES.....	8
2	SITE EVALUATIONS.....	9
2.1	INTRODUCTION.....	9
2.2	MILL CREEK BRIDGE.....	9
2.3	TURKEY CREEK BRIDGE.....	10
2.4	COW CREEK BRIDGE.....	10
2.5	SUMMARY.....	12
3	LITERATURE REVIEW.....	13
4	FINITE ELEMENT MODELING OF CONCRETE SHRINKAGE.....	17
4.1	INTRODUCTION.....	17
4.2	EVALUATION OF SHRINKAGE RATE.....	17
4.3	FINITE ELEMENT MODEL.....	18
5	EXPERIMENTAL PROGRAM.....	21
5.1	INTRODUCTION.....	21
5.2	DESIGN AND FABRICATION.....	26
5.3	SITE LAYOUT.....	31
5.4	SLAB PLACEMENT.....	32
5.5	TOPPING REINFORCEMENT.....	34
5.6	TOPPING PLACEMENT.....	35
5.7	SUMMARY.....	46
5.8	INSTRUMENTATION.....	49
5.9	RESTRAINED SHRINKAGE RINGS.....	52
5.10	LOAD TESTS.....	53
6	RESULTS AND DISCUSSION.....	57
6.1	COMPRESSIVE STRENGTH AND MODULUS OF ELASTICITY.....	57
6.2	PRESSURE TENSION TEST.....	57
6.3	RESTRAINED RING TEST.....	59
6.4	THERMOCOUPLE DATA.....	61
6.5	TOPPING OBSERVATIONS.....	62
6.6	LOAD TESTS.....	64
7	SUMMARY AND CONCLUSIONS.....	71
8	REFERENCES.....	73
	APPENDIX A – SLAB CALCULATIONS.....	75
	APPENDIX B – TOPPING PLACEMENT SUMMARY.....	91
	APPENDIX C – CYLINDER TEST RESULTS.....	99
	APPENDIX D – WEATHER DATA.....	103
	APPENDIX E – THERMOCOUPLE DATA.....	106
	APPENDIX F – CONSTRUCTION DRAWINGS.....	111
	APPENDIX G – JOINT DEPTH VARIATION.....	119

1 INTRODUCTION

1.1 BACKGROUND

Precast flat slab bridges are a practical alternative to traditional deck/girder designs used for short span bridges. Using precast slabs reduces the price of bridge construction by virtually eliminating the need for formwork thus making it economically attractive. It allows for faster construction time and quicker project turnover.

Flat slab bridges consist of prestressed, precast concrete deck panels that span from bent to bent. The panels act as permanent forms for a cast-in-place deck. The top surface of the flat slab is roughened to transfer horizontal shear. In some cases, transverse reinforcement is placed to ensure horizontal shear transfer. A topping is then placed over the precast flat slab, which allows the composite to act as a single unit. Some panels incorporate a shear key to transfer transverse shear. The keys usually contain welded wire mesh, reinforcing bars or both as well as non-shrink grout. The topping contains transverse and longitudinal reinforcement intended to provide crack control and lateral transfer of shear between the panels. Figure 1 shows recently erected prestressed slabs before topping placement. These panels have horizontal shear reinforcement and shear keys.



Figure 1. Typical prestressed slab panels

Poor curing techniques and improper placement of reinforcement has caused excessive shrinkage cracking in a number of flat slab bridges in Florida. Excessive cracking is unsightly, can affect the durability of the wearing surface, and can lead to corrosion of the reinforcement

1.2 RESEARCH OBJECTIVES

The focus of this research was to evaluate techniques for providing crack control in the cast portion of a precast flat slab bridge. A review of methods that have been used to control cracking on bridge decks was conducted. Several systems were considered and chosen for use in the experimental program based on their effectiveness, ease of implementation and application, and effect on the labor and construction cost of the bridge. These systems were then evaluated on full-scale precast flat slab bridge spans. Specimen size and shape were chosen to closely match existing field conditions and steps were taken to ensure that toppings were exposed to

similar curing conditions. They were left outside to weather, and were monitored visually for cracking. Crack width, crack distribution, ease of application, and the overall cost of each system were compared and ranked based on performance. Recommendations are made for changes to flat slab bridge construction techniques based on their performance.

2 SITE EVALUATIONS

2.1 INTRODUCTION

Site visits were conducted by the author to assess crack patterns on selected existing flat slab bridges. Three Central Florida bridges were visited: Mill Creek Bridge (No. 364056), Turkey Creek Bridge (No. 700203), and Cow Creek Bridge (No. 314001). All of these have reflective longitudinal cracks over the joints in the flat slabs, and transverse cracks over the bents.

2.2 MILL CREEK BRIDGE

The Mill Creek Bridge is located on CR318 north of Ft. McCoy. It is a simply supported, two-span bridge composed of 15 in. deep precast flat slabs. The topping has a reflective crack over each flat slab joint (Figure 2) that measures an average of 0.016 in. Cracks were also noted over the middle bent where the flat slabs meet end to end. The control joint is located at the center and runs with the span of the bridge. All of these cracks are relatively small and have not affected the performance of the bridge. No construction drawings were available for this bridge.



Figure 2. Reflective crack on topping of Mill Creek Bridge

2.3 *TURKEY CREEK BRIDGE*

The Turkey Creek Bridge is located on US1 south of Melbourne. It is a simply supported, six-span bridge with 12 in. deep precast flat slabs with shear keys and an 8 in. topping. The topping is reinforced with No. 5 bars at 12 in. on center in each direction. The topping has extensive longitudinal cracks that vary in size. Reflective cracks are located over each flat slab joint. Many of the cracks have been repaired with epoxy (Figure 3) and show no signs of continued cracking. A large number of vehicles were using the bridge on the day of the visit. In addition to showing the most cracking, it also carries the largest traffic volume of the three bridges.

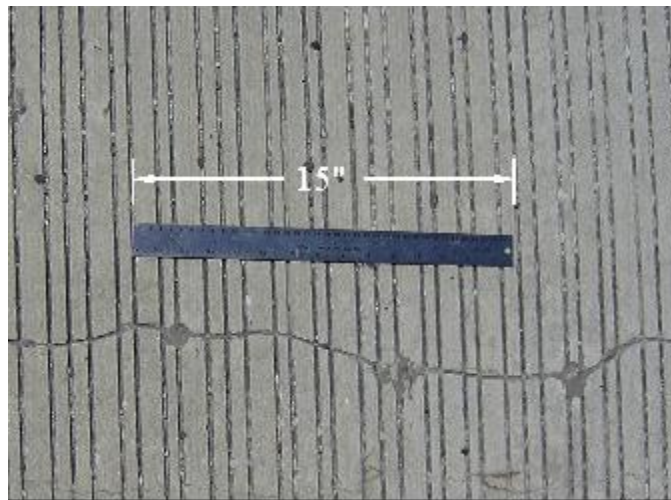


Figure 3. Repairs to cracks on Turkey Creek Bridge

2.4 *COW CREEK BRIDGE*

Cow Creek Bridge is located on CR 340 just west of High Springs. It is a five-span bridge with 12 in. deep flat slabs with shear keys and a 6 in. topping (Figure 4). The flat slabs have horizontal shear reinforcement and the topping has No. 5 reinforcing bars at 6 in. on center in the transverse direction and at 12 in. on center in the longitudinal direction. Previous assessment by the FDOT showed that the longitudinal cracks formed before the bridge was opened to traffic, and the reinforcement bars in the topping were incorrectly installed at 4 to 5 in. below the topping. The topping has a reflective longitudinal crack over each joint in the flat slab. These cracks measured an average of 0.028 in. It also has cracks along most of the saw-cut joints located over the bents. Figure 5 shows the typical saw cut and bearing located over every bent. Concrete has spalled in some areas adjacent to the cuts (Figure 6). This type of cracking occurs when the control joints are cut after the concrete has set. The longitudinal cracks do not appear to have affected the performance of the bridge.

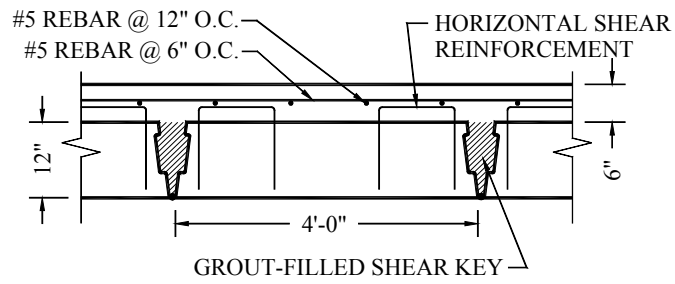


Figure 4. Cow Creek Bridge cross-section

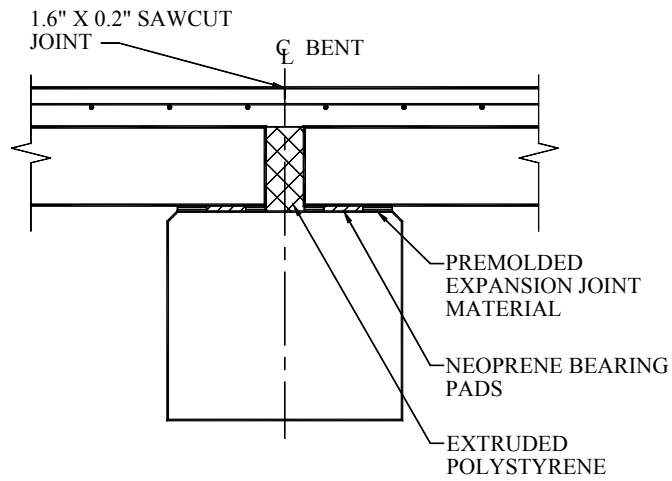


Figure 5. Control joint and bearing detail

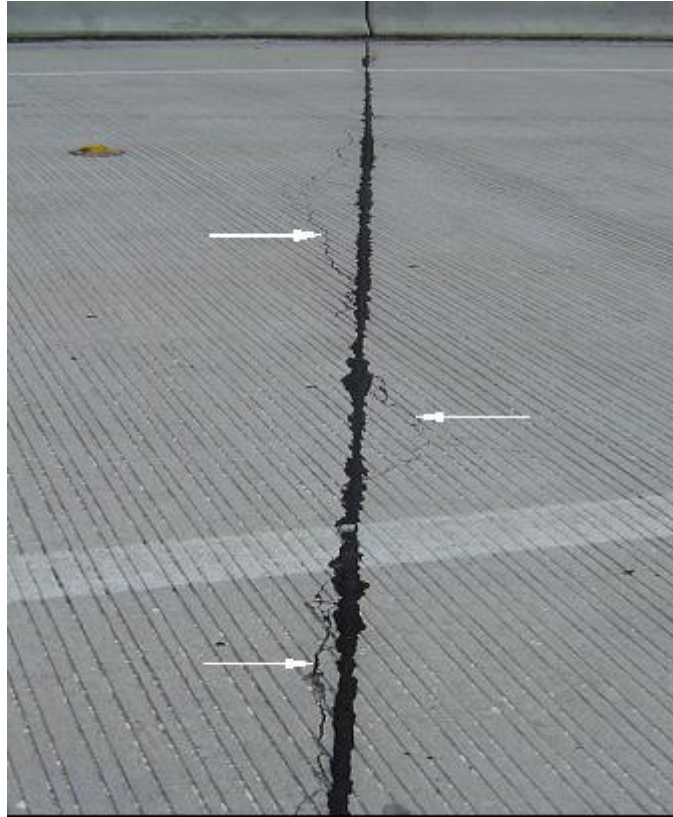


Figure 6. Transverse cracks at a control joint on the Cow Creek Bridge

2.5 SUMMARY

Three precast flat slab bridges with reinforced concrete toppings were visually inspected. The Cow Creek and Turkey Creek bridges had shear keys built into the prestressed slabs. Slab depth varied from bridge to bridge. All of the bridges had a reflective longitudinal crack over each flat slab joint and multiple transverse cracks over the bents where the topping goes into negative moment. The topping on the Cow Creek Bridge was spalling at these locations. The Turkey Creek Bridge showed the most cracking and is the only one to have been repaired.

3 LITERATURE REVIEW

Cracking of bridge decks is not a problem that is specific to flat slab bridges. Although limited research has been conducted dealing specifically with cracking on this type of bridge, a good deal of research has been performed on deck cracking of traditional slab/girder and deck slab bridges. Several of the factors listed by Issa (1999) are common causes of deck cracking.

- Poor curing procedures which promote high evaporation rates and a large amount of shrinkage.
- Use of high slump concrete
- Excessive amount of water in the concrete as a result of inadequate mixture proportions and re-tempering of concrete.
- Insufficient top reinforcement concrete cover and improper placement of reinforcement.

Cracks may not be the result of bad design but rather an outcome of poor construction practice.

Researchers have tested several methods to control cracking that can be easily implemented and though they do not increase the tensile strength of the concrete, they do improve its shrinkage and post crack behavior. Many of these have been implemented by transportation departments and have proven to work in the field.

The New York Thruway Authority (NYTA) and the Ohio Turnpike Commission (OTC) have successfully used shrinkage compensating concrete (SHC) to control shrinkage cracking on bridge decks (Ramey, Pittman, and Webster 1999). Although the NYTA had problems with deck scaling in the bridge decks that used SHC it was determined not to be a factor. The OTC had the greatest success with SHC. They have replaced 269 bridge decks with SHC and only 11 have shown minor or moderate cracking with none showing severe cracking. This same study also showed that good quality SHC requires continuous curing to activate the ettringite formation. The OTC requires contractors to use fog spraying under certain weather conditions, always use monomolecular film to retard evaporation, and control the curing water temperature to avoid thermal shock. They also require wet curing for seven days, which is necessary because SHC will crack if any ettringite is activated after the concrete hardens. Use of SHC requires strict curing techniques to effectively eliminate shrinkage cracks.

Research has shown that shrinkage reducing admixtures (SRA) effectively reduce drying shrinkage of concrete and, subsequently, cracking. Tests show a reduction in drying shrinkage of about 50 to 60% at 28 days, and 40 to 50% after 12 weeks (Nmai et al. 1998). Restrained ring tests showed that concrete mixtures with SRA decrease the rate of residual stress development by decreasing the surface tension of water by up to 54% (Pease et al. 2005). A considerable reduction in crack width occurs as compared with normal concrete depending on the type and amount of SRA used (Shah, Karaguler, and Sarigaphuti 1992). SRA can be integrated in the mixture or applied topically to the concrete surface after bleeding stops. Better results are obtained with larger surface application rates. Mixing SRA integrally, however, is more effective.

Rectangular slabs and ring type specimens have been used to demonstrate the ability of synthetic fibers to control cracking resulting from volume changes due to plastic and drying shrinkage. Synthetic fibers were shown to reduce the amount of plastic shrinkage cracking when compared to the use of welded wire mesh (Shah, Sarigaphuti, Karaguler 1994). They tested polypropylene, steel, and cellulose fibers using a restrained ring test at 0.5%, 0.25%, and 0.5%

by volume, respectively. The maximum crack width was reduced by 70% at those dosage rates. The ability of the fibers to control cracking is partially due to the decrease in the amount of bleed water (Nanni, Ludwig, and McGillis 1991; Soroushian, Mirza, and Alhozaimy 1993). The authors suggested that the presence of fibers reduced settlement of the aggregate particles, thus eliminating damaging capillary bleed channels and preventing an increase in inter-granular pressures in the plastic concrete. Adding synthetic fibers also decreases the initial and final set times of the concrete. Decreasing the time that the concrete is left exposed to the environment in a plastic state promotes reduced shrinkage cracking.

A series of tests run by Balaguru (1994) on steel, synthetic, and cellulose fibers reveals that the fiber's aspect ratio (length/diameter) seems to be a major factor contributing to crack reduction. An increase in fiber content also contributed to a smaller crack area and width. The same results were obtained by Banthia and Yan (2000), and Grzybowski and Shah (1990) (Figure 7-Figure 10). Fibers with a high aspect ratio have more contact area with the concrete mixture consequently, more stress is transferred by the fiber before pull-out. Increases in fiber content usually lead to smaller crack widths. Too much fiber, however, may affect the workability of the concrete mixture and cause entanglement into large clumps. Fiber length, volume, and specific fiber surface (total surface area of all fibers within a unit volume of composite) are all major contributing factors to the amount of cracking.

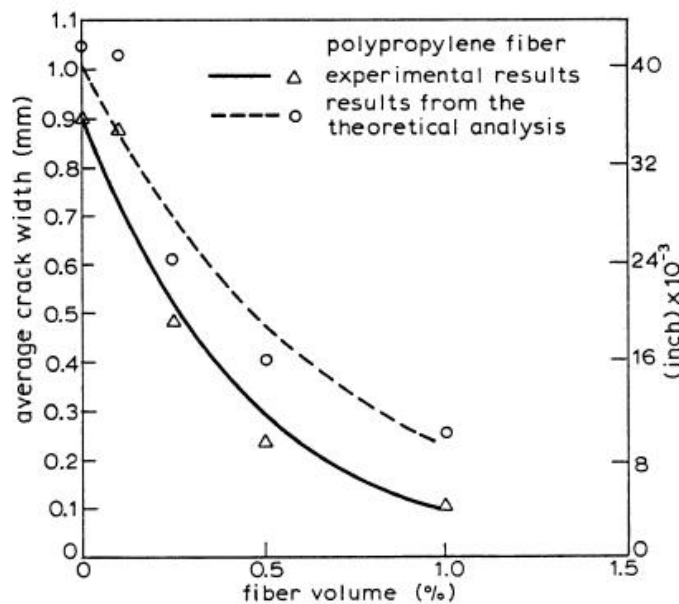


Figure 7. Average crack width vs. fiber volume for polypropylene fibers (Grzybowski and Shah 1990)

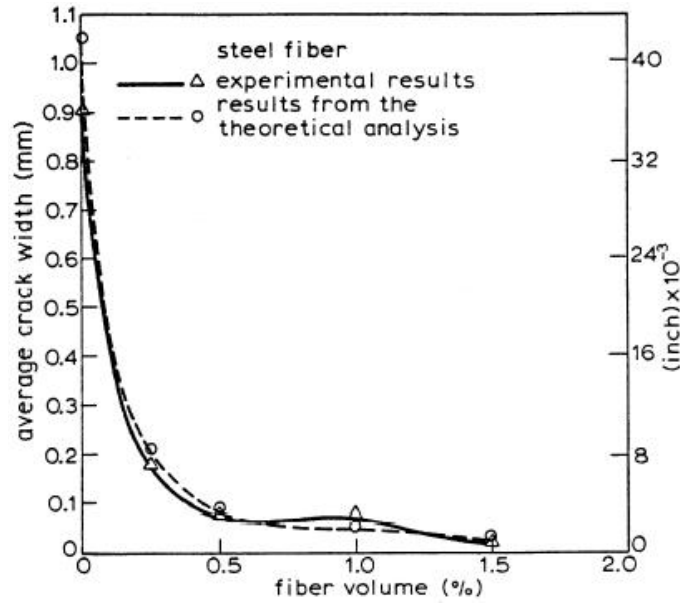


Figure 8. Average crack width vs. fiber volume for steel fibers (Grzybowski and Shah)

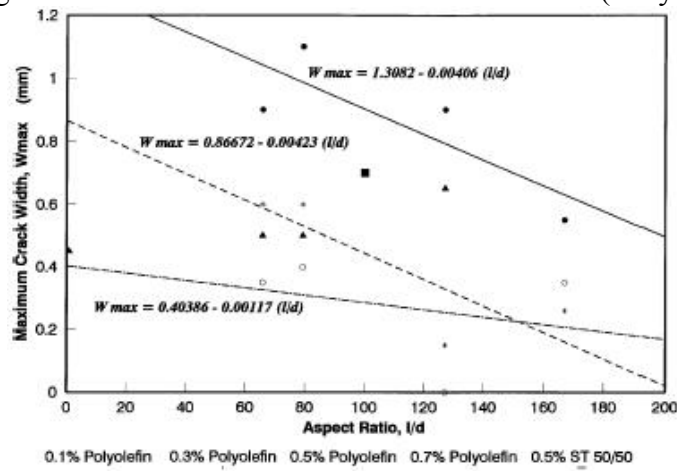


Figure 9. Maximum crack width vs. aspect ratio (Grzybowski and Shah 1990)

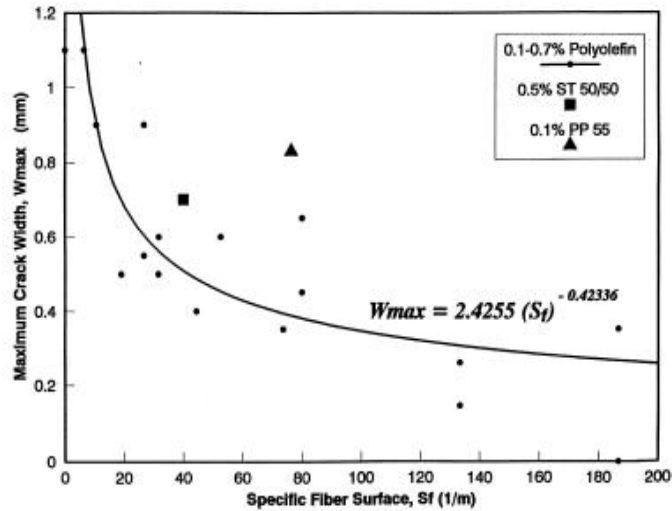


Figure 10. Maximum crack width vs. specific fiber surface (Grzybowski and Shah 1990)

Little research was found on use of a rigid carbon fiber reinforced polymer (CFRP) composite grid to control bridge deck cracking. A CFRP grid would make it possible to reinforce the concrete near the surface. Flexure testing by Makizumi, Sakamoto, and Okada (1992) placed a carbon-fiber grid, prestressed strands, and in some cases, reinforcing bars, in small beams. The grid was placed 3mm from the extreme face in tension. Cracks were reduced by half in cases with reinforcing bars. Specimens that contained only grid and prestressing met the minimum crack size requirements proposed by the Japan Society of Civil Engineers (JSCE).

4 FINITE ELEMENT MODELING OF CONCRETE SHRINKAGE

4.1 INTRODUCTION

Figure 11 shows two idealized restrained concrete slabs. Figure 11a shows a slab restrained at the ends. If the slab is unreinforced, then a single crack will form whose size is equal to the total shrinkage strain. In Figure 11b the base provides frictional restraint to the slab, generating cracks at the free surface that are equally distributed. The cracks that form under these conditions are referred to as primary cracks. Secondary cracks can also form between the primary cracks as a result of combined shrinkage strains and externally applied tensile stress. Furthermore, when the axial stresses increase and no more primary cracks form, the secondary cracks begin to widen. The contribution of drying shrinkage to concrete cracking can be controlled by preparing a proper mix design, proportioning the concrete member to minimize differential shrinking stresses, optimizing curing procedures, and proper use and application of joints.

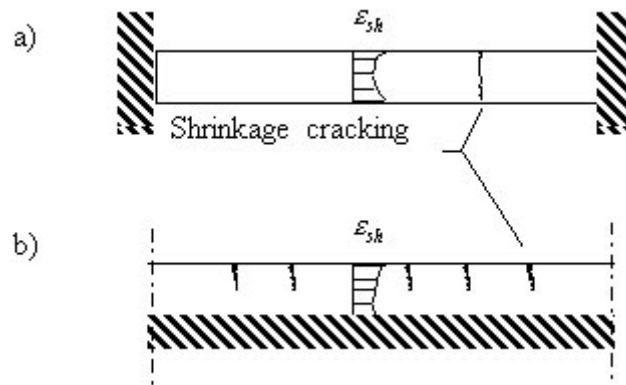


Figure 11. Typical cases of internally loaded and time dependent strains caused by shrinkage

4.2 EVALUATION OF SHRINKAGE RATE

The total shrinkage of concrete, in general, consists of three components: 1) autogenous shrinkage caused by volume change due to chemical reactions during hydration, 2) carbonation shrinkage due to the reaction of calcium hydroxide from cement paste with atmospheric carbon dioxide, and 3) drying shrinkage. The autogenous shrinkage is relative small, about 5 to 8% of the maximum drying shrinkage, and can be neglected. So can the carbonation shrinkage, since carbon dioxide penetrates only a very thin surface layer.

According to the ACI 209, the development of drying shrinkage over time is predicted as:

$$\varepsilon_{sh} = 780 \times 10^{-6} (\beta_{cp} \beta_h \beta_d \beta_s \beta_f \beta_{ce} \beta_{ac}) \quad (1)$$

where β_{cp} takes into account the effect of curing periods, β_h is used to estimate the effect of relative humidity, β_d is the coefficient used for the effect of average thickness of structural member, β_s estimates the effect of concrete consistency, e.g., slump of fresh concrete, β_f is used to take into account the content of fine aggregates, the coefficient β_{ce} indicates the effect of cement content, and β_{ac} is used to estimate the effect of air content.

Of our interests only the effects of relative humidity and thickness of the member are considered to estimate the shrinkage strain. The coefficient β_h is calculated as follows:

$$\beta_h = 1.4 - 0.010 \square H \quad \text{if } 40 \leq H \leq 80\% \quad (2)$$

$$\beta_h = 1.4 - 0.010 \square H \quad \text{if } 80 < H \leq 100\%$$

The effect of thickness of the member is taken into account as shown Table 1:
if $50 \leq d \leq 150 \text{ mm}$,

Table 1. The coefficient β_h

d (mm)	50	75	100	125	150
β_d	1.35	1.25	1.17	1.08	1.00

Thus, for example, if a concrete slab with 150 mm thickness undergoes drying shrinkage in a relative humidity of 50%, then the shrinkage strains are evaluated along the depth (Table 2).

Table 2. Shrinkage strains in a 50% relative humidity condition ($\beta_h = 0.9$)

depth (mm)	50	75	100	125
$\varepsilon_{sh} (\times 10^{-6})$	$780 \times (0.9 \times 1.35)$ = 947.7	$780 \times (0.9 \times 1.25)$ = 877.5	$780 \times (0.9 \times 1.17)$ = 821.3	$780 \times (0.9 \times 1.08)$ = 758.2

However, since drying shrinkage occurs over time, the development of shrinkage can be expressed by:

$$\varepsilon_t = \frac{t}{35+t} \varepsilon_{sh} \quad (2)$$

where t is the duration of drying in days. Therefore, the development of shrinkage strain through thickness of the slab at 30 days after casting is summarized in Table 3.

Table 3. Shrinkage strains of normal weight concrete after 30-day surface exposure

depth (mm)	50	75	100	125
$\varepsilon_t (\times 10^{-6})$ at 30days	0.46×947.7 = 436.0	0.46×877.5 = 403.7	0.46×821.3 = 377.8	0.46×758.2 = 348.8

4.3 FINITE ELEMENT MODEL

4.3.1 CONSTITUTIVE RELATIONSHIP

The effect of shrinkage in stress development is modeled essentially the same manner as thermal expansion: the thermal expansion coefficient α is replaced with an equivalent coefficient of shrinkage rate and temperature change over time is simulated as the development of shrinkage, ε_t . Prior studies have noted, however, that shrinkage gradients through the depth of concrete pavement and slab are nonlinear, and thus, shrinkage induced stresses should be considered due to both the total shrinkage strains at a time and the shrinkage gradients through thickness of the member. In this study, the concrete cover is divided into three sub-layers along

the thickness of 150 mm so that the shrinkage gradients are modeled as tri-linear shrinkage gradients whereas the precast concrete deck is assumed to yield no shrinkage. The generalized Hooke's law is employed to compute the shrinkage stresses:

$$\sigma_{sh} = -\beta(\varepsilon_t) \quad (3)$$

where β represents an equivalent shrinkage constant to thermal expansion coefficient.

4.3.2 MODEL DESCRIPTION

A three dimensional slab is modeled to study the effect of boundary constraints. The 150 mm slabs (i.e., concrete cover) were 2400 mm long and 1200 mm wide, with a Poisson's ratio of 0.19, a mass density of 2200 kg/m^3 . A modulus of elasticity is calculated using a 28-day modulus of elasticity of normal weight concrete $E_{28} = 35000 \text{ MPa}$ as follows

$$E_t = (0.01 \times t + 0.7) \times E_{28} \quad (3)$$

4.3.3 SIMULATION RESULTS

Time-varying shrinkage stress analyses were then performed to compute time-histories of stress states throughout the three-dimensional 8-node brick meshes. Thus, the three-dimensional volume change due to drying shrinkage was modeled as prescribed nodal temperature boundary conditions. Using the time history of temperature distributions equivalent to shrinkage strains obtained from the ACI 209 method, nodal temperatures of the finite element model were chosen.

Due to plane symmetry of the geometry, partial symmetry finite element models were used. In order to investigate the effects of boundary restraint on contraction-induced shrinkage stress in the concrete cover, two different mechanical boundary conditions were considered. A finite element model was constructed such that both vertical (z-direction) and translational (xy-direction) constraints were imposed on the bottom plane of the precast concrete deck and, along the symmetry boundary, displacement in the perpendicular direction was constrained as well. However, no constraint along the xy direction was imposed on the second model, i.e., Model B. In both boundary condition cases, two different relative humidity conditions were considered so that an actual humidity condition was bracketed, e.g., a range of 50 to 80% of relative humidity. The results are shown in Table 4.

Table 4. Maximum tensile stresses developed in concrete cover

Model	Relative humidity (%)	Time (days)	Maximum Tensile (psi)	Maximum stress component
A (fixed boundary)	80	10	351	σ_{xx}
		20	648	
		30	914	
A (fixed boundary)	50	5	557	σ_{xx}
		10	1050	
		30	2740	
B (released boundary)	80	10	338	σ_{yy}
		20	622	
		30	872	
B (released boundary)	50	5	537	σ_{yy}
		10	1010	
		30	2617	

More noticeably, the magnitude of the maximum principal stresses are similar in both boundary condition cases, but stresses change significantly with respect to the boundary constraint imposed on the bottom of the precast deck.

Secondly, comparison of the stress development in a case where the corner of the precast deck was not restrained in upward vertical motion (contact) reveals that development of the maximum principal stresses can change noticeably in response to the constraints imposed on the edge boundaries of the structural system. More severe tensile stresses, normal stresses to the plane in the near corner interface zone between the concrete cover and the precast deck were developed when the corner nodes of the model were constrained to only displace vertically. The maximum principal stresses obtained from simulations are presented in Table 5.

The results of this FEM study indicated that the slab system might exhibit curling at the corners due to the differential shrinkage strains that generally occur in slabs on grade. This led to the placement of deflection gages at the corner of each slab specimen to monitor for movement. Furthermore, tensile stresses generated in the model, even with no edge restraint, were above the tensile strength of the concrete with 50% R.H. but not as high when 80% R.H. was considered. Even at 80% R.H., however, the predicted tensile stresses were estimated to be near 1000psi after 30 days time. Based on these projections, we expected that the control specimen would exhibit cracking relatively soon after casting.

Table 5. Maximum principal tensile stresses developed in a contact model

Model	Relative humidity (%)	Time (days)	Maximum principal tensile stress (psi)
C (Nonlinear spring-contact boundary)	50	5	537
		10	967
		30	2279
C (Nonlinear spring-contact boundary)	80	10	310
		20	566
		30	760

5 EXPERIMENTAL PROGRAM

5.1 INTRODUCTION

Several methods of controlling cracking were considered for testing (Table 6). The concrete toppings that were evaluated contained either: synthetic fiber, steel fiber, a blend of steel and synthetic fibers, a shrinkage-reducing admixture, or a carbon-fiber grid. They were selected based on their ease of application and their estimated effect on the construction and labor cost of the bridge deck. Several of these are presently commercially available and commonly used in the construction industry. A standard FDOT Class II (bridge deck) mixture was also used as a basis for comparison.

Table 6. Methods considered for controlling shrinkage cracking

Method of control	Advantages	Disadvantages	Comments	Test
Control	n/a	n/a	n/a	Yes
Transverse post-tensioning: precast panels are post-tensioned together before topping is placed.	Reduce transverse reinforcement requirements.	Difficult and costly on small, low-volume projects Curing must still be carefully implemented	n/a	No
Shrinkage compensating cement: Concrete will increase in volume after setting and during early age hardening by activation of ettringite (ACI 223-98)	No special equipment or techniques are needed	Delay in pouring causes loss in slump (ACI 223-98) Curing must be carefully monitored	Concrete must remain as wet as possible during curing in order to activate ettringite. Concrete expands during wet cure No effect on creep (ACI 223-98) No modification of formwork is needed (ACI 223-98) Used to control dry shrinkage	No
Shrinkage-reducing admixtures: Reduces capillary tension that develops within the concrete pores as it cures (Pease et al. 2005)	Easily mixed in at jobsite or at cement plant Considerable reduction in crack width as compared with plain concrete (Shah, Karaguler, and Sarigaphuti 1992)		Volume of water added into mix must be reduced by volume of admixture added into mix (Pease et al. 2005)	Yes
Fiber reinforced concrete: Randomly distributed fibers carry tensile stresses after cracking	Discontinuous and distributed randomly Loss in slump, not in workability (ACI 544.1R) Easily incorporated into mix	Balling may become a problem if fiber lengths are too long (ACI 544.1R)	Many types and lengths available All bonding is mechanical (ACI 544.1R)	

Table 6. Continued

Method of control	Advantages	Disadvantages	Comments	Test
Synthetic fibers: Commercially available fibers shown to distribute cracks and decrease crack size (ACI 544.1R)			Most fibers will not increase the flexural or compressive strength of the concrete (ACI 544.1R) Fiber dimensions influence shrinkage cracking Mostly used in flat slab work to control bleeding and plastic shrinkage (ACI 544.1R)	
Acrylic		Not much research has been conducted	Has been used to control plastic shrinkage (ACI 544.1R)	No
Aramid		Expensive when compared to other fibers	Mostly used as asbestos cement replacement in high stress areas (ACI 544.1R)	No
Carbon	Reduces creep Reduces shrinkage significantly (ACI 544.1R)	Difficult to achieve a uniform mix (ACI 544.1R)	Research shows that carbon fibers have reduced shrinkage of unrestrained concrete by 90% (ACI 544.1R)	No
Nylon	Widely used in industry	Moisture regain must be taken into account at high fiber volume content (ACI 544.1R)	Shown to have decreased shrinkage by 25% (ACI 544.1R)	No
Polyester		No consensus on long term durability of fibers in portland cement concrete (ACI 544.1R)	Not widely used in industry	No
Polypropylene	Significantly reduces bleed water (ACI 544.1R) Widely used in industry		Shown to reduce total plastic shrinkage crack area and maximum crack width at 0.1 % fiber volume fraction (Soroushian, Mirza, and Alhozaimy 1995)	Yes

Table 6. Continued

Method of control	Advantages	Disadvantages	Comments	Test
Polyvinyl Alcohol (PVA)	Higher stiffness and strength than other synthetic fibers.	Strong chemical bond with paste leads to fiber rupture and low elongation.	Relatively new material	No
Steel Fibers	Many shapes and sizes available Use of high aspect ratio fibers provide high resistance to pullout (ACI 544.1R) Widely used in industry	Surface fibers may corrode (surface staining?) If large cracks form, fibers across opening may corrode (ACI 544.1R)	May not reduce total amount of shrinkage but increase number of cracks reducing crack size (ACI 544.1R)	Yes
Natural Fibers	Very inexpensive	Requires special mix proportioning to counteract retardation effects of glucose in fibers (ACI 544.1R)	Not widely used in industry	No
Carbon FRP Grid - Grid system carries tensile stresses after cracking at depth of installation	Available in different sizes Can be placed at a specific depth	May not be available in large sheets Manufacturer recommended that concrete be screeded at level where mesh is placed	Not much information available on its use to control cracking FDOT allows placement of grid at ½ in. below surface	Yes
Glass FRP Grid - Grid system carries tensile stresses after cracking at depth of installation	Available in different sizes Can be placed at a specific depth	Concrete may need to be screeded at level where mesh is placed	Not much information available on its use to control cracking FDOT allows placement of grid at ½ in. below surface	No

Each concrete mixture that was used for the precast slabs (Class IV) and the toppings (Class II) conformed to the parameters set forth in the FDOT Standard Specifications for Road and Bridge Construction (2004a) (Table 7, Table 8, and Table 9). The concrete toppings had the same proportion of ingredients within acceptable tolerances. They varied only in the type of system that was incorporated into the mixture to control cracking.

Table 7. Concrete type for bridge superstructures

Component	Slightly Aggressive Environment	Moderately Aggressive Environment	Extremely Aggressive Environment
Precast Superstructure and Prestressed Elements	Type I or Type II	Type I or Type III with Fly Ash or Slag, Type II, Type IP, Type IS, or Type IP(MS)	Type II with Fly Ash or Slag
C.I.P. Superstructure Slabs and Barriers	Type I	Type I with Fly Ash or Slag, Type II, Type IP, Type IS, or Type IP(MS)	Type II with Fly Ash or Slag

Table 8. FDOT structural concrete specifications

Class of Concrete	Specified Minimum Strength (28-day) (psi)	Target Slump (in)	Air content Range (%)
II (Bridge Deck)	4,500	3*	1 to 6
IV	5,500	3	1 to 6
*The engineer may allow higher target slump, not to exceed 7 in when a Type F or Type G admixture is used.			

Table 9. Master proportional limits

Class of Concrete	Minimum Total Cementitious Materials lbs/yd ³	*Maximum Water Cementitious Materials Ratio lb/lb
II (Bridge Deck)	611	0.44
IV	658	0.41
*The calculation of the water to cementitious materials ratio (w/cm) is based on the total cementitious material including silica fume, slag, fly ash, or Metakaolin.		

Four full-scale bridge decks were constructed to test the performance of the toppings. The Cow Creek Bridge was selected as a model for the design because it displays the type of crack patterns that this project is investigating and it has similarities in design with the other evaluated bridges and other existing flat slab bridges in Florida. A redesign of the bridge deck was conducted to ensure that the full-scale model conforms to the latest design codes. Each deck was approximately 12 ft wide and spanned 30 ft. The toppings were 6 in. deep and exposed to similar environmental conditions as existing flat slab bridges in Florida.

5.2 DESIGN AND FABRICATION

The flat slab analysis and design was done using LRFD Prestressed Beam Program v1.85 (Mathcad based computer program) developed by the FDOT Structures Design Office. It is available on their website, www.dot.state.fl.us/structures. The program analyzes prestressed concrete beams in accordance with the AASHTO LRFD Specification (2001) and the FDOT's Structures Manual (2004b). Input and output from the program are found in Appendix A.

Twelve full-scale precast slabs were constructed by Dura-Stress Inc., a Precast/Prestressed Concrete Institute (PCI) certified plant, in Leesburg, Florida. The slabs were similar in size and design to the Cow Creek slabs with a length of 30-ft. Unlike the Cow Creek Bridge, the flat slabs used to construct the test specimens did not have shear keys. The Texas DOT has had success with flat slab bridges without shear keys (Cook and Leinwohl 1997) and eliminating them would help reduce labor and construction costs. Each slab had twelve 1/2 in. diameter lo-lax prestressing strands tensioned to 31 kips each. The two center strands were debonded 3 ft. from each end of the slab. The slabs were also reinforced with mild steel. Vertical shear reinforcement was provided every 12 in. U-shaped reinforcing bars, spaced at 12 in., provided horizontal shear reinforcement. Mild steel was also provided at each end of the slabs for confinement. All of the steel had a minimum concrete cover of 2 in. Reinforcement details are shown in Figure 12 and Figure 13. Complete reinforcement details are found in Appendix F. Figure 14 and Figure 15 show the constructed reinforcement system.

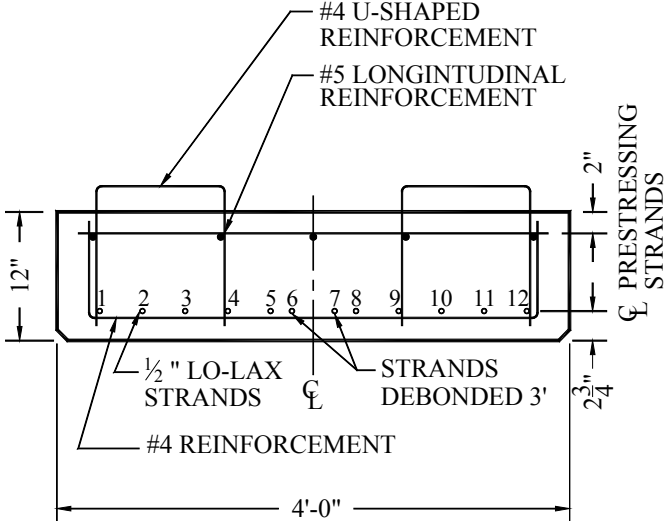
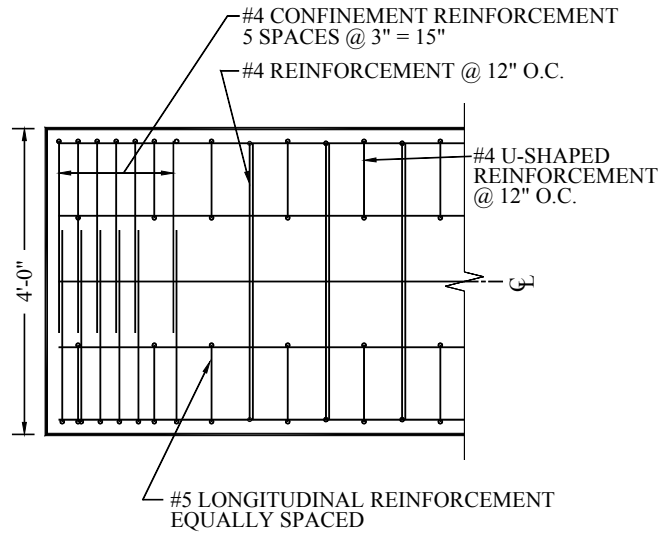


Figure 12. Typical cross-section through precast slab specimen



PRESTRESSING STRANDS NOT SHOWN FOR CLARITY.

Figure 13. Reinforcement detail at end of slab



Figure 14. Reinforcement at end of flat slab



Figure 15. Flat slab reinforcement layout

The concrete used for the slabs was a Class IV FDOT concrete mixture. The mixture design provided by the manufacturer is shown in Table 10. Based on the specifications found in Table 7, the concrete is intended for use in a mildly aggressive environment as defined by the FDOT's Standard Specification for Road and Bridge Construction (2004a). It was batched onsite and delivered to the casting bed in trucks equipped with pumps to place the concrete.

Table 10. Concrete mixture components for precast slabs.

Material	Type	Amount per CY
Cement	AASHTO M-85 Type II	800 lbs
Mineral Admixture	NA	NA
Water	--	308 lbs
Aggregate	Sand 2	1150 lbs
Aggregate	#67 Granite 2	1750 lbs
Admixture	Air Entraining	0 oz
Admixture	Water Reducer	24 oz
Admixture	Superplasticizer	72 oz

The slabs were constructed in three groups of four as indicated in Table 11. The layout on the casting bed is shown in Figure 16. Steel plates and plywood were used as formwork for the slabs. A truck pumped the concrete onto the bed starting at slab No. 4 and moved towards slab No. 1 as the concrete was placed (Figure 17). Each truck transported approximately 5 cubic yards (CY) of concrete. One truck immediately continued placing concrete as the previous one finished. A total of three deliveries were needed to complete the casting of one group of slabs. The concrete was not screeded as it was placed. Personnel from the prestressing yard raked the

concrete into place as it was pumped onto the casting bed. The surfaces were raked to ensure a rough finish to aid in horizontal shear transfer from the topping to the slab and a hoisting anchor was embedded into each corner of the precast slabs (Figure 18). Curing agents were not applied to the surface of the concrete.

Table 11. Flat slab identification number and location

Designation	Casting Date & Time	Location on Casting Bed	1 Day Compressive Strength	Release Date & Time	28-Day Compressive Strength
FS1-1	5/5/2004 1:30PM	1	3870 psi	5/7/2004 ≈ 7:00AM	8960 psi
FS1-2		2			
FS1-3		3			
FS1-4		4			
FS2-1	5/11/2004 10:30AM	1	3400 psi	5/13/2004 ≈ 7:00AM	8400 psi
FS2-2		2			
FS2-3		3			
FS2-4		4			
FS3-1	5/14/2004 11:00AM	1	3690 psi	5/17/2004 ≈ 7:00AM	7980 psi
FS3-2		2			
FS3-3		3			
FS3-4		4			

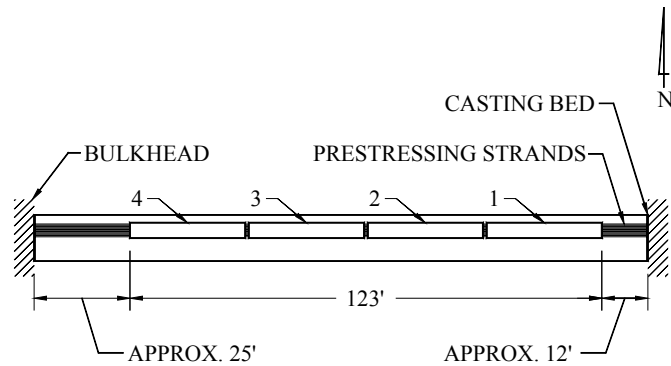


Figure 16. Typical slab layout on casting bed



Figure 17. Casting of flat slabs



Figure 18. Finished flat slab with hoisting anchors installed

Cylinders were taken to ensure adequate strength at release, document 28-day strength, and for possible future use. The cylinders collected for future use have yet to be tested. Additionally, plant quality control personnel collected five cylinders from each group to check the release and 28-day strength. The designed minimum release strength and 28-day strength were 4500 psi and 5500 psi respectively. Two cylinders were tested 24 hours after casting to determine the strength of the slabs. None of the slabs attained the minimum release strength within 24 hours. They remained on the casting bed for an additional day to allow the concrete to gain strength. It was assumed that the minimum release strength would be exceeded 48 hours

after casting; therefore, additional cylinders were not tested to verify it. Twenty-eight day strength, transfer dates and times are shown in Table 11.

The precast slabs were stored at the prestressing yard for approximately six weeks while the test site was prepared. The slabs were stored in three stacks. Each stack contained four flat slabs. The slabs and the cylinders were exposed to the environment during this period.

5.3 SITE LAYOUT

Four single span flat slab bridge superstructures were constructed at the FDOT Maintenance Yard located at 2612 Springhill Rd. in Tallahassee, FL. Reinforced concrete supports for the flat slabs were constructed by the FDOT Structures Lab personnel to elevate the slabs to a convenient working height above the ground. The precast slabs were supported by neoprene bearing pads placed using a three-point system shown in Figure 19. This pattern was used on the Cow Creek Bridge and is currently used successfully by the Texas DOT (Cook & Leinwohl 1997). A view of the site before the placement of the precast slabs is shown in Figure 20. Each specimen consisted of three flat slab panels to ensure the possibility that at least one of the two joints would produce reflective cracks

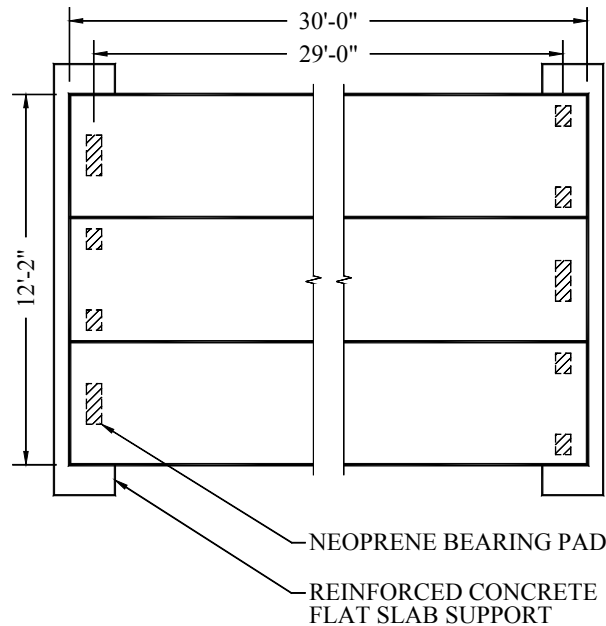


Figure 19. Typical bearing pad placement



Figure 20. Concrete supports with neoprene bearing pads before placement of precast slabs

5.4 SLAB PLACEMENT

The flat slabs were delivered and placed on June 29, 2004. The panels were transported to the site on flat-bed trailers. Each trailer carried two flat slabs. The first delivery was at 9:00 AM and approximately every half hour thereafter. A crane was onsite to unload and place the flat slabs on the supports. The panels were unloaded and installed in the order that they arrived. Concrete cylinders that were cast along with the slabs were also brought to the site and placed near the precast slabs. Figure 21 shows an overview of the specimens and flat slab orientation that made them up. A single specimen was composed of three adjacent flat slabs with a 1 in. gap between them. A 1-½ in. diameter backer rod was installed between the panels near the surface of the precast slab to retain the fresh concrete (Figure 22).

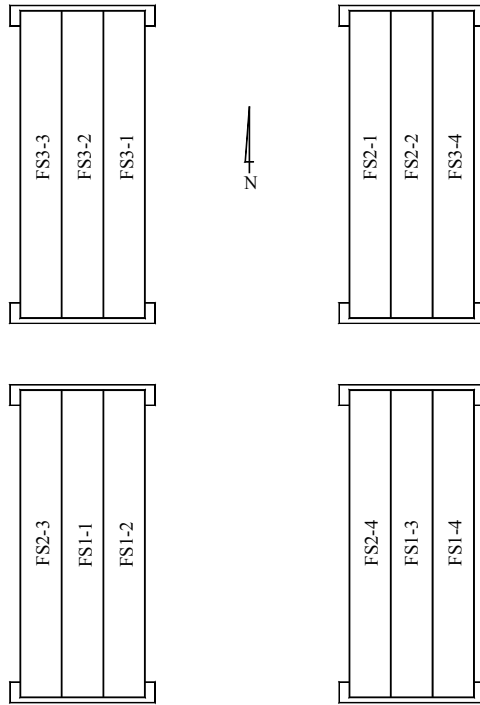


Figure 21. Slab site layout

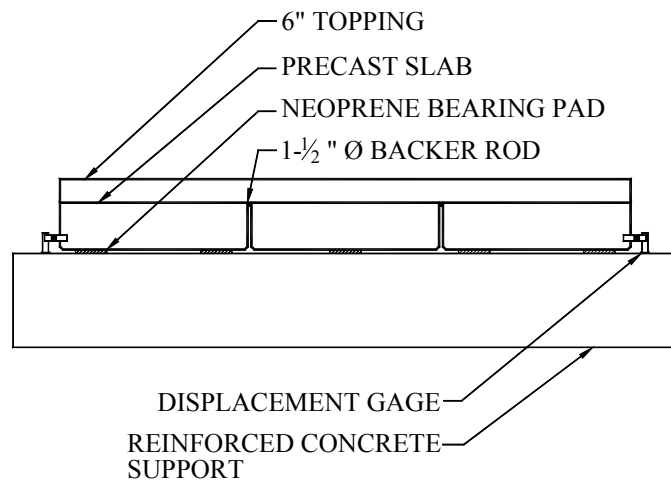


Figure 22. Typical superstructure end elevation view

Formwork was erected on the edges of each deck for the placement of the topping. It was composed of $\frac{3}{4}$ in. plywood that had one side sealed to prevent moisture absorption from the concrete mixture (Figure 23). Once the formwork was erected the topping reinforcement was installed. The formwork was removed seven days after casting the toppings.



Figure 23. Reinforcement and formwork on precast slabs before topping placement

5.5 TOPPING REINFORCEMENT

The size and spacing of the reinforcement was designed using the AASHTO LRFD Specification (2001) and the FDOT Structures Manual (2004b). No. 5 reinforcing bars were installed in the longitudinal and transverse directions spaced at 12 in. on-center with 2 in. of concrete cover. This spacing is the minimum reinforcement required for shrinkage and temperature control. The maximum allowable spacing was used to maximize the shrinkage tensile stresses in the concrete.

The longitudinal reinforcement was placed first and tied to the flat slab's horizontal shear reinforcement with wire ties. The transverse reinforcement was then placed over it and tied (Figure 24).

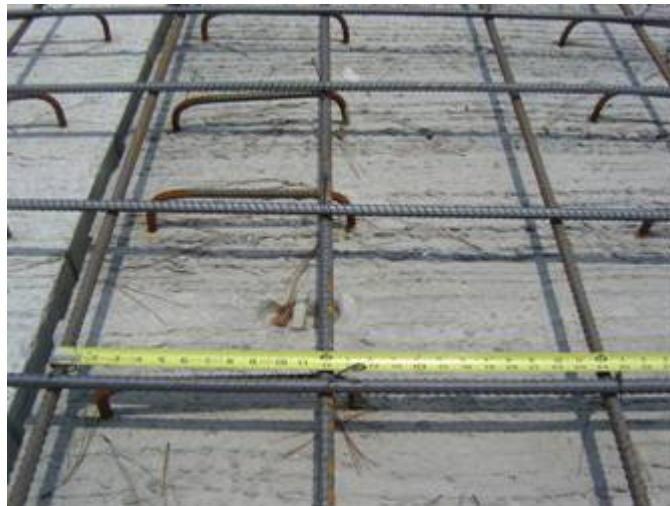


Figure 24. Topping reinforcement layout

5.6 TOPPING PLACEMENT

The toppings were cast daily during the week of July 26, 2004. Figure 25 shows the layout of the toppings with their respective designations shown in Table 12. Toppings that had a similar mixture were paired to minimize shrinkage cross-over effects over a span. The STL and BND toppings were combined because each had steel fibers incorporated into their concrete mixtures. To ensure that the CTL topping was not affected by cross-over effects and that it remained valid as a basis for comparison it was cast on a single span. The SRA topping was also cast on a single span because of the lower overall shrinkage expected of this type of concrete. The remaining two toppings, GRD and SYN, were cast on a single span. Any toppings that shared a span were cast within 2 days of each other.

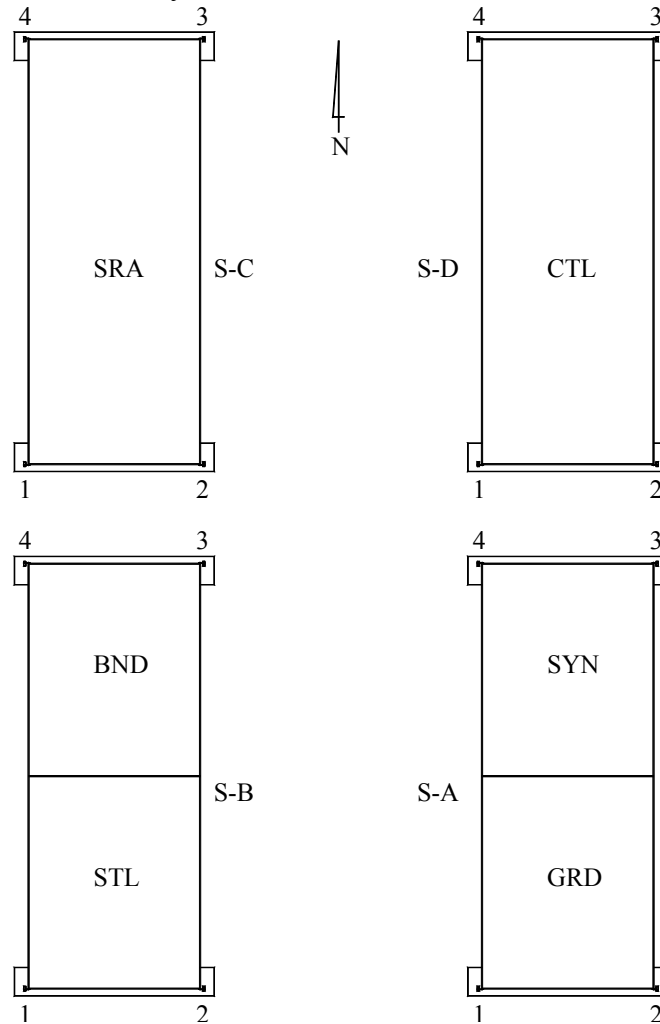


Figure 25. Displacement gage locations and superstructure and topping designation

Table 12. Specimen designation and topping treatment

Symbol	Topping Treatment
SYN	Synthetic fibers
BND	Blended fibers
GRD	Carbon-fiber grid
STL	Steel fibers
SRA	Shrinkage-reducing admixture
CTL	None

The toppings were exposed to direct sunlight from sunrise to sunset except for the CTL topping. A large tree located on the northeast corner of S-D (Figure 25) cast a large shadow on the topping until early afternoon. The CTL topping was purposely located on S-D to determine if cracks would develop under the best curing conditions at the site. Ideally, if the CTL topping cracked, the other toppings would have either cracked or restrained the formation of cracks.

Before the concrete placement, the surface was cleaned of debris with a blower and then wetted to prevent excessive water absorption from the fresh concrete topping. Front or rear discharge ready-mix trucks delivered the concrete to the site. Addition of water to the concrete mixes was performed by the concrete plant's personnel. Following the addition of the topping treatment the truck deposited the concrete directly onto the slabs. The concrete was leveled with a vibratory screed and finished with a 3 ft bull float. A curing compound was sprayed on the surface after the bleed water, if any, had evaporated. The compound was manufactured by W.R. Meadows and met the standards of the FDOT Standard Specification for Road and Bridge Construction (2004a).

The fresh concrete was tested for air content and slump in accordance with ASTM C173 and ASTM C143, respectively. The initial slump was measured upon delivery and after the addition of water and/or crack control system. The air content was measured after all modifications were made to the delivered mix.

Twenty-seven cylinders were cast for each topping in accordance with ASTM C31. Lids were placed on the cylinders after collection and removed the following day. The cylinders remained in their molds and were allowed to cure on their respective topping until they were tested. Tests were conducted for compressive and tensile strength as well as for modulus of elasticity at the ages shown in Table 13.

Tensile strength was measured using the pressure tension test (Figure 26). The equipment consisted of a cylindrical chamber for pressurizing the specimen, nitrogen filled tank, collars for the ends of the specimen, and a computer that records data supplied by a pressure transducer. This procedure required the operator to open a valve by hand to apply pressure to a 4 in. by 8 in. concrete cylinder for each test. The load rate was determined by watching a monitor that plotted a load versus time line, which should be in the range of 35 psi/sec. Li (2004) details the test equipment and procedure.



Figure 26. Pressure tension testing equipment (Li 2004)

Table 13. Cylinder test schedule

Cylinder Age (days)	Pressure Tension Test	Compressive Test ASTM C39	Elastic Modulus ASTM C469
3	yes	NA	NA
7	yes	yes	NA
28	yes	yes	yes
56	yes	yes	yes

Workability of the fresh mixture was ranked by the author from 1 to 4 according to the scale outlined in Table 14. The rankings were subjective, based on visual and physical observations as well as feedback from personnel casting the topping. Very good workability is defined as a mixture that easily flowed down the chute and consolidated around reinforcement with little to no vibration. A mixture with good workability flowed down the chute and consolidated around the reinforcement with some vibration. If the mixture flowed down the chute with aid and consolidated around reinforcement with vibration it was classified as having poor workability. A mixture with very poor workability required physical effort to aid it down the chute and required excessive vibration to consolidate it.

Table 14. Workability ranking scale

Rank	Workability
1	Very good
2	Good
3	Poor
4	Very poor

5.6.1 SYNTHETIC FIBER (SYN)

Polypropylene/polyethylene monofilament fibers (Figure 27) were used in the SYN topping at a dosage rate of 6 lbs/CY. The material properties provided by the fiber's

manufacturer are given in Table 15 and the concrete mixture's constituents are shown in Table 16.



Figure 27. Synthetic fibers used in SYN topping

Table 15. Material properties for fibers used in SYN topping

Specific Gravity	0.92
Absorption	None
Modulus of Elasticity	1,378 ksi
Tensile Strength	90 ksi
Melting Point	320°F
Ignition Point	1,094°F
Alkali, Acid and Salt Resistance	High

Twenty-four pounds of fibers were fed into the mixing drum over a period of 4 min. They were dispersed manually to prevent balling and allowed to mix for 70 revolutions of the drum as per manufacturer's recommendations. Even after mixing, however, some of the fibers were entangled and not fully coated with cement paste. Seven gallons of water were added to the mixture after a slump test measured 1¾ in. This volume of water was based on the delivery ticket, which subsequently was discovered to have been incorrect. Consequently, the actual w/c ratio was 0.38, which was significantly lower than the target value. At the time of casting, the mixture had a slump of 3¼ in. and an air content of 2.5%.

The workability of the SYN mixture was less than ideal. The fresh concrete did not flow down the chute and required excessive raking and vibrating during placement. Low w/c ratio, low air content, and incorrect amount of fly ash and cement contributed to poor workability. Following screeding, only a light sheen formed on the surface with no bleed water or bleed channels visible.

Table 16. Mixture proportions for SYN topping

Material	Design Qty.	*Required	Batched	Difference	Difference (%)	Moisture (%)
#57 Stone (lbs)	1640	6685	6620	-65	-0.97	1.90
Sand (lbs)	1324	5460	5430	-30	-0.55	3.10
Cement (lbs)	495	1980	1965	-15	-0.76	NA
Fly Ash (lbs)	120	480	345	-135	-28.13	NA
Air (oz)	1.8	7.2	7	-0.20	-2.78	NA
WR (oz)	33.8	135.2	135	-0.20	-0.15	NA
Water (gal)	25	65.58	65	-0.58	-0.89	NA
*Amount required for 4 CY. Quantities provided by ready-mix plant.						

5.6.2 BLENDED FIBER (BND)

The BND topping was a blended fiber concrete mixture composed of synthetic (Figure 28) and steel fibers (Figure 29). The synthetic fibers were ¾-in. long multifilament nylon fibers while the steel fibers were 2-in. long with a crimped profile. Table 17 and Table 18 outline the material properties of the synthetic and steel fibers provided by the manufacturer. Synthetic and steel fibers were used at a dosage rate of 1 lb/CY and 25 lbs/CY respectively. Table 19 shows the batched quantities of the ingredients in the BND mixture.

Synthetic fibers were incorporated into the mixture first so that the steel fibers would help disperse them in the mixture. A slump test, run after the drum revolved 70 times, measured 3¾ in. Eight gallons of water were added to the mixture to increase the workability and the w/c ratio. The concrete mixture had a final w/c ratio of 0.44, air content of 3.5%, and slump of 4¾ in.

The mixture flowed down the chute without any agitation and had good workability. It was easily screeded and finished. Bleed water or bleed channels were not visible on the surface of the topping.



Figure 28. Synthetic fibers used in BND topping



Figure 29. Steel fibers used in BND and STL toppings

Table 17. Properties for synthetic micro fibers

Specific Gravity	1.16
Absorption	4.5%
Modulus of Elasticity	750 ksi
Tensile Strength	130 ksi
Melting Point	435°F
Ignition Point	1,094°F
Alkali and Acid Resistance	High
Filament Diameter	23 microns
Fiber Length	0.75 in

Table 18. Properties for steel fibers used in BND and STL toppings

Specific Gravity	7.86
Absorption	None
Modulus of Elasticity	29,000 ksi
Tensile Strength	Minimum 100 ksi
Melting Point	2,760°F
Fiber Length	2 in
Equivalent Diameter	0.035 in
Aspect Ratio	57

Table 19. Mixture proportions for BND topping

Material	Design Qty.	*Required	Batched	Difference	Difference (%)	Moisture (%)
#57 Stone (lbs)	1640	6672	6700	28	0.42	1.70
Sand (lbs)	1324	5455	5420	-35	-0.64	3.00
Cement (lbs)	495	1980	1985	5	0.25	NA
Fly Ash (lbs)	120	480	445	-35	-7.29	NA
Air (oz)	1.8	7.2	7	-0.20	-2.78	NA
WR (oz)	33.8	135.20	135	-0.20	-0.15	NA
Water (gal)	31	88.60	89	0.40	0.45	NA

*Amount required for 4 CY.
Quantities provided by ready-mix plant.

5.6.3 CARBON-FIBER GRID (GRD)

A 1.6 in. by 1.8 in. carbon-fiber grid (Figure 30) was embedded in the GRD topping (Figure 31) to provide crack control near the surface of the topping. Results from tensile tests performed on grid specimens are shown in Table 20. The material properties supplied by the manufacturer are listed in Table 21. The grid was placed one inch below the surface of the topping to prevent spalling or delamination. This positioned it below the minimum $\frac{1}{2}$ in. wearing surface required by the FDOT Structures Manual (2004b). The concrete was screeded at the embedment depth to provide a level surface for the placement of the grid. A float was used to fully coat the grid with concrete paste. The topping placement was then completed with a 1 in. layer of concrete placed over the grid. Bleed water was clearly visible on the surface of the topping as it cured.



Figure 30. Carbon-fiber grid used in GRD topping

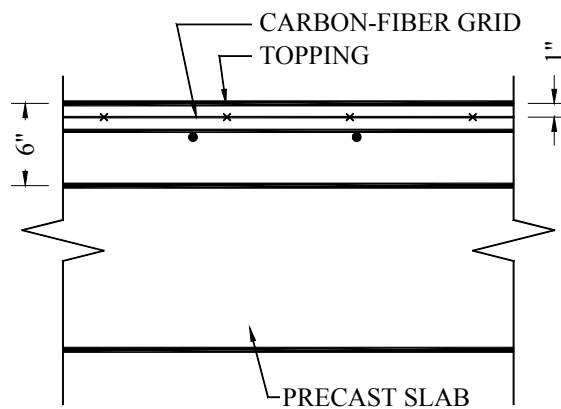


Figure 31. GRD topping grid location cross-section

Table 20. Carbon-fiber strand strength

Specimen	Fiber Direction	Strength (ksi)	Tensile Modulus (ksi)
*1	Vertical	68.5	7665
2	Vertical	126.2	8549
3	Hoop	98	9671
4	Hoop	110.8	11516
*Specimen had a thick epoxy layer that increased the cross-sectional area used to determine strength therefore underestimating strength.			

Table 21. Physical properties for carbon-fiber grid

Fiber Type	Carbon
Grid Spacing (in)	1.6 x 1.8
% of Grid Openness	69
Nominal Tensile (lbs/strand: warp x fill)	1000 x 1000
Nominal Tensile (lbs/foot)	6,650 x 7,500
Crossover Shear Strength (lbs)	40
Resin Type	Epoxy
Fabric Weight (oz/SY)	11

An initial slump of 4¾ in. was measured before any water was added to the mixture. Five gallons of water were added to increase the w/c ratio to 0.40, which brought the slump to 6¾ in. It could not be increased any further because the mixture would have become too fluid and possibly segregated. Table 22 shows the batched constituents that make up the GRD concrete mixture. At the time of casting, the concrete had a slump of 6¾ in. and 3% air content. The fresh concrete had good workability and flowed easily into place.

Table 22. Mixture proportions for GRD topping

Material	Design Qty.	*Required	Batched	Difference	Difference (%)	Moisture (%)
#57 Stone (lbs)	1640	6678	6760	82	1.23	1.80
Sand (lbs)	1324	5455	5410	-45	-0.82	3.00
Cement (lbs)	495	1980	2005	25	1.26	NA
Fly Ash (lbs)	120	480	465	-15	-3.13	NA
Air (oz)	1.8	7.2	7.0	-0.20	-2.78	NA
WR (oz)	34	136	136	0.00	0.00	NA
Water (Gal)	31	80.81	81	0.19	0.24	NA
*Amount required for 4 CY. Quantities provided by ready-mix plant.						

5.6.4 STEEL FIBER (STL)

The STL and BND toppings contained the same type of steel fibers. Their properties are listed in Table 18 and batched quantities are shown in Table 23. A dosage rate of 60 lbs/CY was used to provide a high fiber count per CY and better performance comparison with the SYN and BND toppings. Unlike the previous toppings, water was added to the mixture before the fibers. Sixteen gallons of water were added to the mixture to overcome the decrease in workability and slump caused by the fibers. The fibers were separated as they were deposited into the mixing drum to prevent balling within the mixture. Unlike any of the other toppings, heat generated by the hydration of the cement was notable. It is believed that an incorrect amount of water was added after inspecting the consistency of the mixture. The concrete was extremely stiff and did not flow down the chute or consolidate around the reinforcement and formwork. Eight gallons of water were added but the concrete was still not sufficiently workable. No more water was added because the concrete was already at a w/c ratio of 0.44.

The workability of the STL mixture was poorer than the BND mixture. Like the BND topping, the concrete did not flow down the chute and needed to be raked and vibrated into place. It was extremely difficult to screed and level off the concrete. The poor workability was attributed to an incorrect water dosage and low air content. A high range water reducer could be added to help reduce friction within the mixture thereby improving workability. No bleed water was visible on the surface of the topping.

Table 23. Mixture proportions for STL topping

Material	Design Qty.	Required	Batched	Difference	Difference (%)	Moisture (%)
#57 Stone (lbs)	1640	6678	6670	-8	-0.12	1.80
Sand (lbs)	1324	5455	5430	-25	-0.46	3.00
Cement (lbs)	495	1980	2110	130	6.57	NA
Fly Ash (lbs)	120	480	465	-15	-3.13	NA
Air (oz)	1.8	7.2	7.0	-0.20	-2.78	NA
WR (oz)	34	136	136	0.00	0.00	NA
Water (gal)	31	80.81	80	-0.81	-1.00	NA
*Amount required for 4 CY. Quantities provided by ready-mix plant.						

5.6.5 SHRINKAGE-REDUCING ADMIXTURE (SRA)

A shrinkage-reducing admixture (SRA) was added at a recommended dosage rate of 1-7/8 gal/CY. Table 24 shows the batched materials for the SRA topping. Slump tests conducted before and after dosing indicated that the SRA did not affect the slump. Twenty gallons of water were added to increase the w/c ratio to a level comparable to the other toppings. The mixture

easily flowed down the chute and around the reinforcement. It had very good workability and was screeded and finished without any difficulty.

Table 24. Mixture proportions for SRA topping

Material	Design Qty.	*Required	Batched	Difference	Difference (%)	Moisture (%)
#57 Stone (lbs)	1640	13356	13330	-26	-0.19	1.80
Sand (lbs)	1324	10910	10810	-100	-0.92	3.00
Cement (lbs)	495	3960	4030	70	1.77	NA
Fly Ash (lbs)	120	960	930	-30	-3.13	NA
Air (oz)	1.8	14.4	14	-0.40	-2.78	NA
WR (oz)	33.8	270.4	270	-0.40	-0.15	NA
Water (gal)	31	145.62	145	-0.62	-0.43	NA
*Amount required for 8 CY. Quantities provided by ready-mix plant.						

5.6.6 CONTROL TOPPING (CTL)

The same concrete mixture that was used for the GRD topping was ordered for the CTL topping (Table 25). Like the SRA topping, 20 gallons of water were added to increase the w/c ratio. The final mixture had very good workability and easily flowed around the reinforcement. Bleed channels were clearly visible on the topping as the bleed water surfaced and ran off the sides of the topping. This topping produced the most bleed water.

Table 25. Mixture proportions for CTL topping

Material	Design Qty.	*Required	Batched	Difference	Difference (%)	Moisture (%)
#57 Stone (lbs)	1640	13774	13670	-104	-0.76	1.80
Sand (lbs)	1324	11251	11150	-101	-0.90	3.00
Cement (lbs)	495	4083.8	4045	-38.8	-0.95	NA
Fly Ash (lbs)	120	990	940	-50	-5.05	NA
Air (oz)	1.8	14.85	15	0.15	1.01	NA
WR (oz)	33.8	278.85	279	0.15	0.05	NA
Water (gal)	31	167.30	167	-0.30	-0.18	NA
*Amount required for 8 1/4 CY. Quantities provided by ready-mix plant.						

5.7 SUMMARY

While these topping treatments can easily be incorporated into a concrete mixture, the variability in workability between the topping treatments needs to be addressed. As Table 26 shows, there was a correlation between the workability rating and the slump. The mixtures that received a poor or very poor rating had slumps less than 3¼ in. and low air contents when compared to the 6% allowed by the FDOT Standard Specifications for Road and Bridge Construction (2004a) (Table 8). The effect of the air content is more pronounced in the poorly rated mixtures because of the friction caused by the presence of fibers. Higher air contents would provide more air bubbles that act like ball bearings for the fibers to slide against which would reduce friction within the fresh concrete mixture. The workability of the SYN topping was also affected by the 28% shortage of fly ash in the mixture (Table 16). This shortage prevented the fibers from being fully coated with cement paste after initial mixing thus degrading its workability. Its workability was partially improved by adding water to the mixture to ensure that the fibers were coated but it could have been further improved by adding enough water to increase the w/c ratio to 0.44. Some of the workability issues in the STL topping may be attributed to an incorrect water dosage. This was based on observing the mixture during slump test No. 3. The workability of the concrete would have improved after adding 24 gal of water. The workability of the poorly rated mixtures could have been improved by increasing the amount of air-entraining admixture, water-reducing admixture or adding a high-range water-reducing-admixture.

Table 26. Workability rating/slump relationship

Topping	Workability Rating	Slump (in)
SYN	3	3¼
BND	2	4¾
GRD	1	6¾
STL	4	2
SRA	1	5
CTL	1	5

A summary of the test results and tasks completed with each topping is outlined in Table 27. The air content of all the toppings was low given that the FDOT allows up to 6%. Table 28 documents a timeline for tasks completed on each topping. The batched and cast w/c ratios of the concrete mixtures are shown in Table 29.

Table 27. Concrete mixture summary

Topping	Slump Test #1 (in)	Admixture (Gal)	Fiber Amount (lbs/CY)	Slump Test #2 (in)	Additional Water (gal)	Slump Test #3 (in)	Air Content (%)
SYN	4½	NA	6	1¾	7	¾	2.5
BND	2¾	NA	1 micro 25 steel	3¾	8	4¾	3.5
GRD	4¾	NA	NA	NA	5	6¾	3
STL	2	NA	60	NA	24	2	2
SRA	1¾	15	NA	2	20	5	1.5
CTL	2¾	NA	NA	NA	20	5	1

Table 28. Timeline from batching to casting

Topping	Delivery	Batch Start	Plant Departure	Arrival Time	Casting Start
SYN	July 26 th	8:47AM	8:57AM	9:10AM	9:45AM
BND	July 27 th	8:42AM	8:50AM	9:07AM	9:35AM
GRD	July 28 th	8:45AM	8:57AM	9:07AM	9:22AM
STL	July 28 th	9:56AM	10:15AM	10:26AM	10:58AM
SRA	July 29 th	8:32AM	8:49AM	9:05AM	9:35AM
CTL	July 30 th	8:30AM	8:50AM	9:02AM	9:20AM

Table 29. Concrete mixture w/c ratios

Topping	Batched w/c Ratio	Jobsite w/c Ratio
SYN	0.36	0.38
BND	0.42	0.44
GRD	0.39	0.40
STL	0.37	0.44
SRA	0.35	0.39
CTL	0.39	0.43

As Figure 32 shows, workability issues with the STL and SYN mixtures affected the finishing time of the toppings. Toppings with fiber treatments took the longest to complete. Screeding of the toppings commenced once casting was approximately half completed except on the BND topping which started immediately after it was cast. More time was spent screeding the GRD topping because it was performed twice, once to level the surface for placement of the grid, and a second time to level off the concrete. The time it took to install the grid includes the screeding time yet it was completed faster than the others because of good workability of the mixture. Timeline data for the SRA and CTL toppings were not listed for comparison because they were twice the size of the documented toppings.

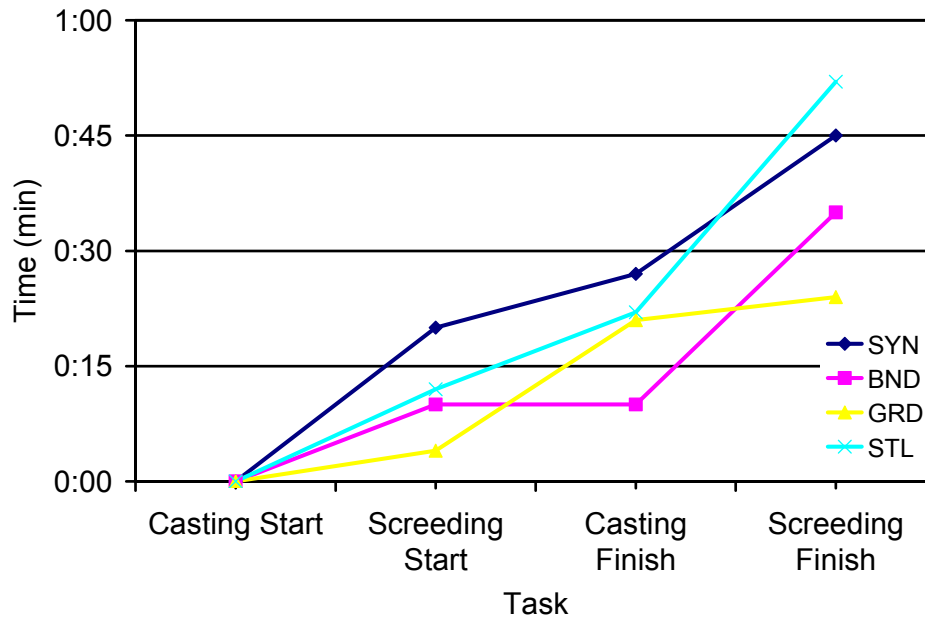


Figure 32. Normalized timeline for construction of the half-span toppings

Though the most expensive of the topping treatments tested, the SRA required the least amount of effort to incorporate into the mixture. The SRA was packaged in 5 gal pails that were easily poured into the mixing drum. This treatment should have minimal impact on the labor cost as it only took an additional 10 min. to incorporate and mix into the concrete. Some ready-mix plants will deliver a concrete mixture with SRA. No shrinkage-reducing admixtures are currently on the FDOT’s qualified products list and will need to be approved before they can be used in the field.

The fiber treatments were the least expensive measure tested to control cracking. They are available from numerous manufacturers in a variety of materials and lengths, and due to their popularity, fiber reinforced mixtures can be ordered from ready-mix plants. If fibers are added at the job site, they should be scattered by hand as they are placed in the mixing drum to prevent balling. Mixtures with higher fiber volumes such as those used for the SYN and STL toppings should incorporate a high-range-water-reducer to improve the workability. This will reduce the risk of an excessive amount of water added to the mixture at the job site.

Carbon-fiber grids are not as commonly available as the other methods that were tested and, if not planned for ahead of time, projects may experience delays because they must be obtained from a specialty supplier. Constructing a GRD topping in the field requires more time to implement than the other treatment methods due to the double screeding of the topping. Quality control plays a larger role with this system because the grid must be installed at the specified depth to be effective. If it is placed too deep in the topping it will not provide its maximum reinforcement potential. An advantage of this system is that no modifications need to be made to current FDOT approved mixtures and it allows the designer to specify where the crack control system should be installed.

5.8 INSTRUMENTATION

The bridge decks were instrumented to monitor temperature gradients through the depth of the toppings and displacements at the corners. The temperature was monitored at three locations in the toppings during the placement of the concrete. Displacement gages were installed at the corners of the bridge deck to measure movement due to curling or thermal changes.

Type K thermocouples were installed at three locations in each topping (Figure 33). Each monitoring location consisted of three thermocouples distributed in the vertical plane through the depth of the topping (Figure 34). Each set of thermocouples was tied to a 5 in. long No. 3 reinforcing bar to keep them in place while the concrete was placed. The No. 3 bar was tied to the topping reinforcement or the flat slab's horizontal shear reinforcement. The wires ran along the top of the flat slab to the nearest joint. They were fed past the backer rod and ran towards the side of the specimen. All the wires for a given topping were tied together and labeled with the location that was being monitored. Male type K plugs were installed at the ends of the wires.

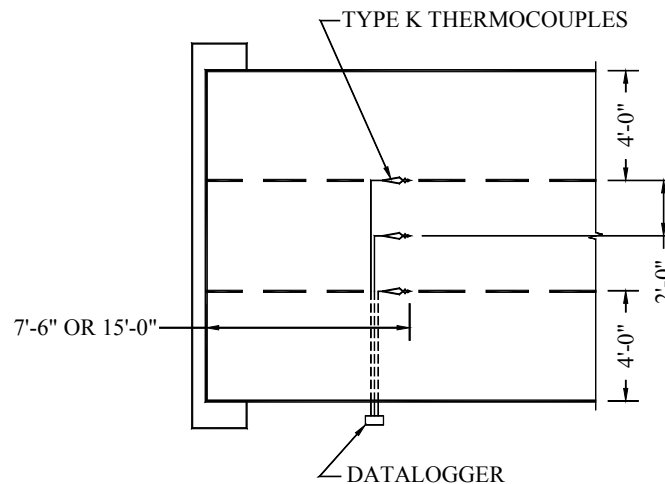


Figure 33. Partial plan view of specimens with typical thermocouple layout

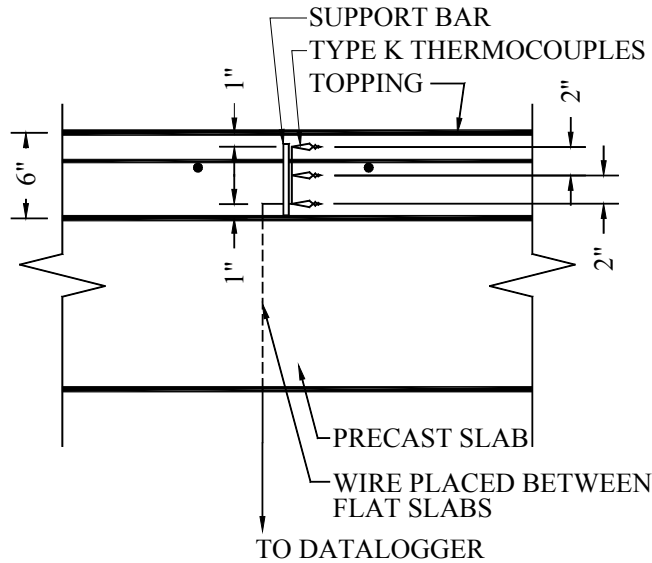


Figure 34. Partial section view of specimen with typical thermocouple profile layout

Nine locations were monitored for each topping (Figure 35). Two four-channel data loggers (eight total channels) were used to record the temperature data. One of the channels was used to monitor the temperature at two locations. The plugs were alternated on this channel approximately every half hour. The time and wire label was documented every time they were alternated. The data loggers were not left on-site overnight due to security concerns therefore temperature data were collected for approximately 8 to 10 hours on the days of the topping placement. Since the CTL and GRD toppings are the same FDOT approved mixture, temperature data were only collected for the CTL topping.

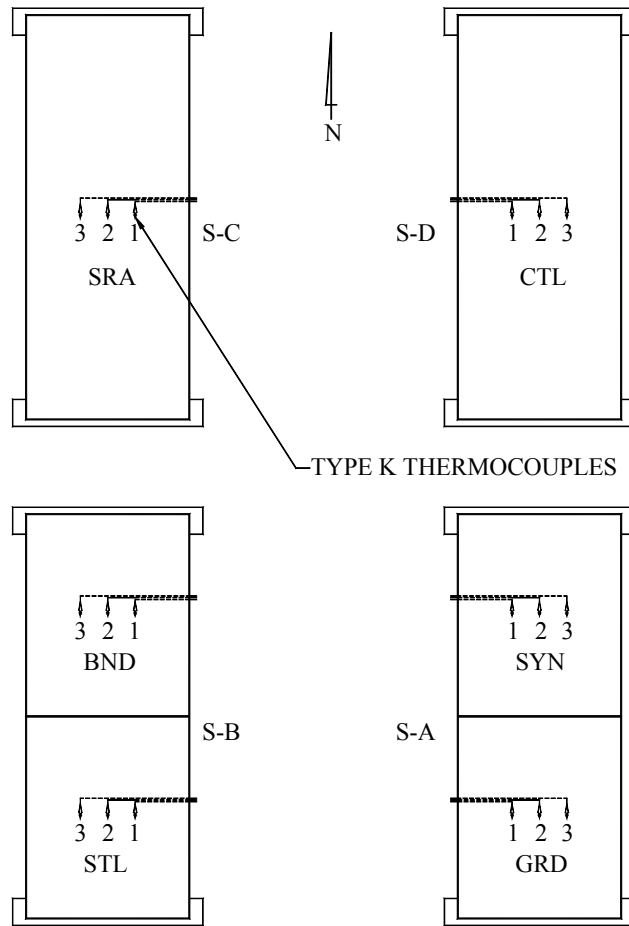


Figure 35. Monitored locations for each topping

Displacement gages were installed at the corners of the bridge decks to monitor vertical or in-plane movement (Figure 25). They were manufactured by Preservation Resource Group, Inc. and had a measurement range of 0.79 in. in the vertical direction and 1.57 in. in-plane. As shown in Figure 36, steel brackets were used to mount the gages to the superstructure support. The opposite end of the gage was attached to the flat slab with screws (Figure 37).



Figure 36. Displacement gage attachment bracket

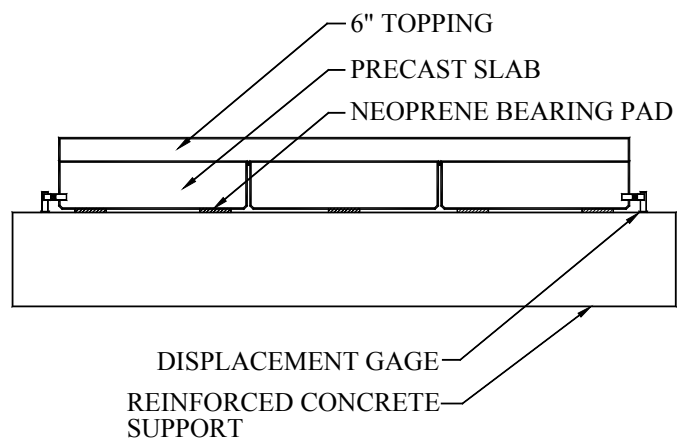


Figure 37. Profile view of displacement gage placement at span end

5.9 RESTRAINED SHRINKAGE RINGS

A restrained shrinkage ring test was performed on all of the toppings. The test was used to compare the time to cracking and the number and size of cracks between the concrete mixtures used for the toppings. The test was modeled after a ring test used to measure the cracking potential of concrete and mortar (See, Attiogbe, and Miltenberger 2003). The dimensions of the apparatus were similar but, unlike the test it was modeled after, strain gages were not used and the tests were conducted outdoors, exposed to changing temperature and humidity levels (Figure 38 & Figure 39). A concrete ring was cast for each of the toppings and the top of the ring was sealed with a curing compound to induce drying from the outer surfaces only. The formwork

was removed from the ring after 24 h. They were measured weekly for two months and biweekly thereafter with a shop microscope.

The ring with the GRD mixture was the only one that did not incorporate its respective crack control treatment. Hence, the results do not take into account the performance of the carbon-fiber grid.

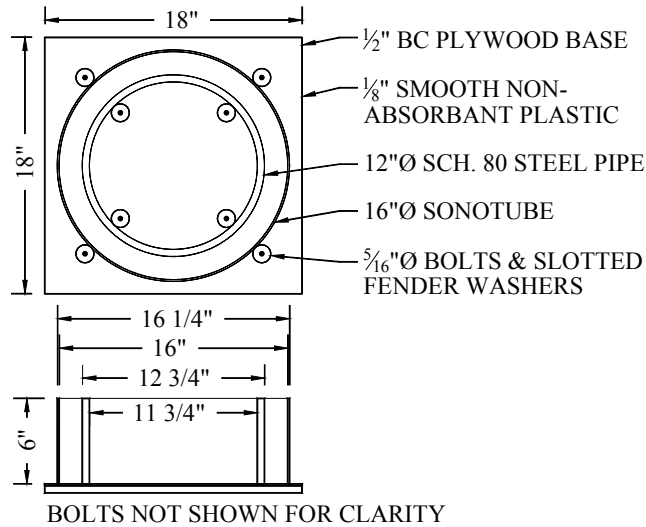


Figure 38. Restrained shrinkage ring



Figure 39. Typical restrained ring specimen

5.10 LOAD TESTS

Visible reflective cracking did not occur in any of the specimens, including the control, during the nearly 8-month monitoring period. One possible explanation is that the placement and curing were conducted in relatively ideal conditions which contributed to the lower shrinkage strains. Another is that the slabs were constructed in the very humid summer months in which ambient humidity was at 80% or above, providing improved curing conditions over that which might occur in the dryer winter months. Yet another is that these specimens were not as

wide as is generally seen in the bridges where reflective cracking has been observed. It is suspected that a wider cross-section would lead to more lateral restraint in the center of the cross-section.

To provide a comparison of the crack control capability of the topping additives, load tests were conducted to generate cracks at the joints. Initially, negative moment was created at the joints by shifting the bearing pads (Figure 40). The pads supporting the outside precast panels were removed by alternately lifting each end of the specimen. The pads under the interior panel were adjusted so that the two outside panels were carried by balanced cantilever action. Calculations indicated that the flexural tensile stresses at the joints under self weight were in excess of the tensile strength, which should have led to cracking. Following adjustment of the pad location, however, cracks appeared only in the control slab.

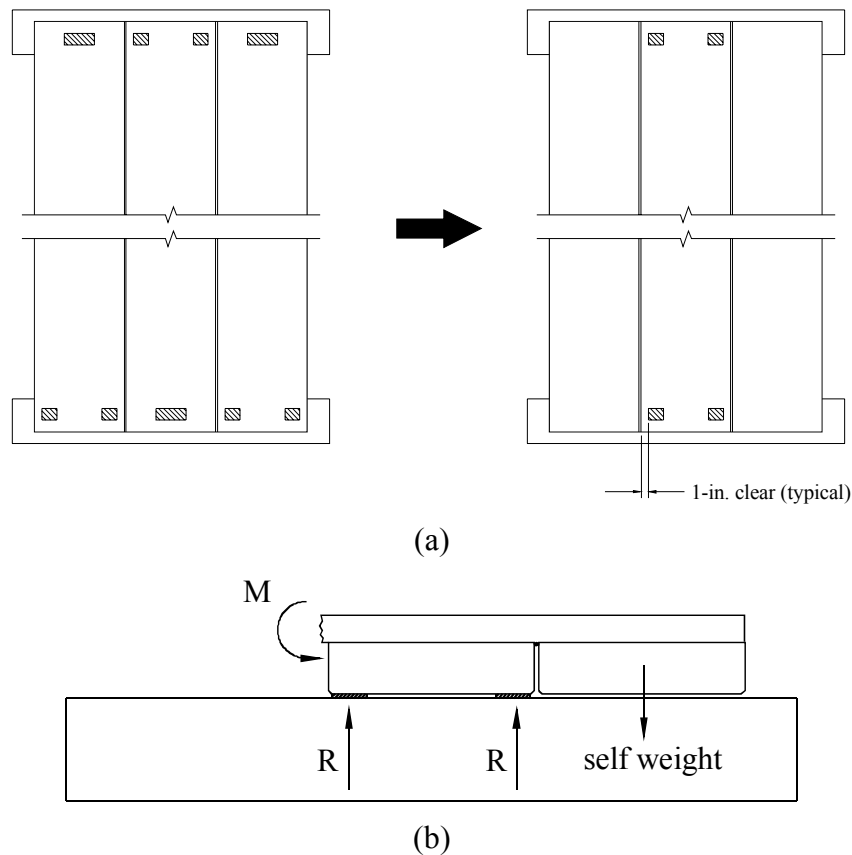


Figure 40. Adjusted bearing pad location and resulting flexural stresses. (a) repositioning of pads under interior specimen (b) free-body diagram of cross-section showing moment at joint caused by pad relocation.

One explanation for the lack of cracking is the variation in topping thickness at the joint. Prior to topping placement a backer rod was placed in the joint to prevent concrete from escaping. In some cases this backer rod slipped, causing a variation in topping thickness along the joint. Tensile stresses from the cantilever are a function of the topping thickness at the joint. If the topping is thicker then the tensile stresses are reduced.

Measurements of the topping thickness were taken every 1-ft. along the length of the joint (Appendix G). The average thicknesses along with the coefficient of variation (COV) are shown in Figure 41

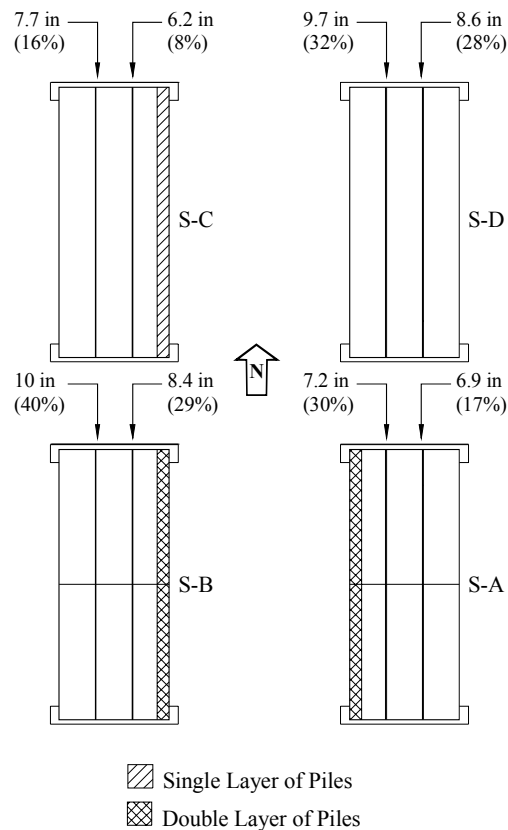


Figure 41. Average and COV of measured topping thickness at joint. Position and number of piles to add load.

Additional load was necessary to induce cracking in the remaining specimens. Figure 42 shows the 20-in. square concrete pile sections that were used to add load. The sections were cut from precast prestressed bridge piles to a length of approximately 48-in. that ranged in weight from 1600 lbs to 1700 lbs. As shown in the figure, the piles were stacked along one edge of the specimen to increase the transverse flexural tensile stresses in the topping over one of the joints while leaving the flexural stresses from the self weight in the opposite joint.

Figure 41 shows the location where they were placed in two stacks along the east edge of S-A and S-B, while a single layer was placed along the east edge of S-C (see). No piles were placed on the control slab. The piles were placed at the outer edge of the slab to induce the highest negative moment at the topping.

Cracks were located visually and widths were measured using a portable microscope at predetermined locations along the length of the joint. Measurements were taken at varying intervals (from two to twelve days) over a period of approximately four months. The piles were placed on the slabs on May 13, 2005.

Figure 43 shows the locations of each measurement point. Eight locations were monitored for each additive with four locations equally spaced along each joint. The W and E designation indicate west and east joints, respectively.

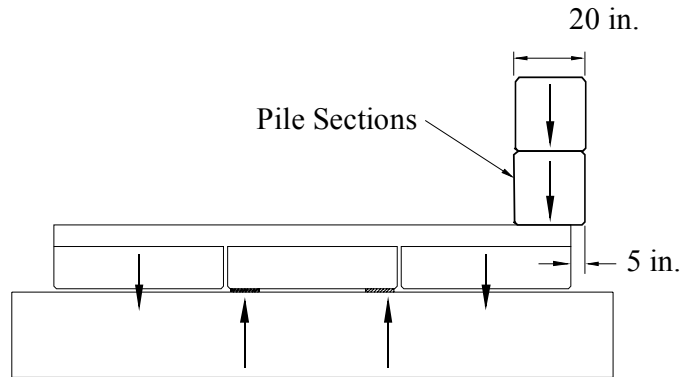


Figure 42. Pile sections stacked on slab S-B in the foreground and S-C in the background.

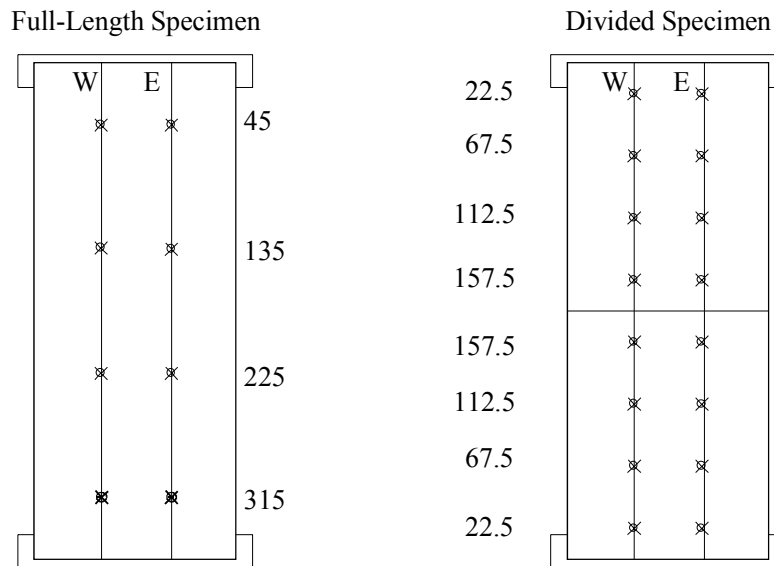


Figure 43. Location of Crack Measurements

6 RESULTS AND DISCUSSION

6.1 COMPRESSIVE STRENGTH AND MODULUS OF ELASTICITY

Cylinder tests were conducted at 3, 28, and 56 days for compressive strength and at 28 and 56 days for modulus of elasticity in accordance with ASTM C39 and ASTM C469, respectively. Results are based on an average of three tests.

Table 30 shows the results of the compressive strength for each of the toppings. The CTL topping had a 28-day compressive strength of 6156 psi, well above the 4500 psi design strength. The STL topping had the highest compressive strength of all the toppings due to the presence of steel fibers and an over-dosage of cement (Table 23). However, steel fibers in the BND mixture did not correlate with an increase in strength. The lower overall strength of the SYN topping may be attributed to an under-dosage of fly ash and cement in the mixture (Table 16). Low w/c ratios did not indicate a higher strength concrete.

Table 30. Compressive strength of concrete cylinders

Topping	3-Day (psi)	28-Day (psi)	56-Day (psi)	w/c ratio
SYN	3610	5760	6380	0.38
BND	2770	6000	6570	0.44
GRD	3130	6500	7070	0.40
STL	4020	7120	8140	0.44
SRA	3130	6290	6490	0.39
CTL	2920	6160	7060	0.43

The modulus of elasticity results are shown in Table 31. Different testing equipment was used to conduct 28 and 56-day modulus and may account for the slight decrease in modulus within some of the toppings. Results indicate that the treatments had a minimal effect on the modulus of elasticity.

Table 31. Modulus of elasticity of concrete cylinders

Topping	28-Day Modulus (ksi)	56-Day Modulus (ksi)
SYN	4220	4260
BND	4330	4210
GRD	4330	4370
STL	4700	4400
SRA	4640	4260
CTL	4440	4200

6.2 PRESSURE TENSION TEST

The concrete tensile strength was measured using the pressure tension test. Results were based on an average of three tests and are shown in Table 32 and Figure 44. Unexpectedly, the tensile strengths of the specimens were found to decrease over time. The decrease was attributed

to the variability inherent in the test system because it was difficult to maintain the same load rate for each specimen, and throughout a test. The load rates were analyzed and their coefficients of variation (COV) are presented in Figure 45. As more tests were conducted, the COV of the load rates decreased. The COV within each test, made up of three specimens, was calculated and found not to be largely affected by the variability in the load rate (Figure 46). Based on the results of the 56 day test, the treatments had a minimal effect on the tensile strength of the concrete.

Table 32. Tensile strength of concrete cylinders using pressure tension test

Topping	3-Day (psi)	7-Day (psi)	28-Day (psi)	56-Day (psi)
SYN	656	659	839	667
BND	744	738	526	604
GRD	705	702	570	649
STL	752	613	607	691
SRA	806	794	563	655
CTL	657	728	638	658

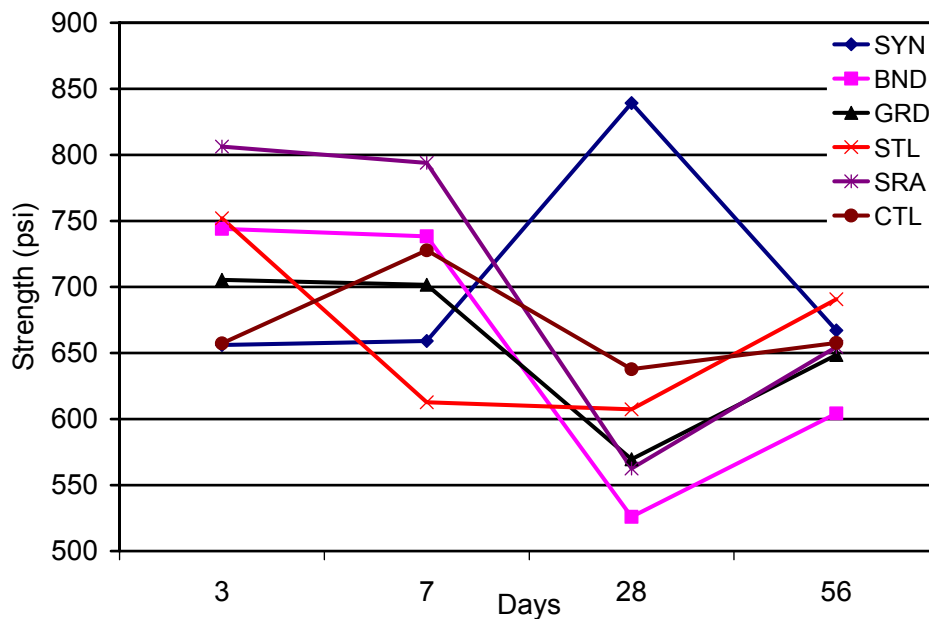


Figure 44. Tensile strength using pressure tension test

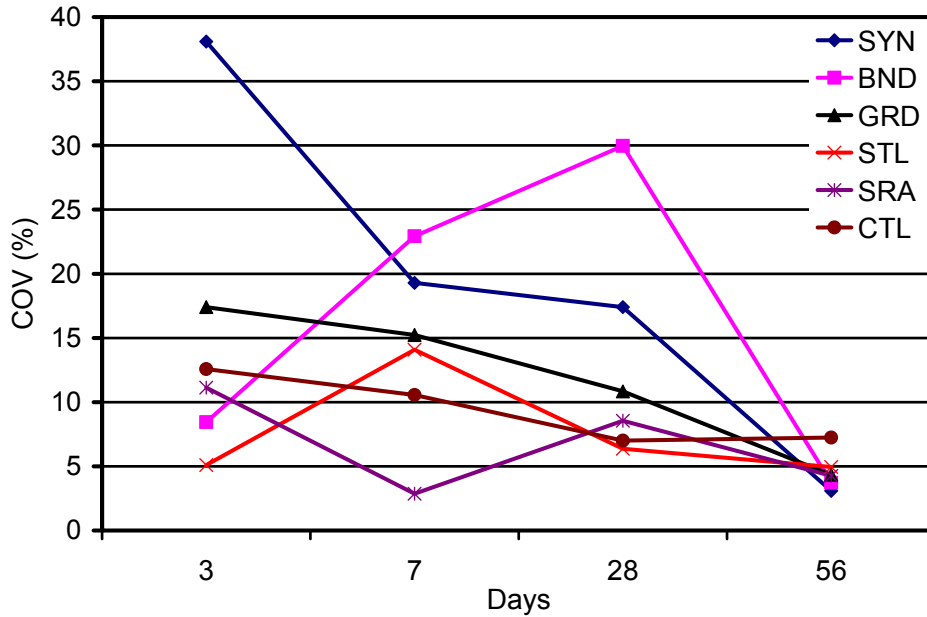


Figure 45. Coefficient of variation for load rate using pressure tension test

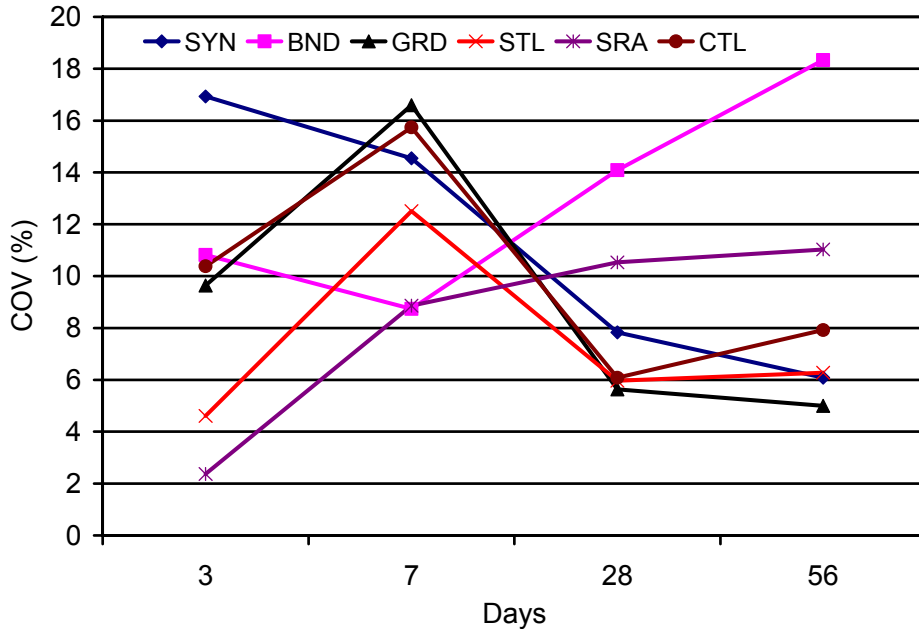


Figure 46. Coefficient of variation for tensile strength using pressure tension test

6.3 RESTRAINED RING TEST

Cracks were first observed on the SYN, BND, GRD, and STL rings approximately 60 days after casting. Though microcracks may have been present, cracks became visible after the humidity levels remained below 70% for an eight day period (Figure 47). The BND and GRD rings had two cracks, one across from the other, while the SYN and STL rings had one. No cracks were observed on the concrete toppings. Approximately 40 days later, cracks were observed on the SRA and CTL rings, after the humidity level went below 70%. Again, no cracks

were observed on the toppings. The variability in the humidity and temperature at the site contributed to the long time to cracking of the rings when compared to research that shows cracking at much earlier ages when the rings are kept in a controlled environment (Grzybowski and Shah 1990; Shah, Karaguler, Sarigaphuti 1992).

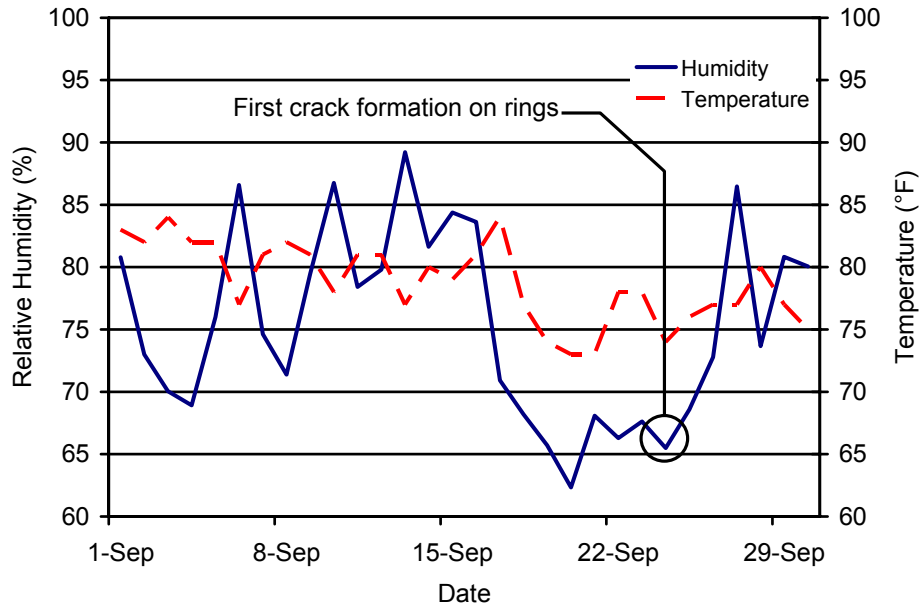


Figure 47. Humidity and temperature for Sept. 2004

Average crack widths are presented in Table 33 and Table 34. Crack widths on the STL ring were smaller than the other rings and consistent with previous research (Grzybowski and Shah 1990). Their research showed decreasing average crack widths with increasing fiber volume. This was confirmed in comparing the performance of the STL and BND rings. Ignoring the presence of synthetic micro fibers in the BND ring, the STL ring, with the higher fiber volume, performed better in reducing crack width.

Table 33. Average crack width for GRD, SRA, and CTL rings

Approx. Days After Casting	GRD (in.)		SRA (in.)		CTL (in.)
	No. 1	No. 2	No. 1	No. 2	No. 1
57	0.004	0.003	NA	NA	NA
64	0.004	0.003	NA	NA	NA
83	0.004	0.003	NA	NA	NA
99	0.004	0.004	0.002	0.002	0.008
113	0.008	0.005	0.002	0.002	0.008
127	0.008	0.005	0.002	0.002	0.008
141	0.01	0.006	0.002	0.002	0.028
160	0.01	0.006	0.002	0.002	0.028
169	0.01	0.006	0.002	0.002	0.028

Table 34. Average crack width for SYN, BND, and STL rings

Approx. Days After Casting	SYN(in.)	BND (in.)		STL (in.)	
	No. 1	No. 1	No. 2	No. 1	No. 2
57	0.004	0.001	0.001	0.001	NA
64	0.004	0.001	0.001	0.001	NA
83	0.005	0.002	0.001	0.001	NA
99	0.006	0.004	0.002	0.001	0.001
113	0.006	0.004	0.002	0.001	0.001
127	0.006	0.004	0.002	0.001	0.001
141	0.007	0.004	0.002	0.001	0.001
160	0.007	0.005	0.002	0.001	0.001
169	0.007	0.005	0.002	0.001	0.001

Crack widths on the SRA ring were significantly smaller than those on the untreated mixtures. The rings with the two unmodified mixtures, CTL and GRD, had the widest cracks of all the rings. The GRD ring unexpectedly developed a second crack opposite of the first one possibly due to restraint at the concrete/steel interface. As previously stated, the results of the GRD ring do not take into account the effectiveness of the carbon-fiber grid.

6.4 THERMOCOUPLE DATA

Temperature data measured through each topping's depth at the time of casting is presented in Appendix F. While most of the toppings had a temperature difference of approximately 5°F, a 13.2°F temperature gradient was measured approximately five hours after casting in the SRA topping (Figure 48) at location 3. This may promote the formation of internal micro cracks in hot weather concreting.

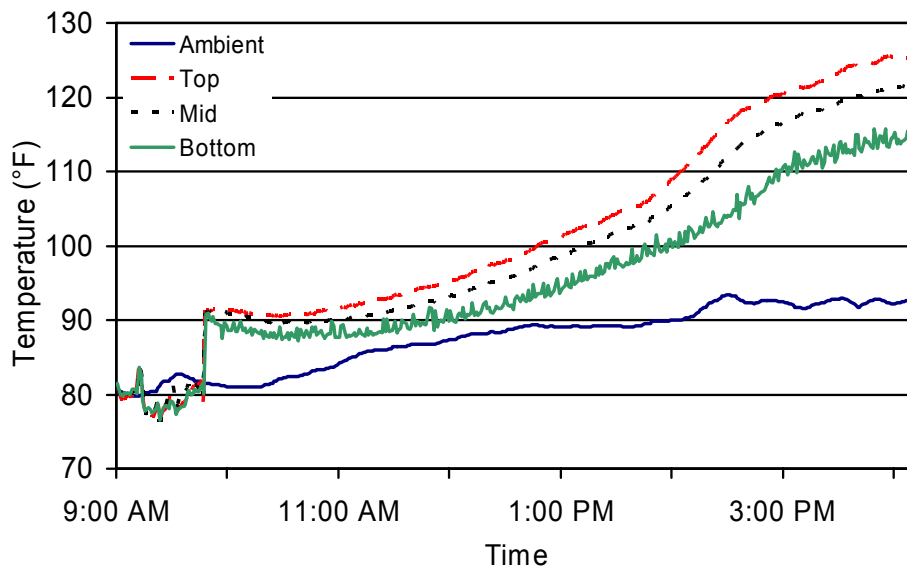


Figure 48. Temperature data through depth of topping for SRA-3

6.5 TOPPING OBSERVATIONS

After 30 weeks of observation, no cracks in the topping, over the flat slab joints, were visible. Several factors inherent in the design and construction may have prevented the formation of cracks.

The FDOT’s Standard Specification for Road and Bridge Construction (2004a) was strictly adhered to. All of the concrete mixtures were at or below the maximum 0.44 w/c ratio and were within tolerances allowed for air content and slump. Reinforcement in the toppings was also installed with 2 in. of cover as outlined in the FDOT’s Structures Manual (2004b). These factors provided a bridge deck that was in compliance with current FDOT standards.

Use of a curing compound may have aided in the prevention of cracks. An FDOT approved compound was sprayed on the topping after the bleed water, if any, had evaporated. It sealed the surface and prevented water from evaporating out of the topping in the first few weeks after casting which is when the majority of drying shrinkage occurs.

Finally, the restraint of the specimens may not have matched the restraint provided on existing flat slab bridges. For cracks to develop, the system must be restrained to induce internal tensile stresses in the concrete as it tries to shrink. The bearing pads may not have provided adequate restraint for the bridge deck. The neoprene pads were 1½ in. thick whereas those used on the Cow Creek Bridge measured 1 in. thick. The pads may have undergone a shear deformation to accommodate the shrinking topping. The displacements would be too small measure with the gages. They also showed no signs of lifting or curling at the corners (Figure 49-Figure 52). The readings provide clues that show the system either acted in an unrestrained manner or insufficient strain was generated in the topping. Furthermore, measurements show that the superstructures with continuous toppings along the span, S-C and S-D, had a negative displacement while the discontinuous toppings did not.

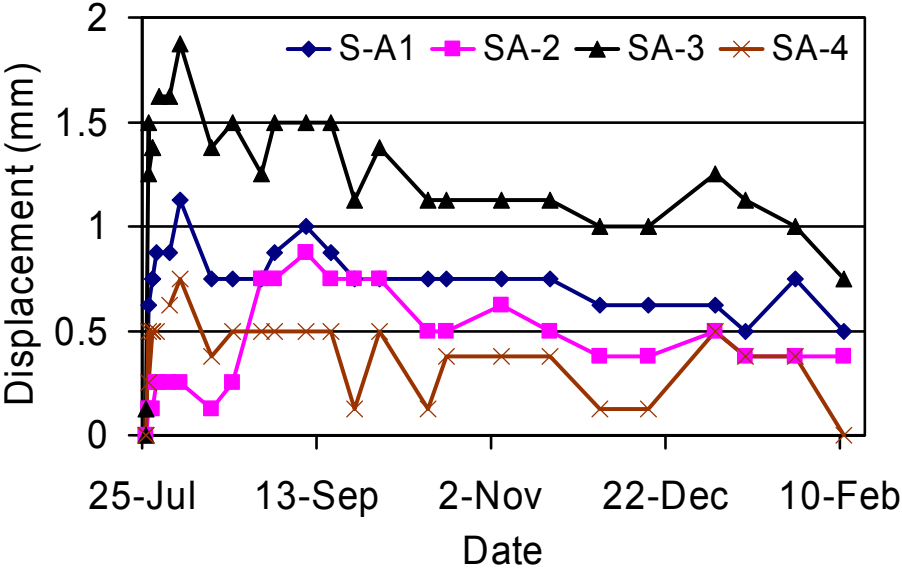


Figure 49. Displacement of superstructure S-A

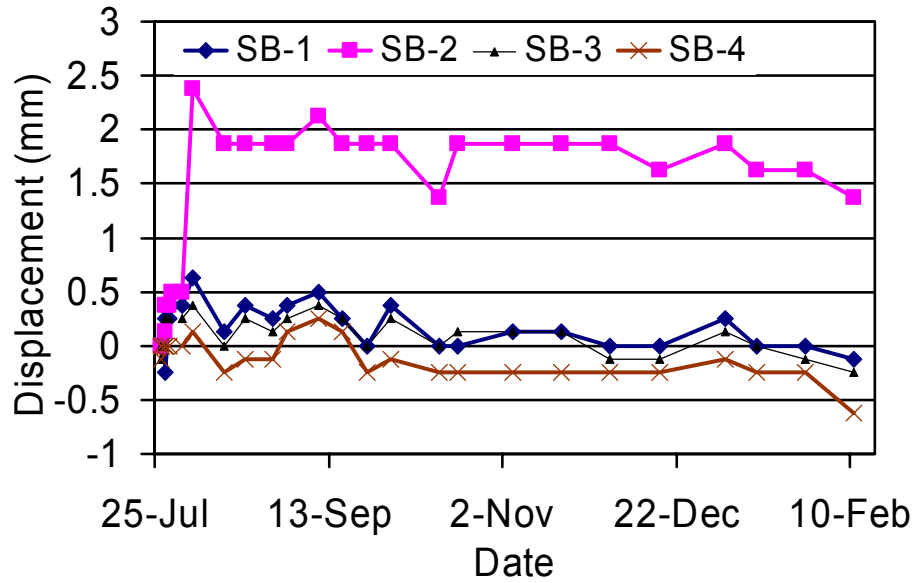


Figure 50. Displacement of superstructure S-B. Gage SB-2 was bumped on August 5, 2004

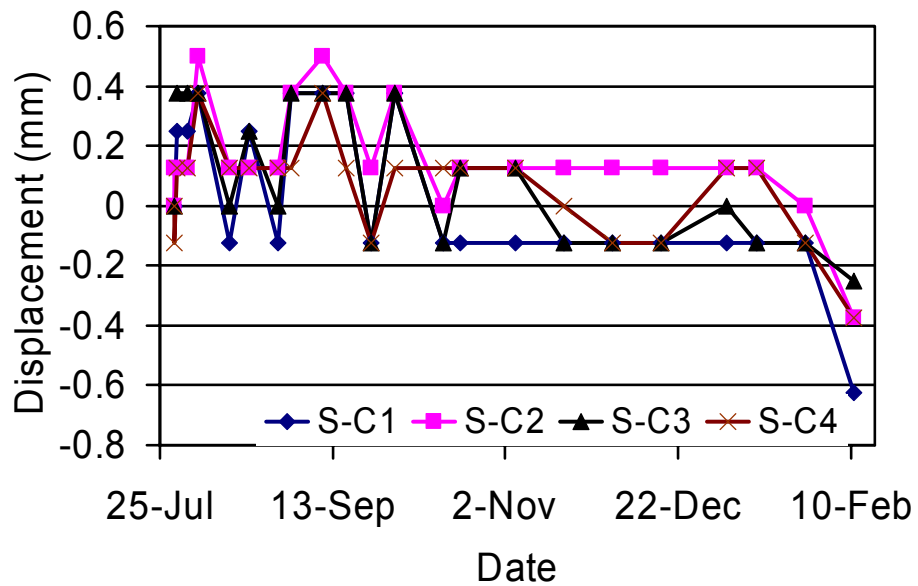


Figure 51. Displacement of superstructure S-C

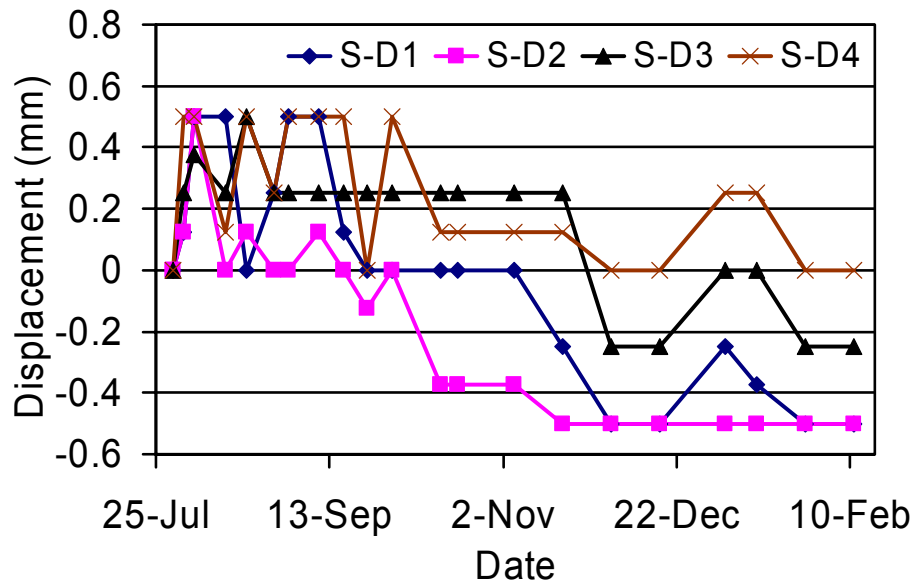


Figure 52. Displacement of superstructure S-D

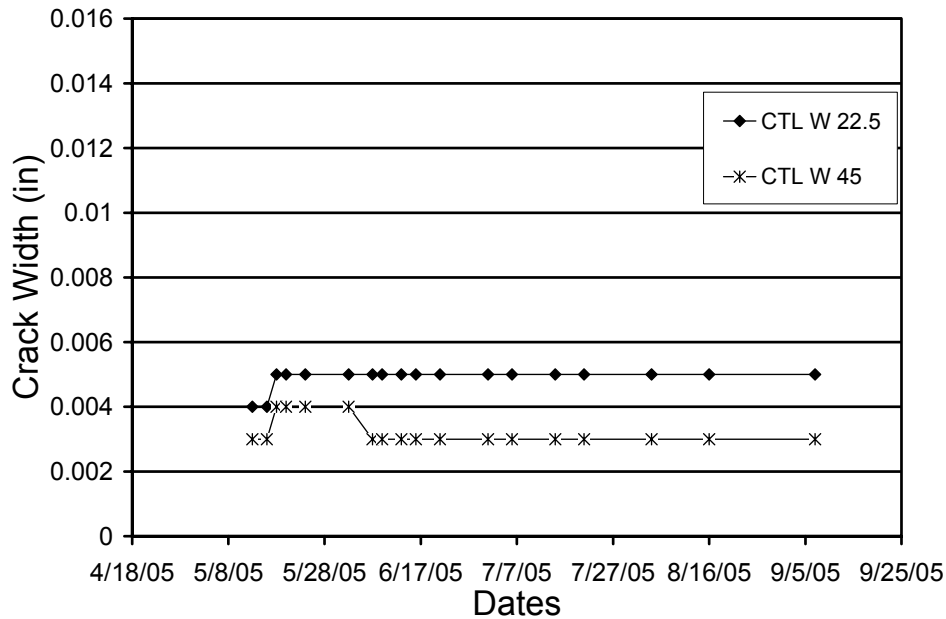
6.6 LOAD TESTS

Because of the lack of reflective cracking, load tests were conducted on the slabs to compare the performance of the additives. This comparison relates the performance when considering strains induced by external loading. The load tests consisted of rearranging the bearing pads and stacking dead weight on the slab to induce flexural stresses in the topping.

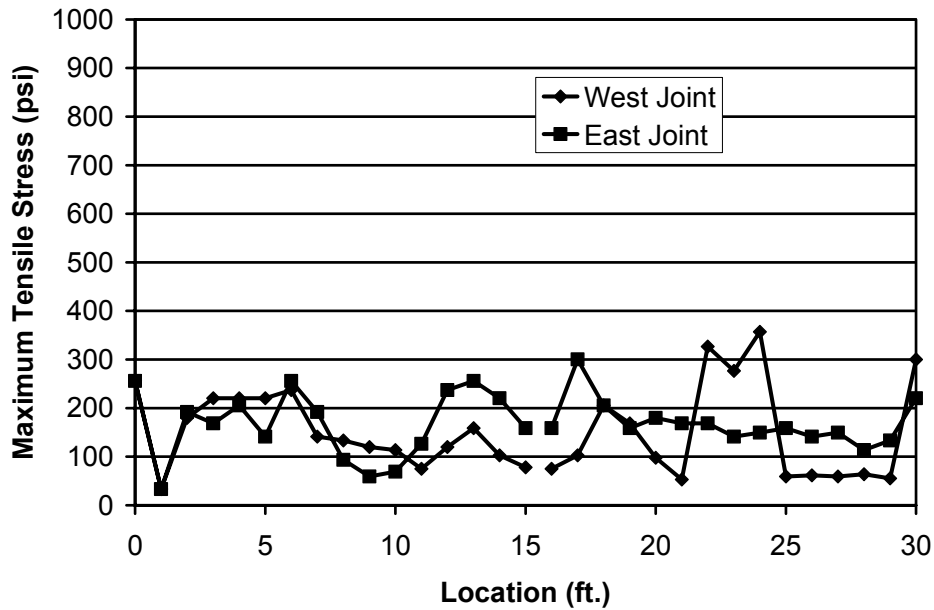
Figure 53a shows the results from the control specimen with cracks appearing at only two locations along the west joint (see Figure 43 for measurement locations). Crack widths initially grew to and stabilized at approximately 0.005 in. during the monitoring period. No growth of the cracks over time was noted. According to ACI 224R-01 (2001) crack widths above 0.006-0.012 in. widths are likely to be bothersome to the general public.

Figure 53b shows the calculated stresses in the extreme tension fiber of the topping based on the gross section properties at the joint, which varied due to the irregular depth of the concrete at the joint. The load used to calculate the stresses was based on the volume of concrete and an assumed unit weight of 150 pounds per cubic foot. Lack of crack growth is unsurprising given the low level of flexural stress caused by the self weight. In general, the calculated tensile stresses were below 300 psi. The calculated tensile strength for 6000 psi is approximately 580 psi (assuming $7.5\sqrt{f'_c}$). Pressure tension test results for cylinders made with the topping concrete were presented earlier. Even considering the variability of the pressure tension test, the results indicate that the tensile strength of the concrete had not been reached.

The control specimen has one of the largest average joint thicknesses with the exception of one in BND and STL specimen. This indicates that the additives were better able to control the cracking under self weight than the control. This will be discussed further in the following section.



(a)

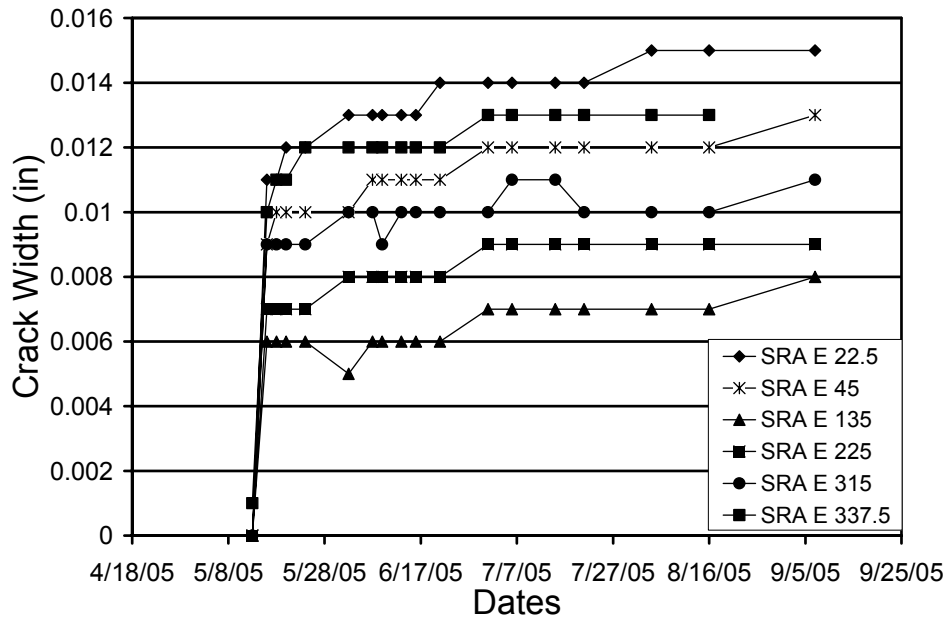


(b)

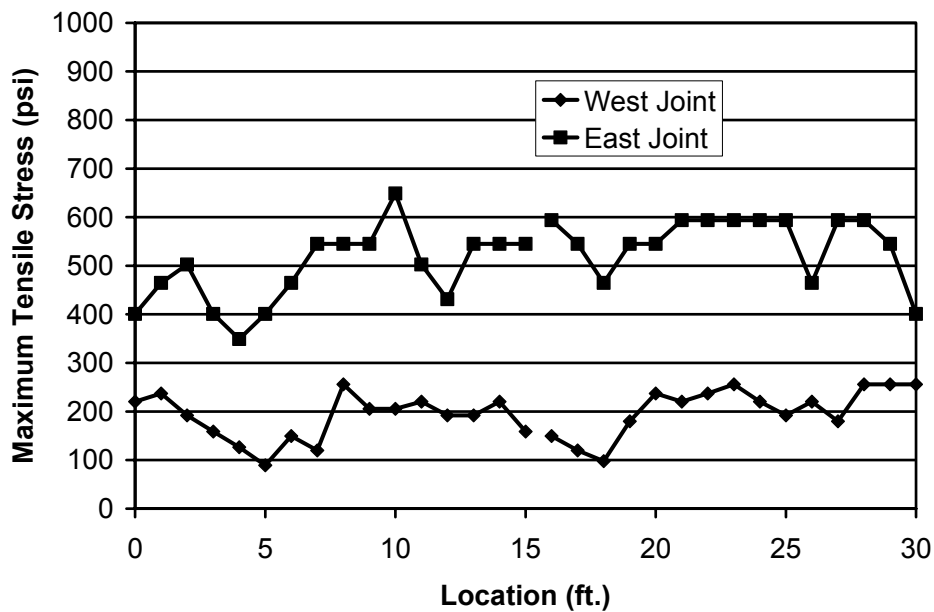
Figure 53. Specimen CTL (a) crack growth with time and (b) calculated transverse flexural tensile stresses.

Cracks formed in the east joint of specimen SRA after a single layer of concrete piles were placed on the outer edge of the slab. Figure 54 shows that the crack widths ranged in size from 0.006 to 0.012 in. and had developed at each measurement location. The crack width growth followed a similar trend at each location. The onset of cracking occurred on May 16, 2005, with the widths increasing in size over the first month, but then stabilizing for the

remainder of the monitoring period. Calculated flexural tensile stresses are shown in Figure 54b. Stresses in the east joint were in the range of 500-600 psi, which is comparable to the predicted tensile strength of the topping concretes.



(a)

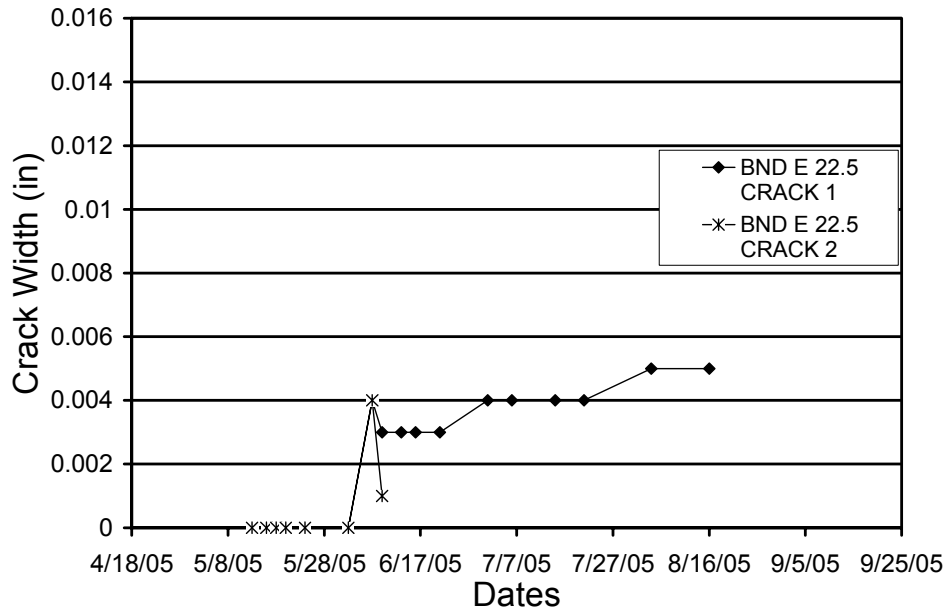


(b)

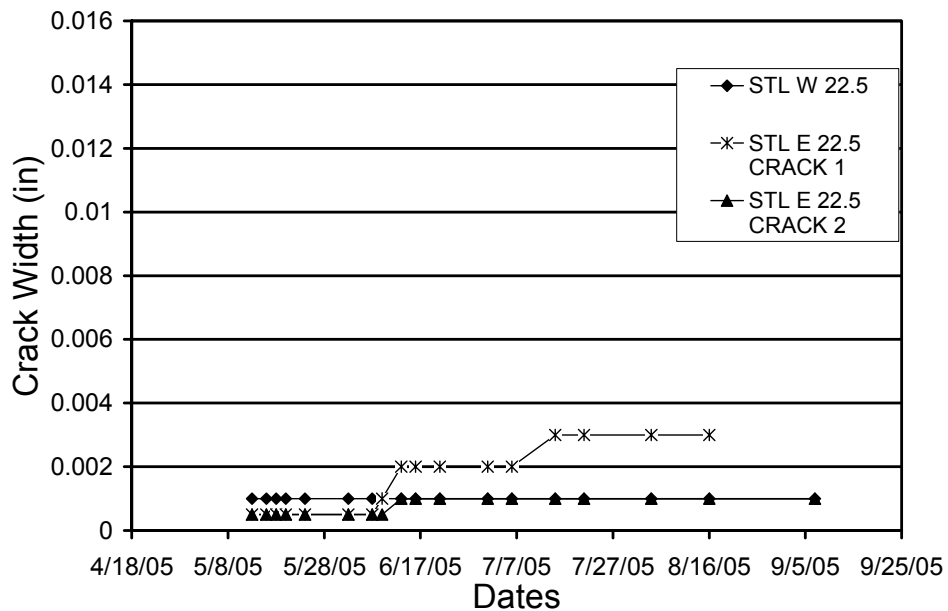
Figure 54. Specimen SRA (a) crack growth with time and (b) calculated transverse flexural tensile stresses.

Two layers of piles were needed to form cracks in specimen BND and STL. Figure 55a shows that two cracks formed at a single measurement location in the BND portion of the

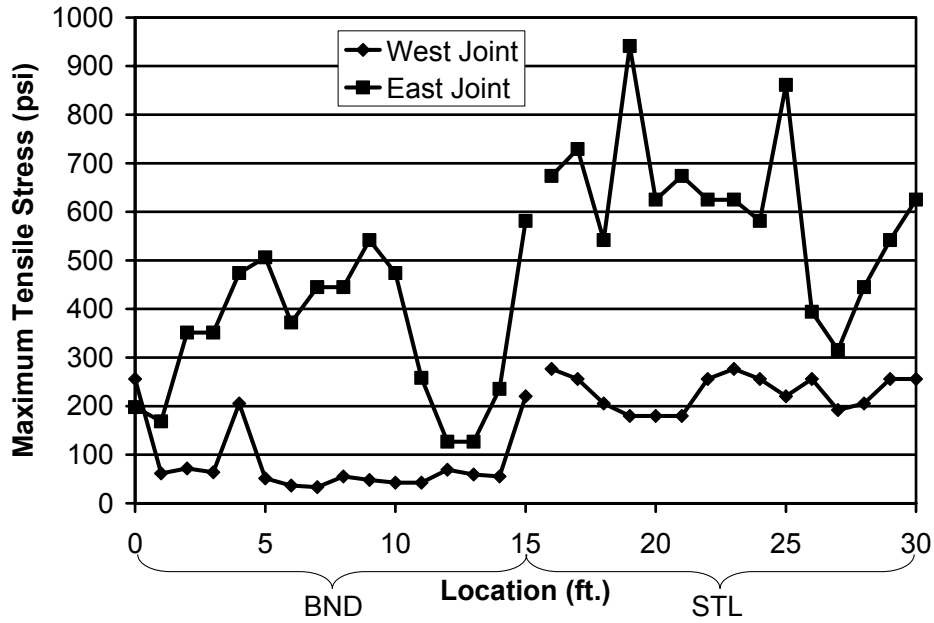
specimen. Maximum crack widths for BND were small at no more than 0.005 in. Figure 55c shows that the calculated stresses for BND were in the range of 400-500 psi. STL performed better yet than that of the BND with two cracks forming at a single location, but with widths no more than 0.003 in. Calculated stresses, however, were much higher (600-700 psi) than that of the BND due to the reduced thickness of the topping.



(a)



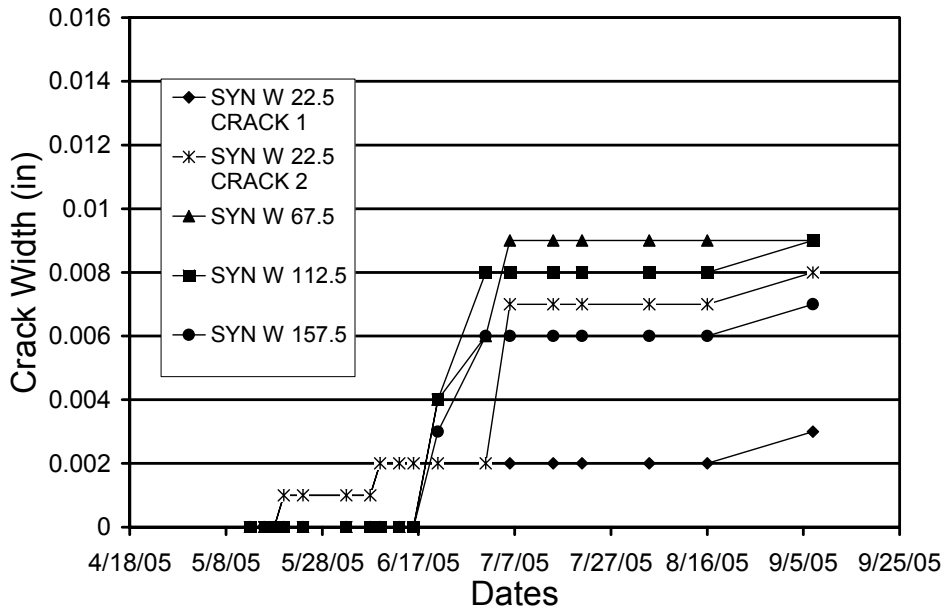
(b)



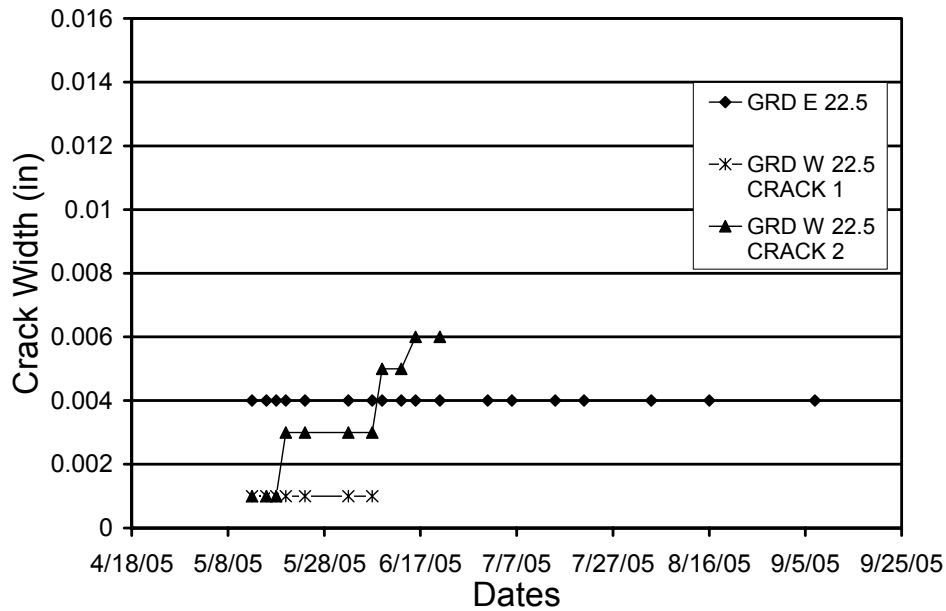
(c)

Figure 55. Crack width growth for slab S-B including (a) BND and (b) STL. (c) shows maximum calculated tensile stresses at precast joints.

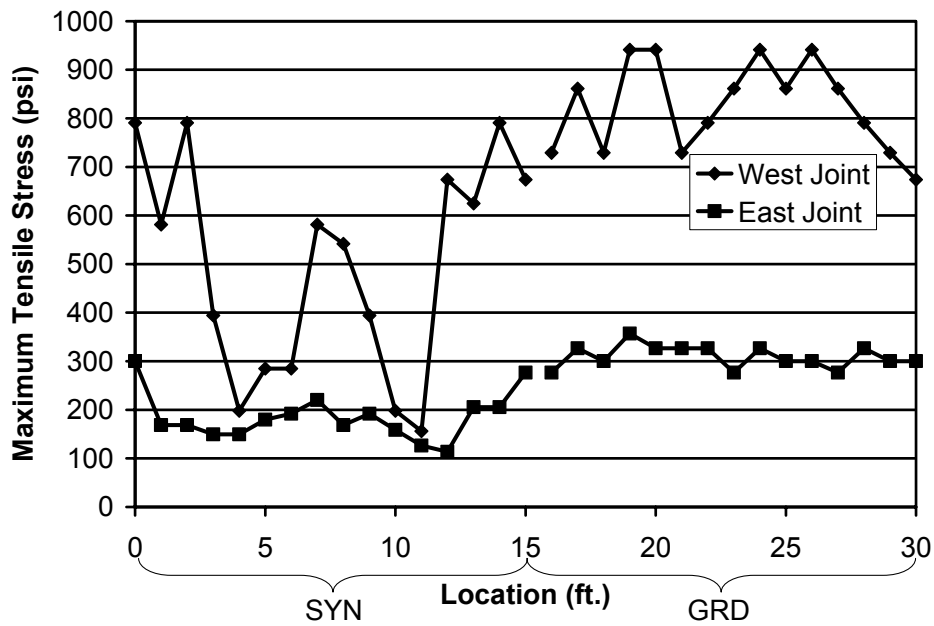
Two layers of piles were also needed to form cracks in specimen SYN and GRD. Figure 56a shows that 0.006 to 0.009-in. wide cracks formed in the west joint of SYN while Figure 56b shows that 0.004 to 0.006-in. wide cracks formed in the west joint of GRD. Crack growth was similar to the other slabs with rapid initial growth followed by stabilization. Comparing the calculated stresses (Figure 56c), however, indicates that the stresses were in the 700 to 900 psi range for the GRD compared to the SYN, which varied widely between 200 and 700 psi.



(a)



(b)



(c)

Figure 56. Crack width growth for slab S-A including (a) SYN and (b) GRD. (c) shows maximum calculated tensile stresses at precast joints.

One of the purposes of this research was to determine the most effective methods to reduce reflective cracking that occurs in the topping at precast joints of bridge decks. This cracking is usually caused by restrained drying shrinkage of the cast-in-place topping. None of the specimens (including the control) cracked during the monitoring period, indicating that

additional means above good concrete placement and curing practice were not necessary for the specimen configuration tested in this research.

Table 35 shows the average crack widths for each of the specimens as generated by relocating the pads and adding load. Also shown are the average flexural tensile stresses (on the uncracked section) at the surface of the bridge deck. To compare the systems, the crack width is divided by the average stress using units of ksi for convenience. Furthermore, the specimens are ranked according to the width/stress ratio. It is apparent and unsurprising that the steel fibers provided the most effective control of crack width under load with a value of 0.003 in/ksi, which is nearly an order of magnitude less than that of the control. The CFRP grid, synthetic fibers, and blended fibers are all comparable with values between 0.012 and 0.014 in/ksi, which are nearly half of that of the control specimen. While these methods do control crack widths over that of concrete with no fibers, they are not as effective as the all steel fiber approach when external load is applied. The CFRP grid was placed with approximately 1-in. of clear cover. The grid performance might be improved by reducing the clear cover to say 1/2-in.

The shrinkage compensating admixture provides no real benefit in the load test over that of the control specimen. The load tests, however, were conducted to determine what effect flexural tensile stresses might have on the additives to determine their ability to resist restrained drying shrinkage strains. While this type of test is probably reasonable when comparing the fiber-reinforced toppings, it does not reflect the ability of the shrinkage reducing admixture to reduce the effects of drying shrinkage. The fibers resist the shrinkage strains through mechanical means, while the shrinkage reducing admixtures provide a limited expansion that will offset the drying shrinkage.

Finally, the table contains the crack widths from the restrained ring crack test in which the crack widths were measured during the full slab monitoring period. It is interesting to note that the steel fiber holds the smallest crack size at 0.002-in., but that the shrinkage compensating admixture is close behind at 0.004-in, which are nearly an order of magnitude better than the control specimen. This confirms that the SRA is likely effective for situations requiring performance under restrained shrinkage but not under load. Otherwise, the trends of the restrained ring test results are comparable with those of the load test with the exception of the CFRP grid specimen. The grid was not added to the restrained ring specimen so the results are on the order of the control specimen.

Table 35. Comparison of average crack widths and calculated stresses in the toppings due to self-weight and superimposed loads.

Specimen	Joint	Average Crack Width (in.)	Average Stress (psi)	Ratio (in/ksi)	Restrained Ring Crack widths (in.)
STL	E	0.002	613	0.003	0.002
GRD	W	0.009	772	0.012	0.016*
SYN	W	0.007	497	0.014	0.007
BND	E	0.005	353	0.014	0.007
SRA	E	0.012	519	0.023	0.004
CTL	W	0.004	166	0.024	0.028
*CFRP grid was not embedded in the concrete used in the restrained ring test.					

7 SUMMARY AND CONCLUSIONS

FDOT has experienced problems with reflective cracking in the topping of some precast flat slab bridges. The cracking usually occurs over the joint between the precast panels on which the topping is placed, hence the term reflective cracking. This research project evaluated techniques for improving crack control in these toppings. Selection was focused on their effectiveness, ease of implementation and application, and effect on the labor and construction cost of the bridge. Commercially available treatments for crack control were reviewed and several were selected for further testing including steel fibers, synthetic fibers, steel/synthetic fiber blend, carbon fiber reinforced composite (CFRP) grid, and shrinkage reducing admixture.

Four full-scale bridge superstructures were constructed to evaluate the crack control treatments. Each superstructure was composed of three 4-ft. x 30-ft precast flat slabs with a 6 in. concrete topping. The precast slabs were constructed off-site by a prestressed concrete manufacturer. The treatments were each incorporated into a standard FDOT approved concrete mixture and cast on-site by FDOT Structures Laboratory staff. Cylinder tests were conducted for compressive and tensile strength, and modulus of elasticity. The cracking performance of the treatments was evaluated using a restrained ring test. The toppings were visually monitored for 30 weeks for crack formation. Plastic shrinkage cracks were visible in the control topping as well as the toppings with the shrinkage reducing admixture (SRA) and CFRP grid (GRD). No further cracking, however, formed during the monitoring period.

In addition to the restrained ring test, and to provide a relative measure of the treatments under transverse tensile stress, load tests were performed on each of the specimens. The bearing pads were relocated so that the self-weight of the specimens caused flexural tensile stresses to form in the topping over the precast joints. Additional weight was needed to generate cracking in some of the specimens.

Based on observations during construction, the results of the materials tests, and the performance of the toppings, the following is concluded:

- Insufficient tensile stresses from drying shrinkage were generated in the toppings to induce cracking. One possible explanation is that the placement and curing were conducted in relatively ideal conditions which contributed to the lower shrinkage strains. Another is that the slabs were constructed in the very humid summer months in which ambient humidity was at 80% or above, providing improved curing conditions over that which might occur in the dryer winter months. This was supported by the fact that the restrained ring specimens did not crack until after the relative humidity dropped below 70 percent. Yet another is that these specimens were not as wide as is generally seen in the bridges where reflective cracking has been observed. It is suspected that a wider cross-section would lead to more lateral restraint in the center of the cross-section.
- Modulus of elasticity and tensile strength were unaffected by the crack control treatments used in this research.
- In both the restrained ring and load test the all steel fiber (STL) topping provided nearly an order of magnitude reduction in crack widths.
- The CFRP grid (GRD) topping reduced the crack widths in the load test by a factor of two.

- In the restrained ring test the blended fiber (BND) and all synthetic fiber (SYN) toppings reduced crack widths by a factor of four. In the load test, BND and SYN toppings reduced the crack widths by a factor of two.
- The topping with shrinkage reducing admixture (SRA) reduced crack widths in the restrained shrinkage test by a factor of seven.

8 Recommendations

As with any concrete construction, proper mixing, transporting, placement, and curing are crucial to a successful finished product. With reasonable care, we have shown that this system (for the width and configuration tested) can be constructed without reflective cracking even when additives are not used. As has been shown, however, added assurance can be attained with the use of additives. While the all steel fiber system (STL) was shown to be the most effective in reducing crack widths under load and in the restrained ring test, it was also rated as the most difficult to place, vibrate, and finish, followed by the all synthetic fibers (SYN) and blended fibers (BND). If the fiber is added directly to an FDOT approved mix, without accounting for the reduction in workability, then the temptation to add water at the job site is heightened by the reduction in workability. When fiber additives are being considered for use in toppings, it is recommended that trial mixes be prepared to ensure that adequate workability will be available without the addition of water. Indeed, fiber-reinforced concrete with fiber volumes such as those used for the steel (STL) and synthetic (SYN) fibers specimens should incorporate a high-range-water reducer to improve workability.

9 REFERENCES

- AASHTO LRFD Bridge Design Specifications, Second Edition (2001 Interim), Customary U.S. Units, American Association of State Highway and Transportation Officials, Washington, D.C., 1998.
- American Concrete Institute Committee 223, “Standard Practice for the Use of Shrinkage-Compensating Concrete,” ACI 223-98, 1998, 28 pp.
- American Concrete Institute Committee 224, “Control of Cracking in Concrete Structures,” ACI 224R-01, ACI Manual of Concrete Practice, 2005, 46 pp.
- American Concrete Institute Committee 544, “State-of-the-Art Report on Fiber Reinforced Concrete,” ACI 544.1R-96, Re-approved 2002, 66 pp.
- Balaguru, P., “Contribution of Fibers to Crack Reduction of Cement Composites.” *ACI Materials Journal*, Vol. 91, No. 3, 1994, pp. 280-288.
- Banthia, N., and Yan, C., “Shrinkage Cracking in Polyolefin Fiber Reinforced Concrete,” *ACI Materials Journal*, Vol. 97, No. 4, 2000, pp. 432-437.
- Cook, R.A., Leinwohl, R.J., “Precast Option for Flat Slab Bridges”, Structures and Materials Research Report No. 97-1, Engineering and Industrial Experiment Station, University of Florida, Gainesville, Florida, August, 1997.
- FDOT Standard Specifications for Road and Bridge Construction, 2004a, State Specifications Office, Florida Department of Transportation, Tallahassee, FL, <http://www.dot.state.fl.us/specificationsoffice/2004BK/toc.htm>, Last accessed Mar. 2005
- FDOT Structures Manual, 2004b, FDOT Structures Design Office, Florida Department of Transportation, Tallahassee, FL http://www.dot.state.fl.us/structures/StructuresManual/2004January/Structures_Manual.htm, Last accessed Mar. 2005.
- Grzybowski, M., and Shah, S. P., “Shrinkage Cracking of Fiber Reinforced Concrete,” *ACI Materials Journal*, Vol. 87, No. 2, 1990, pp. 138-148.
- Issa, M.A., “Investigation of Cracking in Concrete Bridge Decks at Early Ages,” *Journal of Bridge Engineering*, Vol. 4, No. 2, May 1999, pp. 116-124.
- Li, G., “The Effect of Moisture Content on the Tensile Strength Properties of Concrete,” Masters Thesis, Dept. of Civil and Coastal Engineering, University of Florida, 2004.
- Makizumi, T., Sakamoto, Y., and Okada, S., “Control of Cracking by Use of Carbon Fiber Net as Reinforcement for Concrete,” Fiber-Reinforced-Plastic Reinforcement for Concrete Structures — International Symposium, SP-138 (American Concrete Institute 1992), pp. 287-295.

- Nanni, A.; Ludwig, D. A.; and McGillis, T., "Plastic Shrinkage Cracking of Restrained Fiber-Reinforced Concrete," *Transportation Research Record*, No. 1382, 1991, pp. 69-72.
- Nmai, C. K.; Tomita, R.; Hondo, F.; and Buffenbarger, J., "Shrinkage-Reducing Admixtures," *Concrete International*, Vol. 20, No. 4, April 1998, pp. 31-37.
- Pease, B. J., Shah, H. R., Hossain, A. B., and Weiss, W. J., "Restrained Shrinkage Behavior of Mixtures Containing Shrinkage-Reducing Admixtures and Fibers," International Conference on Advances in Concrete Composites and Structures (ICACS), Chennai, India, January 2005,
http://bridge.ecn.purdue.edu/%7Econcrete/weiss/publications/r_conference/RC-032.pdf,
Last accessed Mar. 2005.
- Ramey, G. E., Pittman, D. W., and Webster, G. K., "Shrinkage-Compensating Concrete for Bridge Decks," *Concrete International*, Vol. 24, No. 4, April 1999, pp. 29-34.
- See, H. T., Attiogbe, E. K., and Miltenberger, M. A., "Shrinkage Cracking Characteristics of Concrete Using Ring Specimens," *ACI Materials Journal*, Vol. 100, No. 3, 2003, pp. 239-245.
- Shah, S. P., Karaguler, M. E., and Sarigaphuti, M., "Effects of Shrinkage-Reducing Admixtures on Restrained Shrinkage Cracking of Concrete," *ACI Materials Journal*, Vol. 89, No. 3, 1992, pp. 289-295.
- Shah, S. P., Sarigaphuti, M., and Karaguler, M. E., "Comparison of Shrinkage Cracking Performance of Different Types of Fibers and Wiremesh," *Fiber Reinforced Concrete, Developments and Innovations*, SP-142 (American Concrete Institute 1994), pp. 1-18.
- Soroushian, P., Mirza, F., and Alhozaimy, A., "Plastic Shrinkage Cracking of Polypropylene Fiber Reinforced Concrete," *ACI Materials Journal*, Vol. 92, No. 5, 1993, pp. 553-560.

APPENDIX A – Slab Calculations

Input

LRFD English Prestressed Beam Program Data Input	Project = "Research Design" DesignedBy = "Laz Alfonso" Date = "Dec 12, 2003"
---	---

ExistingDataFile = vec2str(READPRN"PbeamFileName.dat") DataFileToBeCreated := vec2str(READPRN"PbeamFileCreated.dat")

ExistingDataFile = "C:\FDOT_STR\Programs\LRFPbeamE1.85\4 ft original span.dat"

DataFileToBeCreated = "C:\FDOT_STR\Programs\LRFPbeamE1.85\4 ft original span.dat"

Comment = "4 ft wide 12 inch thk 30 ft span"

newComment := "4 ft wide 12 inch thk 30 ft span"

Only change the new values, if current data values are OK, leave the double X (XX) in the newData field.

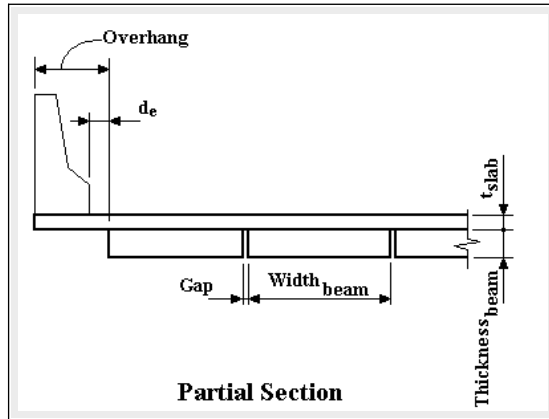
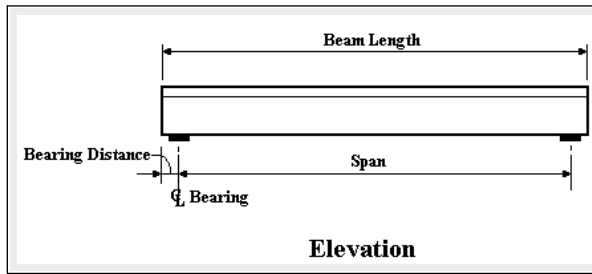
Enter or Change Project Data

newProject := "XX"

newDesignedBy := "XX"

newDate := "XX"

Plan, Elevation, and Cross Section Data





The top of the precast beam is the location of the origin for the coordinate system.

Figure 57. LRFD PSBeam input 1.

Echo of Input

$L_{\text{beam}} = 30\text{ft}$ *see Beam Elevation*
 BearingDistance = 6 in *see Beam Elevation*
 PadWidth = 6 in *width of the bearing pad - used in the shear calculations - see Beam Elevation*
 $\text{Width}_{\text{beam}} = 4\text{ft}$ *see Partial Section*
 $\text{Width}_{\text{adj.beam}} = 4\text{ft}$ *used to calculate the live load distribution to exterior beams. Not used for interior beams*
 Overhang = 0 ft *see Partial Section*
 $t_{\text{slab}} = 6\text{in}$ *see Partial Section, not including integral WS*
 $t_{\text{slab.delta}} = 1\text{in}$ *maximum additional slab thickness over support to accomodate camber, used for additional DL only*
 $d_c = -1.5\text{ft}$ *see Partial Section (3 ft max). (LRFD 4.6.2.2.1) corrected to ASSHTO definition internally*
 BeamPosition = "interior" *This should be either "interior" or "exterior"*
 Thickness_{beam} = 12 in *see Partial Section*
 Gap = 1 in *see Partial Section (LRFD 3.6.1.1.1)*
 $t_{\text{integral.ws}} = 0.5\text{in}$ *wearing surface thickness cast with the deck (SDG 7.2.1)*
 $\text{Weight}_{\text{future.ws}} = 0.015 \frac{\text{kip}}{\text{ft}^2}$ *future wearing surface (SDG Table 3.1)*
 NumberOfBeams = 11 *number of beams in the span cross section (LRFD 4.6.2.2.1)*
 SectionType = "transformed" *transformed = "transformed" gross = "gross"*
 Skew = 0 deg *see Plan View*

Input New Values

newL_{beam} := 30-ft
 newBearingDistance := XX-in
 newPadWidth := XX-in
 newWidth_{beam} := XX-ft
 newWidth_{adj.beam} := XX-ft
 newOverhang := XX-ft
 newt_{slab} := XX-in
 newt_{slab.delta} := XX-in
 newd_c := XX-ft
 newBeamPosition := 
 newThickness_{beam} := XX-in
 newGap := XX-in
 newt_{integral.ws} := XX-in
 newWeight_{future.ws} := XX $\frac{\text{kip}}{\text{ft}^2}$
 newNumberOfBeams := XX
 newSectionType := 
 newSkew := 0-deg

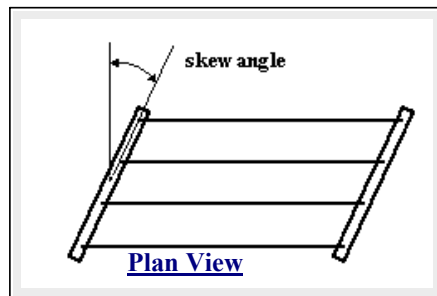


Figure 58. LRFD PSBeam input 2.

Permit Truck Axle Loads and Spacings

PermitAxles = 2 *This is the number of wheel loads that comprise the permit truck, max for dll is 11. A value must be entered for newPermitAxles for changes to newPermitAxleLoad or newPermitAxleSpacing to register*

newPermitAxles := XX

Toggle_{permit.only} = 0 *If this value is 1 only the permit live load is considered otherwise the HL-93 live load is used for stresses and the worst case for Strength checks*

newToggle_{permit.only} :=

Permit_uniform_LL = 0 $\frac{\text{lbf}}{\text{ft}}$ *Uniform live load to be considered in conjunction with the Permit Vehicle (per lane)*

newPermit_uniform_LL := XX $\frac{\text{lbf}}{\text{ft}}$

Indexes used to identify values in the P and d vectors

$$\text{PermitAxleLoad} = \begin{pmatrix} 8 \\ 32 \end{pmatrix} \text{kip}$$

newPermitAxles := if(newPermitAxles = XX, 1, newPermitAxles)
 $q := 0..(\text{newPermitAxles} - 1)$ $qt := 0.. \text{newPermitAxles}$

The PermitAxleSpacing vector contains the spacings between the concentrated loads. The first and last values are place holders and should always be zero

newPermitAxleLoad_q :=

XX·kip
XX·kip
XX·kip
XX·kip
XX·kip
XX·kip
XX·kip
XX·kip
XX·kip

newPermitAxleSpacing_{qt} :=

0·ft
XX·ft
XX·ft
XX·ft
XX·ft
XX·ft
XX·ft
XX·ft
XX·ft
0·ft

$$\text{PermitAxleSpacing} = \begin{pmatrix} 0 \\ 14 \\ 0 \end{pmatrix} \text{ft}$$

Material Properties - Concrete

AggregateType = "Standard" *This should be either "Florida" or "Standard" depending on the type of course aggregate used.*

newAggregateType :=

$f_{c,slab} = 4.5 \text{ksi}$ *strength of slab concrete*

new $f_{c,slab} := XX \text{ksi}$

$f_{c,beam} = 5.5 \text{ksi}$ *strength of beam concrete*

new $f_{c,beam} := 5.5 \text{ksi}$

$f_{ci,beam} = 4.5 \text{ksi}$ *release beam strength*

new $f_{ci,beam} := 4.5 \text{ksi}$

$\gamma_{slab} = 0.15 \frac{\text{kip}}{\text{ft}^3}$ *density of slab concrete, used for load calculations*

new $\gamma_{slab} := XX \frac{\text{kip}}{\text{ft}^3}$

$\gamma_{beam} = 0.15 \frac{\text{kip}}{\text{ft}^3}$ *density of beam concrete, used for load calculations*

new $\gamma_{beam} := XX \frac{\text{kip}}{\text{ft}^3}$

Environment = "moderately" *This should be either "slightly", "moderately" or "extremely"*

newEnvironment :=

Material Properties - Prestressing Tendons

$f_{pu} = 270 \text{ksi}$ *tendon ultimate tensile strength, used for stress calcs*

new $f_{pu} := XX \text{ksi}$

$E_p = 28500 \text{ksi}$ *tendon modulus of elasticity*

new $E_p := XX \text{ksi}$

Figure 59. LRFD PSBeam input 3.

Material Properties - Mild Steel

$f_y = 60 \text{ ksi}$	<i>mild steel yield strength</i>	<code>newfy := XX·ksi</code>
$E_s = 29000 \text{ ksi}$	<i>mild steel modulus of elasticity</i>	<code>newEs := XX·ksi</code>
$H = 75$	<i>% relative humidity (LRFD 5.9.5.4.2)</i>	<code>newH := XX</code>
$t_j = 1.5$	<i>time in days between jacking and transfer (LRFD 5.9.5.4.4b)</i>	<code>newtj := XX</code>
$A_{\text{slab.rebar}} = 0.31 \frac{\text{in}^2}{\text{ft}}$	<i>area of longitudinal slab reinf per unit width of slab, both layers combined</i>	<code>newAslab.rebar := XX·$\frac{\text{in}^2}{\text{ft}}$</code>
$d_{\text{slab.rebar}} = 2.5 \text{ in}$	<i>distance from top of slab to centroid of longitudinal steel</i>	<code>newd_slab.rebar := XX·in</code>
$A_{s,\text{long}} = 1.55 \text{ in}^2$	<i>area of longitudinal mild reinforcing in the flexural tension zone of the beam</i>	<code>newAs_long := 1.55·in²</code>
$d_{\text{long}} = 2 \text{ in}$	<i>absolute distance from top of the beam to the centroid of the longitudinal steel in the flexural tension zone</i>	<code>newd_long := 2·in</code>
$\text{BarSize} = 5$	<i>Size of bars used to create $A_{s,\text{long}}$ needed to calculate development length</i>	<code>newBarSize :=</code> <input type="text" value="XX"/>

Loads

Composite and non-composite dead loads are calculated based on the provided data and FDOT standards. In the main and detailed programs are locations where changes to the non-composite or composite dead loads can be made. These locations are noted as Add_w_{noncomp} and Add_w_{comp} for non-composite and composite loads respectively. Loads can be added by setting these values equal to positive values and subtracted by setting them equal to a negative value. The program will calculate and apply the HL-93 live load automatically. Additional permit loads must be listed in the permit truck section above.

end of data input

Figure 60. LRFD PSBeam input 4.

LRFD PSBeam Output

LRFD English Prestressed Beam Design Program

Project = "Research Design"
 DesignedBy = "Laz Alfonso"
 Date = "Dec 12, 2003"


Legend

Tan = DataEntry

Yellow = CheckValues

Grey = Comments + Graphs

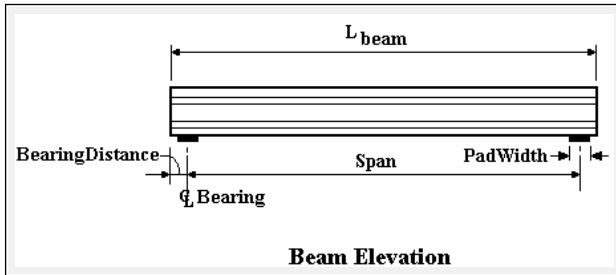
The CR values displayed are Capacity Ratios which give the ratio of the provided capacity divided by the required

Bridge Layout and Dimensions  Reference: C:\FDOT_STR\Programs\LRFDpbeamE1.85\ProgramFiles\section1.mcd(R)

Comment = "4 ft wide 12 inch thk 30 ft span"

filename = "C:\FDOT_STR\Programs\LRFDpbeamE1.85\4 ft original span.dat"

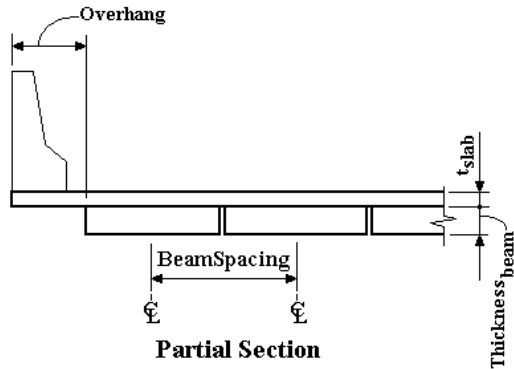
The top of the precast beam is the location of the origin



WRITEPRN"be

DataMessage = "This is a 4 feet wide, 12 inch thick, flat slab section design "

L_{beam} = 30 ft BearingDistance = 6 in Span = 29 ft PadWidth = 6 in



WRITEPRN"coo

Picture_{section}

Overhang = 0 ft BeamSpacing = 4.083 ft t_{slab} = 6 in h_{buildup} = 0 in
 Skew = 0 deg t_{integral ws} = 0.5 in NumberOfBeams = 11 t_{slab.delta} = 1 in

WRITEPRN"loc

BeamTypeTog = "FLT12" *These are typically the FDOT designations found in our standards. The user can also create a coordinate file for a custom shape. In all cases the top of the beam is at the y=0 ordinate.* BeamPosition = "interior" *For calculating distribution factors must be either interior or exterior*

SectionType = "transformed" b_e = 4.083 ft *effective slab width*
LRFD 4.6.2.6

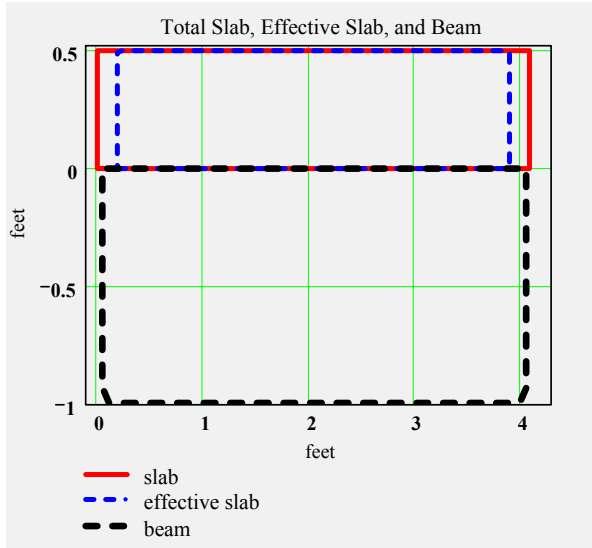
user_g mom = 0

user_g shear = 0

If user_g mom (the moment distribution factor) or user_g shear (the shear distribution factor) is set to zero the program's calculated value will be used. If they are other than zero then this user input value will be used.

Figure 61. LRFD PSBeam output 1.

Section Properties - Beam and Slab



Material Properties - Concrete

<i>Corrosion Classification</i>	Environment = "moderately"	<i>density of slab concrete</i>	$\gamma_{slab} = 0.15 \frac{kip}{ft^3}$
<i>strength of slab concrete</i>	$f_{c,slab} = 4.5$ ksi	<i>density of beam concrete</i>	$\gamma_{beam} = 0.15 \frac{kip}{ft^3}$
<i>strength of beam concrete</i>	$f_{c,beam} = 5.5$ ksi	<i>weight of future wearing surface</i>	$Weight_{future.ws} = 0.015 \frac{kip}{ft^2}$
<i>release beam strength</i>	$f_{ci,beam} = 4.5$ ksi	<i>used in distribution calculation</i>	$n_d = 1.106$
<i>initial conc. modulus of elasticity</i>	$E_{ci} = 3861$ ksi	<i>relative humidity</i>	$H = 75$
<i>concrete modulus of elasticity</i>	$E_c = 4268$ ksi		
<i>type of course aggregate, either "Florida" or "Standard"</i>	AggregateType = "Standard"		

Material Properties - Prestressing Tendons and Mild Steel

<i>tendon ultimate tensile strength</i>	$f_{pu} = 270$ ksi	<i>tendon modulus of elasticity</i>	$E_p = 28500$ ksi
<i>time in days between jacking and transfer</i>	$t_j = 1.5$	<i>ratio of tendon modulus to beam concrete modulus</i>	$n_p = 6.677$
<i>mild steel yield strength</i>	$f_y = 60$ ksi	<i>mild steel modulus of elasticity</i>	$E_s = 29000$ ksi
<i>ratio of rebar modulus to beam concrete modulus</i>	$n_m = 6.794$		
<i>d distance from top of slab to centroid of slab reinf.</i>	$d_{slab.rebar} = 2.5$ in	<i>area per unit width of longitudinal slab reinf.</i>	$A_{slab.rebar} = 0.31 \frac{in^2}{ft}$

Figure 62. LRFD PSBeam output 2.

d distance from top of beam to centroid of mild flexural tension reinf.
Permit Loads

$$d_{\text{long}} = -2 \text{ in}$$

area of mild reinf lumped at centroid of bar locations

$$A_{s,\text{long}} = 1.55 \text{ in}^2$$

Number of wheel loads that comprise the permit truck

$$\text{PermitAxles} = 2$$

$$\text{PermitUniformLoad} = 0 \frac{\text{lbf}}{\text{ft}}$$

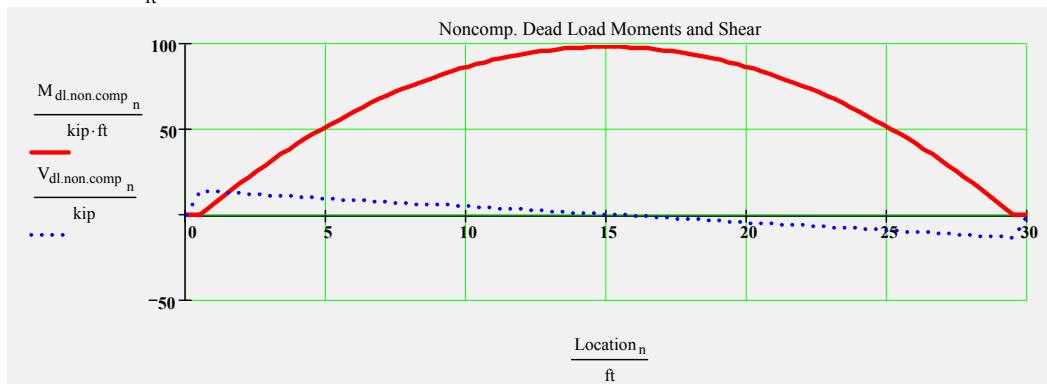
$$\text{PermitAxleLoad}^T = (8 \ 32) \text{ kip}$$

$$\text{PermitAxleSpacing}^T = (0 \ 14 \ 0) \text{ ft}$$

Loads - Release, Non composite, Composite, and Live Load (truck and lane)

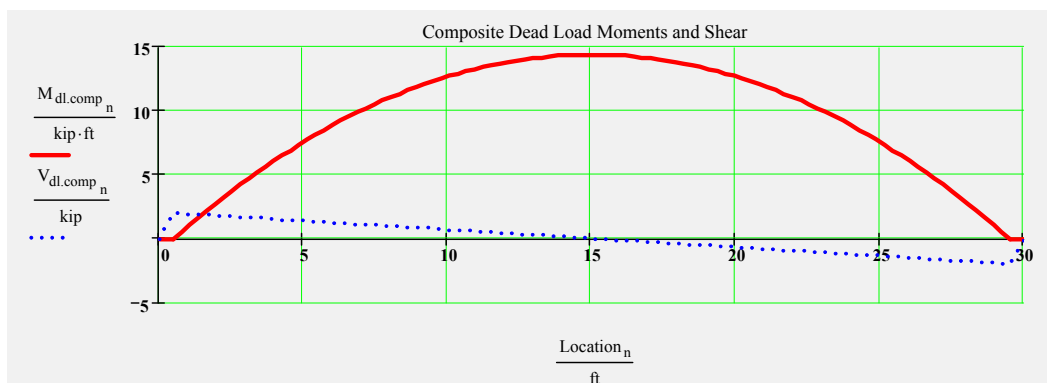


$w_{\text{beam}} = 0.599 \frac{\text{kip}}{\text{ft}}$ $\max(M_{\text{release}}) = 67.4 \text{ kip}\cdot\text{ft}$ *note: at release, span length is the full length of the beam*



$w_{\text{slab}} = 0.332 \frac{\text{kip}}{\text{ft}}$ $w_{\text{beam}} = 0.599 \frac{\text{kip}}{\text{ft}}$ $w_{\text{forms}} = 0 \frac{\text{kip}}{\text{ft}}$ $w_{\text{noncomposite}} = 0.931 \frac{\text{kip}}{\text{ft}}$ $\text{Add}_w \text{ noncomp} = 0 \frac{\text{kip}}{\text{ft}}$
(w_{slab} includes buildup)

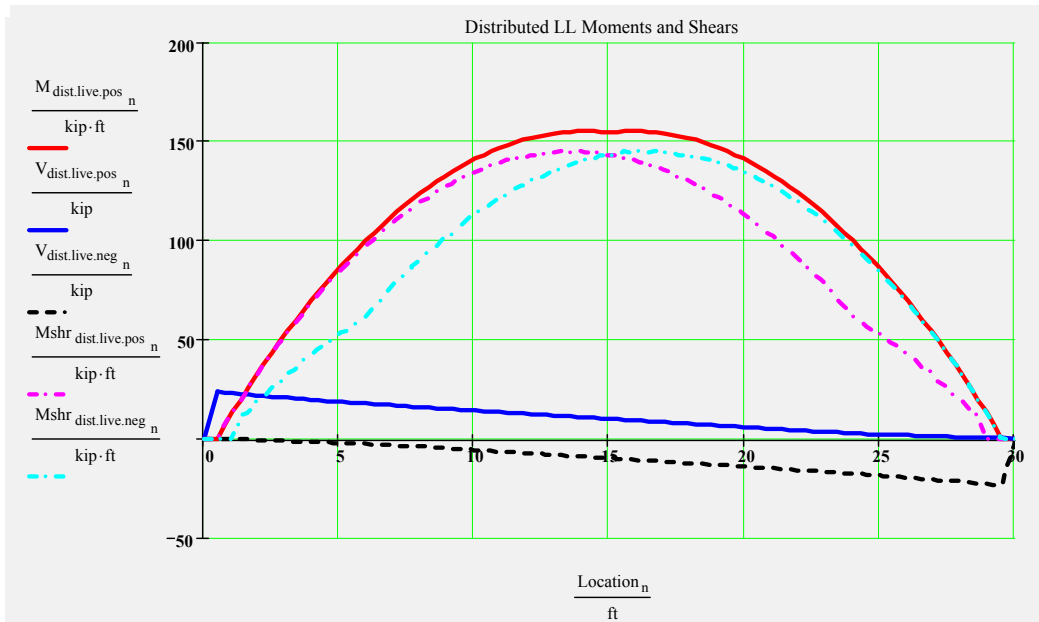
$\max(M_{\text{dl.non.comp}}) = 98.5 \text{ kip}\cdot\text{ft}$ $\max(V_{\text{dl.non.comp}}) = 13.5 \text{ kip}$



$w_{\text{barrier}} = 0.076 \frac{\text{kip}}{\text{ft}}$ $w_{\text{future.ws}} = 0.061 \frac{\text{kip}}{\text{ft}}$ $w_{\text{composite}} = 0.14 \frac{\text{kip}}{\text{ft}}$ $\text{Add}_w \text{ comp} = 0 \frac{\text{kip}}{\text{ft}}$

$\max(M_{\text{dl.comp}}) = 14 \text{ kip}\cdot\text{ft}$ $\max(V_{\text{dl.comp}}) = 2 \text{ kip}$

Figure 63. LRFD PSBeam output 3.



Live load distribution factors BeamPosition = "interior" $g_{shear} = 0.32$ $g_{mom} = 0.32$
 Reaction_{LL} = 24.381 kip (service value includes truck impact) Reaction_{DL} = 16.026 kip (service value)

A suggested method of iteration is to fill the beam with tendons beginning in the middle of the bottom row, filling the row outward, then continuing on to the middle of the next lowest row. Typically, the minimum number of tendon is reached when midspan tensile stress is below the LRFD Service III Limit stress. Next, tendons should be debonded in pairs according to the Structures Design Guidelines until the end compression stress are below the LRFD Service I Limit stress. These two limits typically control the design (see graph below).

Design Prestress Tendon Geometry

Double click on the **Strand Geometry** icon to specify type, location, size, and debonding of strands. Then click on **Stranddata** and press F9 to read in the data.



Strand Geometry

```
Stranddata := a ← READPRN("tendsect.dat")
              w ← READPRN("strand.dat")
              x ← READPRN("area.dat")
              y ← READPRN("shield.dat")
              z ← READPRN("distance.dat")
              (w x y z a)
```

Reference: C:\FDOT_STR\Programs\LRFDpbeamE1.85\ProgramFiles\section

Summary of Initial Compression and Final Tension Prestress for Iteration Purposes. These two stress checks usually control. See graphs in proceeding sections for full details.

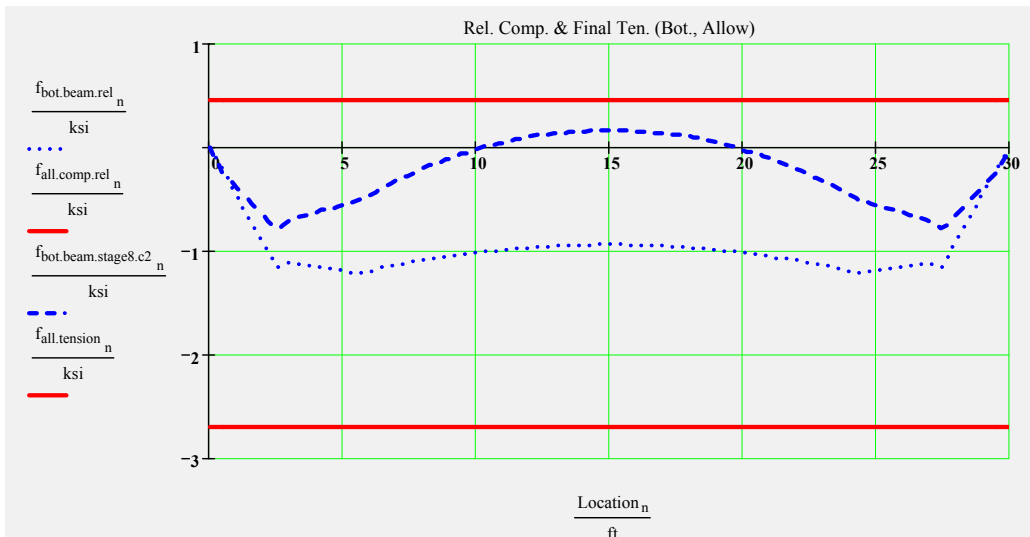


Figure 64. LRFD PSBeam output 4.

$\min(CR_f_{comp,rel}) = 2.212$ Check_ $f_{comp,rel}$ = "OK"

$\min(CR_f_{tension,stage8}) = 2.894$ Check_ $f_{tension,stage8}$ = "OK"

check strand pattern for debonding limits (per row and total) and for debonded strands on outside edge of strand pattern
 Check0 - No Debonded tendon on outside row, Check1 - less than 40% Debonded in any row, Check2 - less than 25% Debonded total

CheckPattern₀ = "OK"

CheckPattern₁ = "OK"

CheckPattern₂ = "OK"

Section and tendon properties

$A_{beam} = 3.996 \text{ ft}^2$ Concrete area of beam $I_{beam} = 6.893 \times 10^3 \text{ in}^4$ Gross Moment of Inertia of Beam

$y_{comp} = -3.152 \text{ in}$ Dist. from top of beam to CG of composite section $I_{comp} = 2.24 \times 10^4 \text{ in}^4$ Gross Moment of Inertia Composite Section

$A_{deck} = 1.847 \text{ ft}^2$ Concrete area of deck slab $A_{ps} = 1.8 \text{ in}^2$ total area of strands

$d_{b,ps} = 0.5 \text{ in}$ diameter of Prestressing strand $\min(\text{PrestressType}) = 0$ 0 - low lax 1 - stress relieved

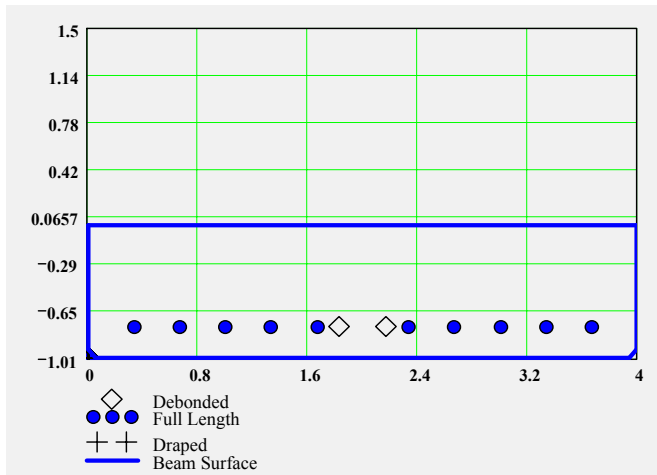
$f_{py} = 243 \text{ ksi}$ tendon yield strength $f_{pj} = 203 \text{ ksi}$ prestress jacking stress

$L_{shielding}^T = (3 \ 0) \text{ ft}$

$A_{ps,row}^T = (0.3 \ 1.5) \text{ in}^2$

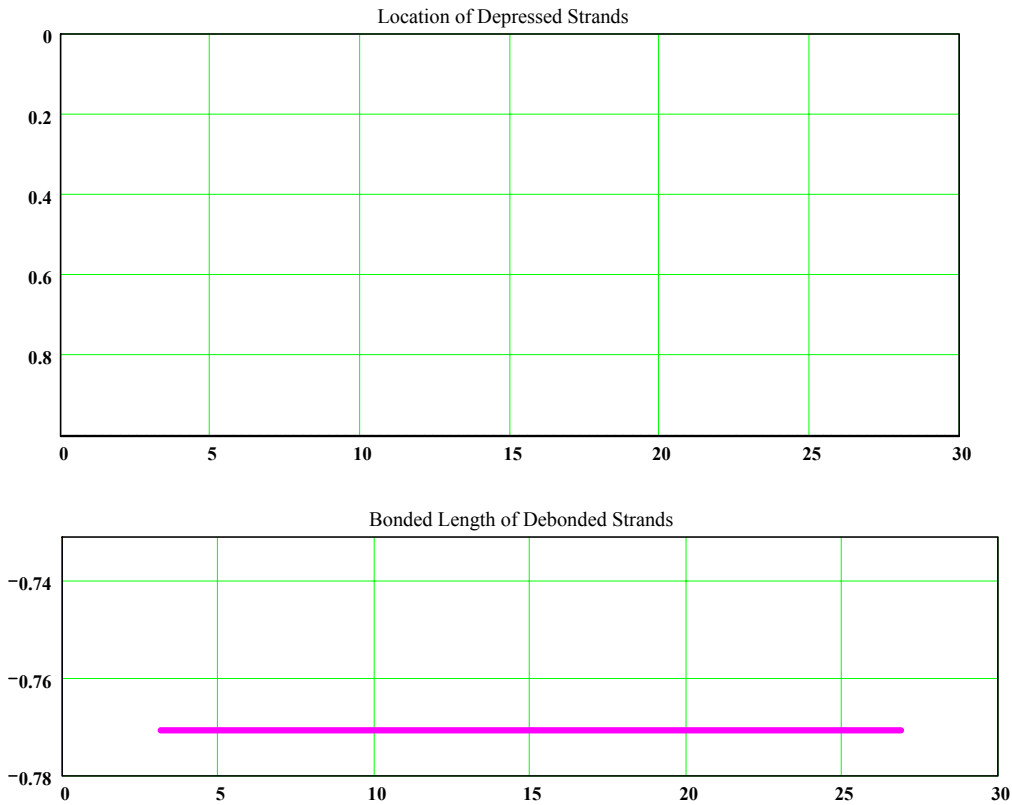
$d_{ps,row} =$		0	1	2	3	4	5	6	7	ft
	0	-0.771	-0.771	-0.771	-0.771	-0.771	-0.771	-0.771	-0.771	-0.771
	1	-0.771	-0.771	-0.771	-0.771	-0.771	-0.771	-0.771	-0.771	-0.771

Tendon Layout

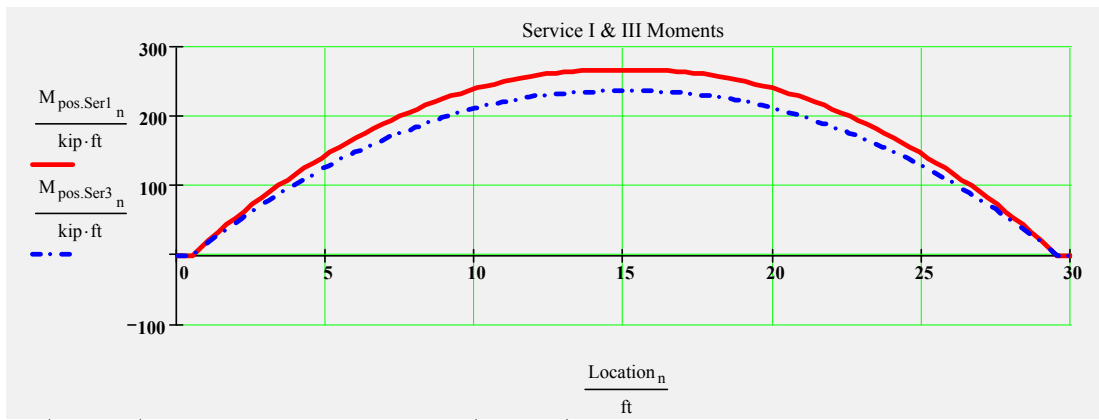


TotalNumberOfTendons = 12
 NumberOfDebondedTendons = 2
 NumberOfDrapedTendons = 0
 StrandSize = "1/2 in low lax"
 StrandArea = 0.153 in²
 JackingForce per.strand = 30.982 kip

Figure 65. LRFD PSBeam output 5.



SERVICE LIMIT STATE



$\max(M_{\text{pos.Ser1}}) = 268 \text{ kip-ft}$

$\max(M_{\text{pos.Ser3}}) = 237 \text{ kip-ft}$

Prestress Losses (LRFD 5.9.5)

$f_{pj} = 202.5 \text{ ksi}$ $\Delta f_{pR1} = -2.2 \text{ ksi}$ $\Delta f_{pES} = -5.8 \text{ ksi}$ $\Delta f_{pi} = -8 \text{ ksi}$ $f_{pi} = 194 \text{ ksi}$

$\Delta f_{pCR} = -7.9 \text{ ksi}$ $\Delta f_{pSR} = -5.8 \text{ ksi}$ $\Delta f_{pR2} = -4.5 \text{ ksi}$ $\Delta f_{pTot} = -26 \text{ ksi}$ $f_{pe} = 176 \text{ ksi}$

percentages $\frac{\Delta f_{pi}}{f_{pj}} = -3.976 \%$ $\frac{f_{pi}}{f_{pj}} = 96.024 \%$ $\frac{\Delta f_{pTot}}{f_{pj}} = -12.929 \%$ $\frac{f_{pe}}{f_{pj}} = 87.071 \%$

Figure 66. LRFD PSBeam output 6.

Stress Limitations for P/S tendons (LRFD 5.9.3)

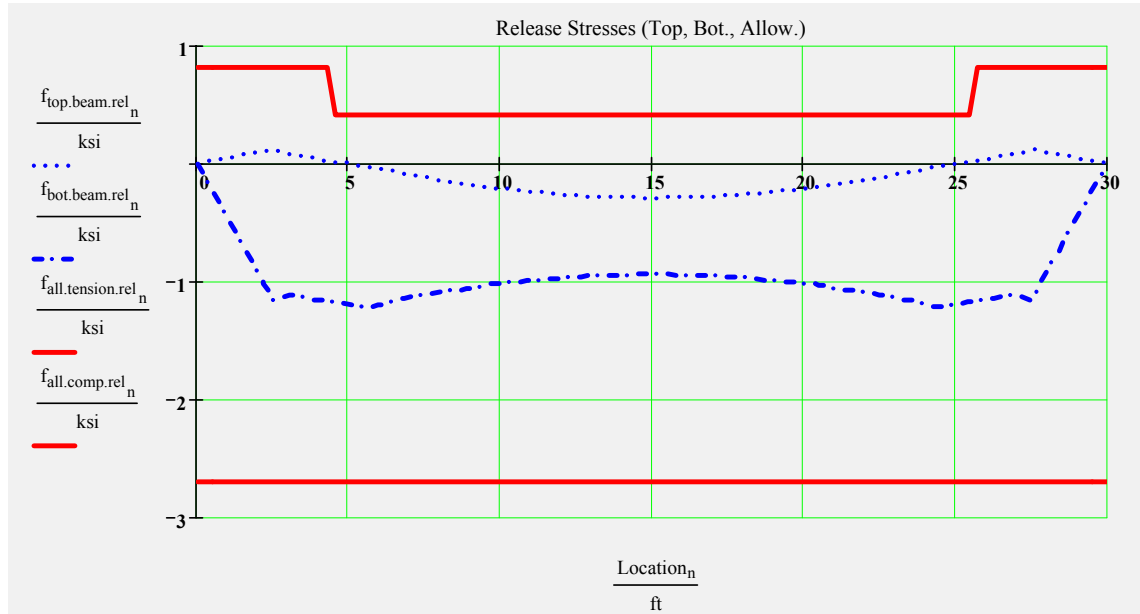
Check_f_{pt} = "OK"

0.8f_{py} = 194 ksi

Check_f_{pe} = "OK"

Stress Limitations for Concrete - Release and Final (LRFD 5.9.4)

Release



min(CR_f_{tension.rel}) = 7.041

Check_f_{tension.rel} = "OK"

min(CR_f_{comp.rel}) = 2.212

Check_f_{comp.rel} = "OK"

Final

min(CR_f_{tension.stage8}) = 2.894

Check_f_{tension.stage8} = "OK"

(Service III, PS + DL + LL*0.8)

min(CR_f_{comp.stage8.c1}) = 3.729

Check_f_{comp.stage8.c1} = "OK"

(Service I, PS + DL)

min(CR_f_{comp.stage8.c2}) = 3.603

Check_f_{comp.stage8.c2} = "OK"

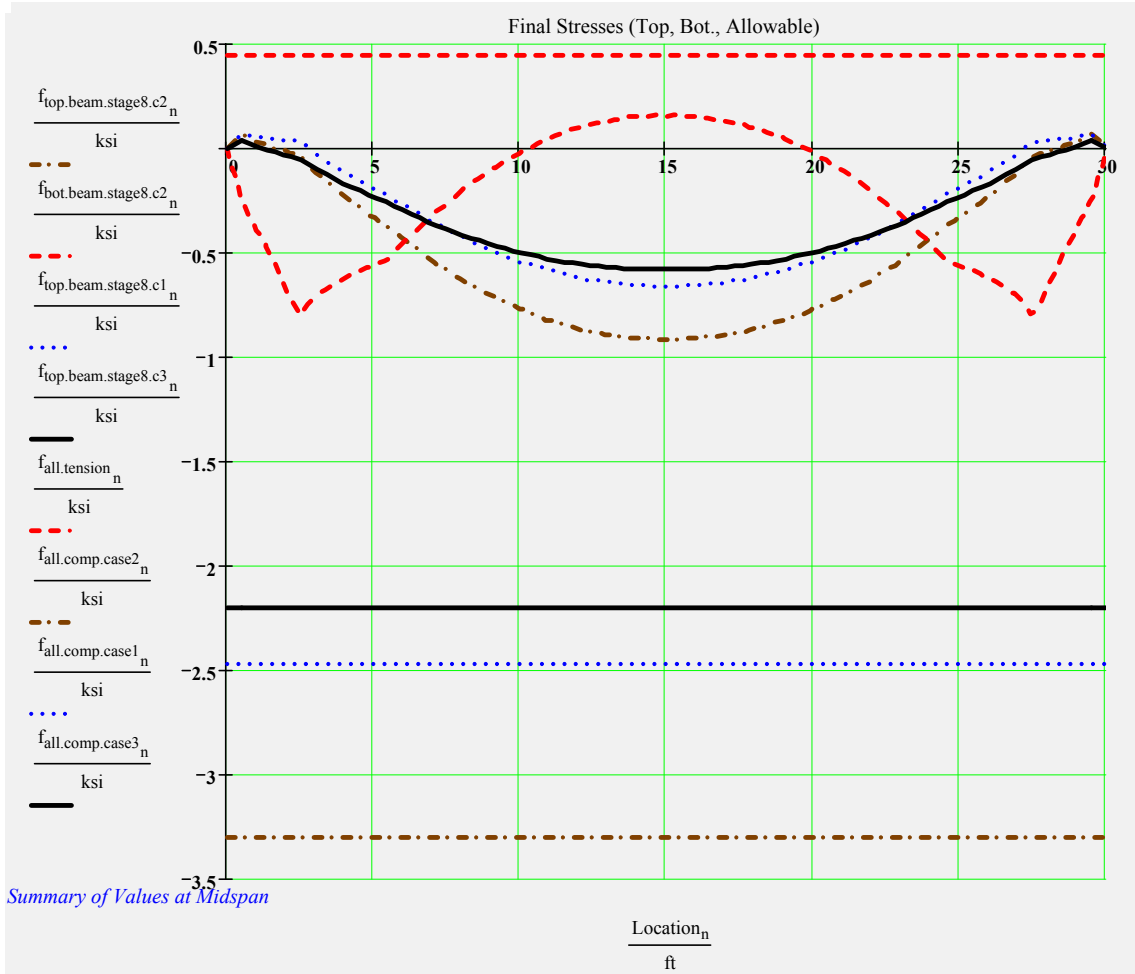
(Service I, PS + DL + LL)

min(CR_f_{comp.stage8.c3}) = 3.766

Check_f_{comp.stage8.c3} = "OK"

(Service I, (PS + DL)*0.5 + LL)

Figure 67. LRFD PSBeam output 7.



Summary of Values at Midspan

Stresses =	"Stage "	"Top of Beam (ksi) "	"Bott of Beam (ksi)")
	1	-0.293	-0.943
	2	-0.328	-0.794
	4	-0.283	-0.839
	6	-0.64	-0.481
	8	-0.916	0.153

Compression stresses are negative and tensile stresses are positive

Stage 1 ----> At release with the span length equal to the length of the beam. Prestress losses are elastic shortening and overnight relax

Stage 2 ----> Same as release with the addition of the remaining prestress losses applied to the transformed beam

Stage 4 ----> Same as stage 2 with supports changed from the end of the beam to the bearing locations

Stage 6 ----> Stage 4 with the addition of non-composite dead load excluding beam weight which has been included since Stage 1

Stage 8 ----> Stage 6 with the addition of composite dead load and live loads applied to the composite section

PrestressForce =	"Condition "	"Axial (kip)"	"Moment (kip*ft)")
	"Release"	-357.3739	-99.0955
	"Final (about composite centroid)"	-323.7221	-164.6951

Properties =	"Section "	"Area (in^2) "	"Inertia (in^4) "	"distance to centroid from top of bm (in)")
	"Net Beam "	582.58	7014.2	-5.92
	"Transformed Beam "	594.84	7147.13	-5.99
	"Composite "	877.07	23140.02	-3.14

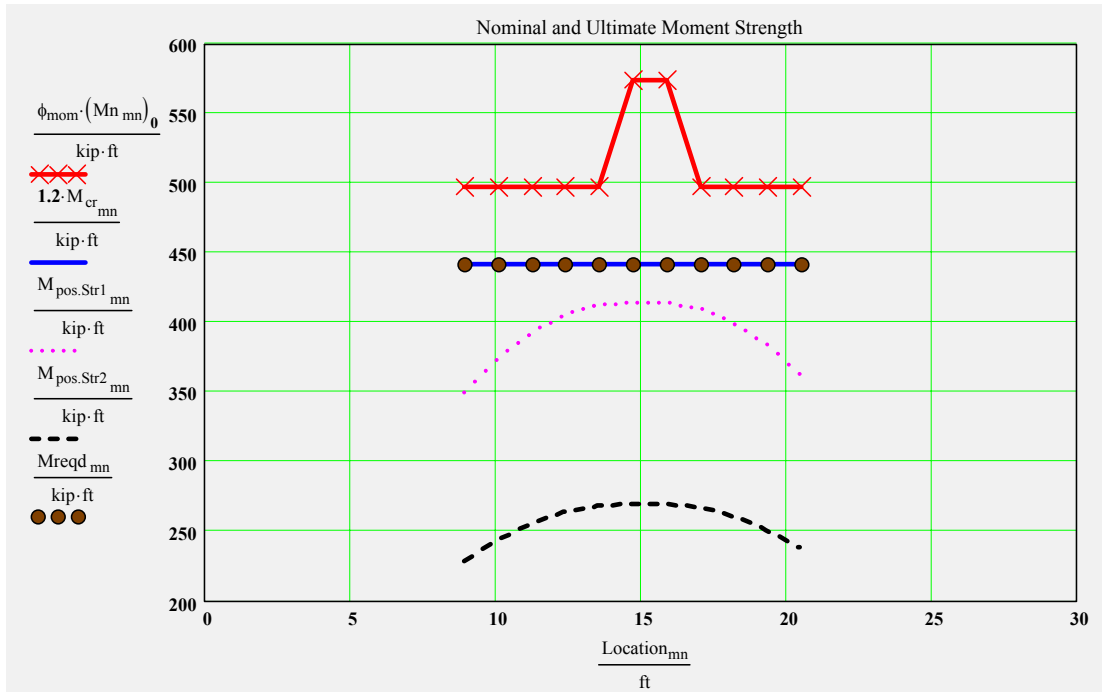
Figure 68. LRFD PSBeam output 8.

	"Type"	"Value (kip*ft)"
ServiceMoments =	"Release"	67.4
	"Non-composite (includes bm wt.)"	98.5
	"Composite"	14.4
	"Distributed Live Load"	154.5

STRENGTH LIMIT STATE

Reference: C:\FDOT_STR\Programs\LRFPbeamE1.85\ProgramFiles\section3.mcd(R)

Moment Nominal Resistance versus Ultimate Strength Cases I and II

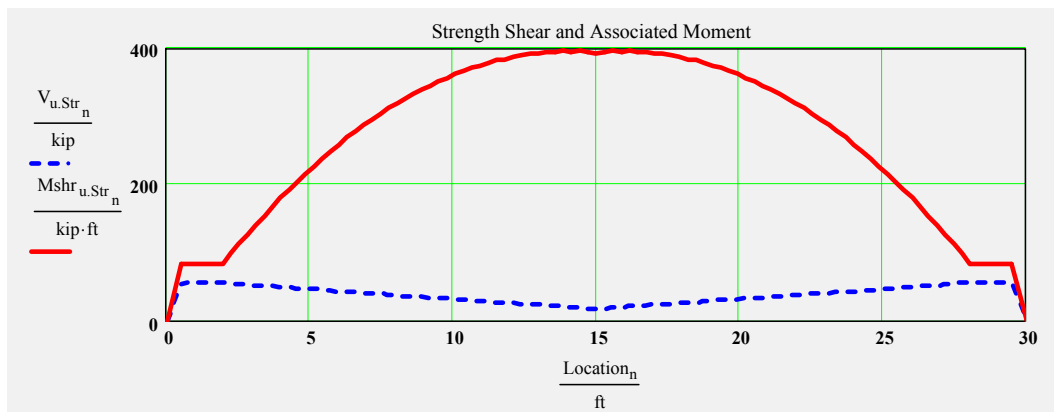


$\max(M_{pos.Str1}) = 414 \text{ kip-ft}$

$\min(CR_{Str1.mom}) = 1.127$

CheckMomentCapacity = "OK"

Strength Shear and Associated Moment



$\max(V_{u.Str}) = 56 \text{ kip}$

$\max(M_{shr_{u.Str}}) = 396 \text{ kip-ft}$

Figure 69. LRFD PSBeam output 9.

Check and Design Shear, Interface and Anchorage Reinforcement
 Locally assigned stirrup sizes and spacings (Values less than 0 are ignored)
 To change the values from the input file enter the new values into the vectors below. Input only those that you wish to change, values that are less than one will not alter the original input values.

The interface_factor accounts for situations where not all of the shear reinforcing is embedded in the poured in place slab

<i>A stirrup</i>	user_s_nspacings := XX·in	user_NumberSpaces_nspacings := XX	user_A_stirrup_nspacings := XX·in ²	interface_factor_nspacings := 0.5
<i>S1 stirrup</i>	XX·in	XX	XX·in ²	1
<i>S2 stirrup</i>	XX·in	XX	XX·in ²	1
<i>S3 stirrup</i>	XX·in	XX	XX·in ²	1
<i>S4 stirrup</i>	XX·in	XX	XX·in ²	1

Reference: C:\FDOT_STR\Programs\LRFDpbeamE1.85\ProgramFiles\section4.mcd(R)

Stirrup sizes and spacings used in analysis

<i>A stirrup</i>	s =	in	NumberSpaces =	A_stirrup =	in ²	
<i>S1 stirrup</i>						(0)
<i>S2 stirrup</i>						(0)
<i>S3 stirrup</i>						(0)
<i>S4 stirrup</i>						(15)

EndCover = 0 in The number of spaces for the S4 stirrup is calculated by the program to complete the half beam length

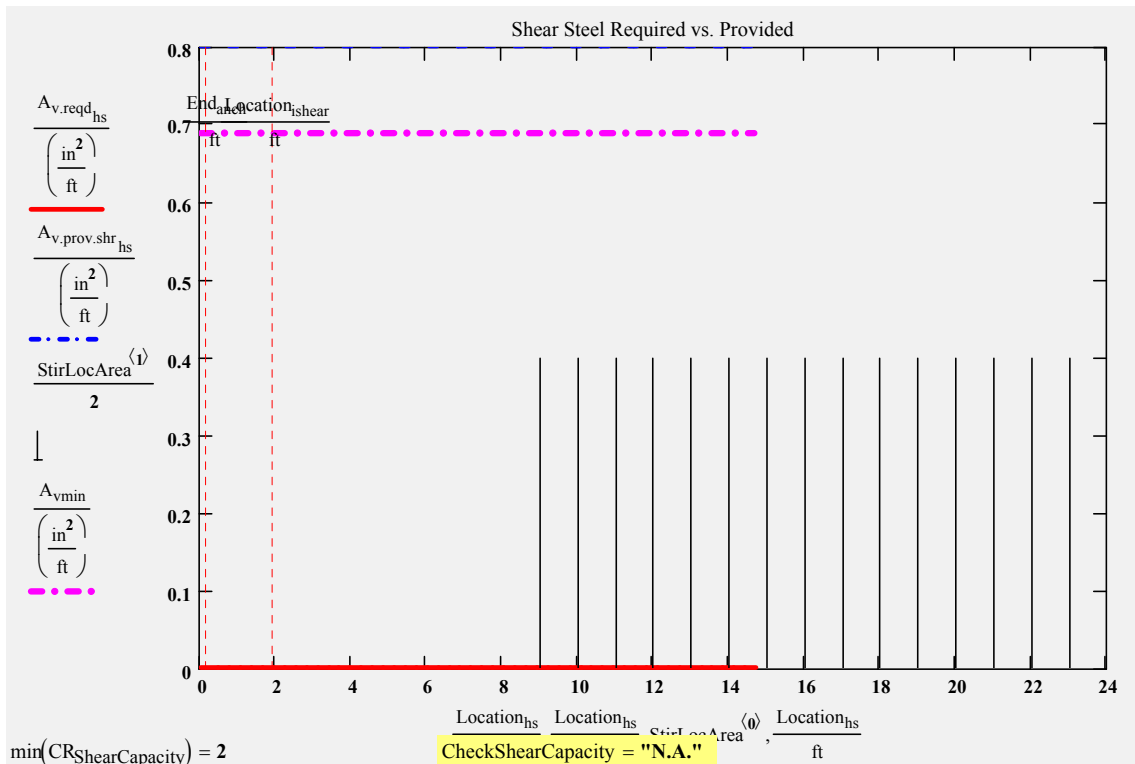
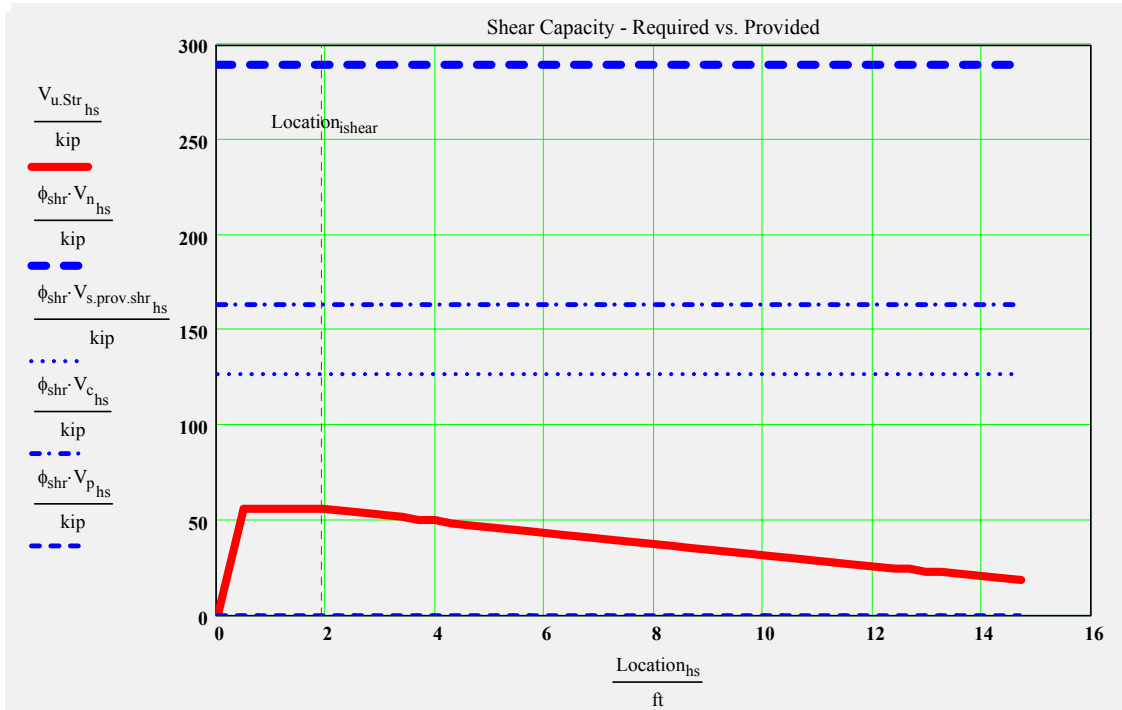
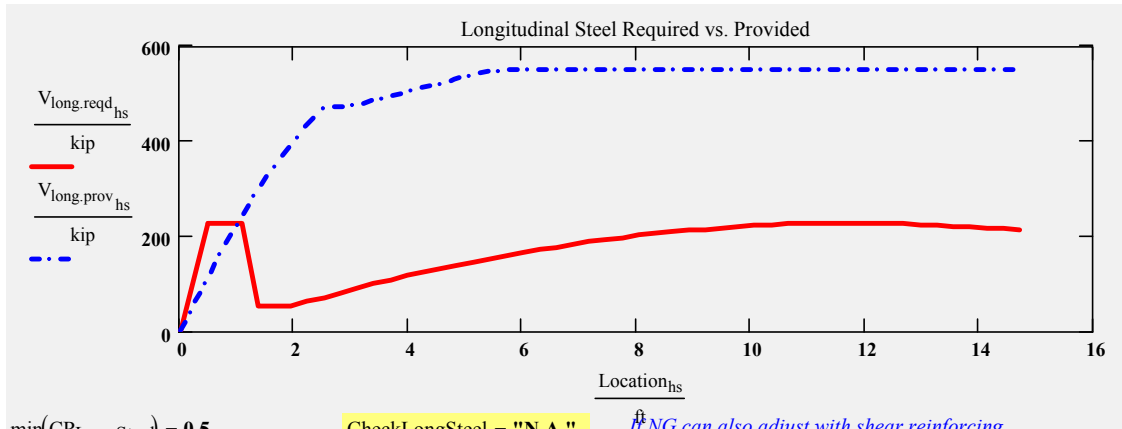


Figure 70. LRFD PSBeam output 10.



Check Longitudinal Steel



$\min(CR_{LongSteel}) = 0.5$ CheckLongSteel = "N.A." *if NG can also adjust with shear reinforcing*

Check Interface Steel

MinInterfaceReinfReqd = "N.A."

$A_{vf.min} = 0 \frac{\text{in}^2}{\text{ft}}$

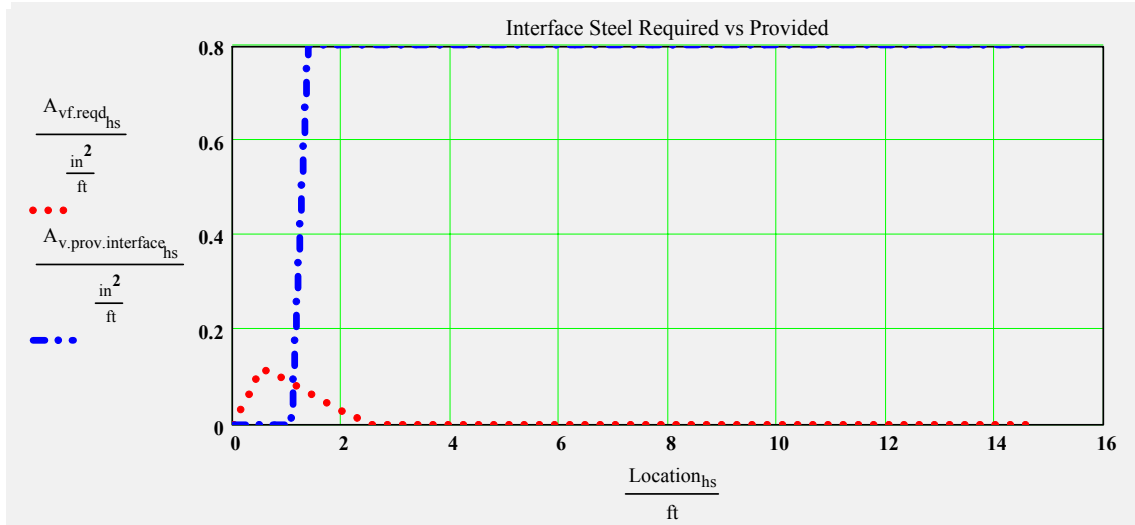
$\max(A_{vf.des}) = 0.1 \frac{\text{in}^2}{\text{ft}}$

Typically shear steel is extended up into the deck slab. These calculations are based on that assumption that the shear steel functions as interface reinforcing. The interface_factor can be used to adjust this assumption. If Avf.design or Avf.min is greater than 0 in ²/ft, interface steel is required.

MinLegsPerRow = 0

CheckInterfaceSpacing = "N.A."

Figure 71. LRFD PSBeam output 11.



$$\text{CheckInterfaceSteel} := \text{if} \left(\frac{\text{TotalInterfaceSteelProvided}}{\text{TotalInterfaceSteelRequired} + 0.001 \cdot \text{in}^2} \geq 1, \text{"OK"}, \text{"No Good"} \right) \quad \text{CheckInterfaceSteel} = \text{"OK"}$$

Check Anchorage Steel for Bursting and Calculate Confinement Steel

use #3 bars @ 6 in for confinement **CheckAnchorageSteel = "N.A."** *value includes bars at both ends*
TotalNoConfineBars = 8

Summary of Design Checks

AcceptInteriorM = "OK"	AcceptExteriorM = "OK"	AcceptInteriorV = "OK"
Check_f _{pt} = "OK"	Check_f _{pe} = "OK"	Check_f _{tension.rel} = "OK"
Check_f _{comp.rel} = "OK"	Check_f _{tension.stage8} = "OK"	Check_f _{comp.stage8.c1} = "OK"
Check_f _{comp.stage8.c2} = "OK"	Check_f _{comp.stage8.c3} = "OK"	CheckMomentCapacity = "OK"
CheckMaxCapacity = "N.A."	CheckStirArea = "N.A."	CheckShearCapacity = "N.A."
CheckMinStirArea = "N.A."	CheckMaxStirSpacing = "N.A."	CheckLongSteel = "N.A."
CheckInterfaceSpacing = "N.A."	CheckAnchorageSteel = "N.A."	CheckMaxReinforcement = "OK"
CheckInterfaceSteel = "OK"	CheckStrandFit = "OK"	

TotalCheck = "OK"

Figure 72. LRFD PSBeam output 12

APPENDIX B – Topping Placement Summary

TOPPING PLACEMENT DAILY SUMMARY

SYN 7-26-2004

- Flat slabs were cleaned with a blower
- Concrete batched at 8:47AM
- Truck leaves plant at 8:57AM
- Truck arrived at site at 9:10AM. Truck #118, Tag N2322B
- Driver did not have material delivery ticket
- Driver's ticket lists a 4" slump was delivered
- Flat slabs were sprayed with water
- Slump test #1 performed at 9:20AM
- 4-1/2" slump
- Started adding Strux 90/40 fibers 9:20AM-9:24AM
- Fibers were introduced by hand into the drum mixer. They were dispersed manually as they were deposited.
- Counted 70 revolutions from 9:24AM to 9:28AM
- Slump test was attempted to see the effect the fibers had on the mix. The fibers were not uniformly mixed in. There was a lot of bundling.
- Slump test #2 performed at 9:30AM
- 1-3/4" slump
- Instructed driver to add 6 gal to achieve a .44 w/c. This was based on a mixture proportions I obtained from Tallahassee Redi Mix (TRM) on a visit last Monday, July 19th.
- Slump test #3 performed at 9:40AM
- 3-1/4" slump
- Placed concrete from 9:45AM-10:12AM
- Workability was terrible. The concrete was raked and vibrated down the chute. It was then raked into place. Most of the concrete was moved between 4' & 5' to its final position. It was then vibrated.
- Screeding started as when the concrete placement was halfway down the topping.
- Screeding finished at 10:30AM
- Floating started as screeding took place. Finished floating at 10:32AM
- An air content of 2.5% was measured

- 27 cylinders were collected and capped. They were collected late in the cycle of events. The collection of cylinders will take place at an earlier time on the remaining toppings.
- The steel ring was cast
- There has not been any bleed water visible on the surface of the topping
- Curing compound was applied at 12:20PM
- Clouds rolled in at 12:36PM and blocked out the sun
- Went to TRM to obtain a copy of the batched materials for today's concrete mixture. Turns out we were low on the amount of water we could add to the mix.

BND 7-27-2004

- Met with Casey Peterson, Quality Control Manager for TRM at about 7:45AM
- Based on yesterday's problems with placing the concrete and the low w/c ratio we wanted to discuss our options to improve the workability of the mixture. He said he could modify the mixture any way we wanted to. We discussed the possibility of reducing the amount of water reducer so as to maximize our w/c ratio while still having a reasonable slump...4"-6". Based on conversations with Dr. Hamilton, I instructed Casey to send the same mix. We would control the w/c ratio at the site.
- Flat slabs were cleaned with a blower
- Concrete batched at 8:42AM
- Truck left plant at 8:50AM
- Truck arrived at the site at 9:07AM
- Flat slabs were sprayed with water
- Collected material ticket from driver and calculated allowable additional water
- Form was filled out incorrectly and we worked under the assumption that we only had 7 oz of water reducer in the mix. This did not affect our calculations and was discovered later on that afternoon.
- Driver's delivery ticket lists a 4" slump was delivered
- Slump test #1 performed at 9:15AM
- 2-3/4" slump
- Fibers were added to the concrete mixture
- Synthetic micro fibers were added at 9:16AM. 11lb/CY
- Steel fibers were added at 9:16AM-9:22AM. 25 lbs/CY

- The steel fibers were added second so that they would help separate the already present micro fibers
- Counted 70 revolutions from 9:22AM to 9:26AM
- Slump test #2 performed at 9:26AM
- 3-3/4" slump
- Instructed driver to add 8 gal to mixture. Based on 1" slump loss for every gallon of water per CY. We were shooting for a .44 w/c and a 5-3/4 slump.
- Slump test #3 performed at 9:35AM
- 4-3/4 slump
- Placed concrete from 9:35AM – 9:45AM
- Concrete had very good workability. It flowed down the chute easily. Most of the concrete was moved between 2' & 3' to its final position. It was then vibrated.
- Backer rod fell through and was reinstalled and secured from 9:45AM until 9:55AM
- Screeding started when the concrete placement was 3/4 of the way down the topping.
- Floating started as screeding took place. Floating started at 10:06AM and finished at 10:17AM
- Screeding was finished at 10:10AM
- An air content of 3.5% was measured
- 27 cylinders were collected and capped while the concrete was placed
- The steel ring was cast while the concrete was placed
- There has not been any bleed water visible on the surface of the topping
- Curing compound was applied at 1:10PM
- Clouds rolled in at 1:20PM and rain started at 1:30PM. Some of the curing compound was washed off.

GRD 7-28-2004

- Both flat slabs were cleaned with a blower
- Concrete batched at 8:45AM
- Truck left plant at 8:57AM
- Truck arrived at the site at 9:07AM
- Flat slabs were sprayed with water

- • Collected material ticket from driver and calculated allowable additional water
- Form was incorrectly filled out again. This was noticed immediately and did not affect any calculations.
- Driver's delivery ticket lists a 4" slump was delivered
- Slump test #1 performed at 9:11AM
- 4-3/4" slump
- Instructed driver to add 5 gal of water to mix. This would put us at a .44 w/c based on the delivery ticket.
- Slump test #2 performed at 9:16AM
- 6-1/4" slump
- Placed concrete from 9:22AM – 9:29AM
- Screeding took place as concrete was placed. This finished the concrete 1" below its final surface to allow for grid installation
- Wooden 2"x6" screed was run over the topping two times
- This process was much easier than I expected
- Grid was laid out from 9:30AM – 9:35AM
- Grid is 42" wide. There is a grid joint at the center with a two hole overlap. The outer strips overlap about 8" with the inner strips
- Grid was floating lightly to have it "stick" to concrete. All the grid came in contact with the concrete. There was no loss of contact due to the grid wanting to roll up.
- Concrete was topped off from 9:35AM – 9:43AM
- Driver was extremely good at placing concrete where it was needed. He backed the truck up and swung the chute as the concrete was placed
- Concrete was screeded as it was topped off.
- The final screeding finished at 9:46AM
- Floating was done from 9:49AM – 9:55AM
- An air content of 3% was measured
- 27 cylinders were collected while the concrete was placed. They were not capped
- The steel ring was cast while the concrete was placed
- Bleed water was visible on the surface as it cured
- Curing compound was applied at 2:00PM
- It started to rain at 3:05PM

STL 7-28-2004

- Concrete batched at 9:56AM
- Truck left plant at 10:15AM
- Truck arrived at the site at 10:26AM
- Flat slabs were sprayed with water
- Collected material ticket from driver and calculated allowable additional water
- Form was incorrectly filled out
- Driver's delivery ticket lists a 4" slump was delivered
- Slump test #1 performed at 10:31AM
- 2" slump
- Instructed driver to add 16 gallons of water. This was based off of the delivery ticket. It would put us at a .44 w/c
- A slump test was not taken after the water was added
- Fibers added to the mix from 10:37AM – 10:49AM
- I could feel the heat generated by the mix as I was adding the fibers
- Counted 70 revolutions from 10:49AM to 10:53AM
- Slump test #2 performed at 10:54 AM
- 2" slump
- Placed concrete at 10:58AM
- The mix was extremely stiff. It seems like there is not enough water in the mix. One wouldn't be able to tell that 16 gallons of water were added to the mix. The mix was raked and vibrated down the chute. This mix is much more difficult to work than the synthetic mix.
- Instructed the driver to add 8 gallons of water at 11:03AM. Based on 1" slump loss for every gallon of water per CY. We were shooting for a 4" slump and expected the w/c ratio to go over the max of .44. A slump test was not performed after the water was added.
- Placement continued at 11:10AM. The mix was somewhat workable after the water was added. It still required the vibrator and the rake to get it down the chute. Most of the concrete was moved between 4' & 5' to its final position.
- Topped off at 11:20AM
- Screeded from 11:25AM – 11:50AM
- Concrete was floated but most of it was difficult to finish. There were many voids on the surface in the area of the initial pour.

- An air content of 2% was measured
- 27 cylinders were collected and capped while the concrete was placed. They were collected after the final 8 gallons of water were added.
- The steel ring was cast while the concrete was placed, after the final 8 gallons of water were added.
- No bleed water was seen on the surface
- Curing compound was applied at 2:40PM
- It started to rain at 3:05PM. At 3:18PM some of the curing compound was washed off

SRA 7-29-2004

- I called the plant earlier to request a 2" slump concrete because we did not know the effect the SRA would have on the mix
- Flat slabs were cleaned with a blower
- Concrete was batched at 8:32AM
- Truck left the plant at 8:49AM
- Truck arrived at the site at 9:05AM
- Collected material ticket from driver and calculated allowable additional water
- Slump test #1 performed at 9:13AM
- 1-3/4" slump
- Added 15 gallons of SRA from 9:16AM – 9:21AM while truck was mixing at high speed
- Much easier to add when compared to fibers. Not as worried about integration into mixture.
- Slump test #2 performed at 9:24AM
- 2" slump
- Instructed driver to add 20 gallons of water at 9:26AM. Based on 1" slump loss for every gallon of water per CY. We were shooting for a 4" slump.
- Slump test #3 performed at 9:30AM
- 5" slump
- Placed concrete from 9:35Am – 9:55AM
- Concrete flowed easily down the chute. Most of the concrete was raked between 2' & 3' to its final position. It had very good workability.
- An air content of 1.5% was measured

- 27 cylinders were collected and capped while the concrete was placed.
- The steel ring was cast while the concrete was placed
- Screeded from 9:48AM – 10:10AM
- Floating was done by a different person today. This may have an effect on plastic cracking.
- Noticed bleed water on the surface
- I left site in order to run p. t. tests in Gainesville
- Curing compound applied by structures lab personnel.

CTL 7-30-2004

- Flat slabs were cleaned with a blower
- Concrete was batched at 8:30AM
- Truck left the plant at 8:50AM
- Truck arrived at the site at 9:02AM
- Collected material ticket from driver and calculated allowable additional water
- Slump test #1 performed at 9:04AM
- 2-3/4" slump
- Instructed driver to add 20 gallons of water to mixture
- Slump test #2 performed at 9:15AM
- 5" slump
- Placed concrete from 9:20AM -9:34AM
- Concrete had good workability
- Concrete screeded from 9:27AM – 9:45AM
- Floating was done by a different person today. This may have an effect on plastic cracking.
- 27 cylinders were collected and capped while the concrete was placed.
- Measured an air content of 1%
- The steel ring was cast while the concrete was placed
- There was a lot of bleed water on the surface. The bleed channels were clearly visible. Water was running off the sides of the formwork.
- Left site in order to run pressure tension tests in Gainesville

- Curing compound applied by structures lab personnel

APPENDIX C – Cylinder Test Results

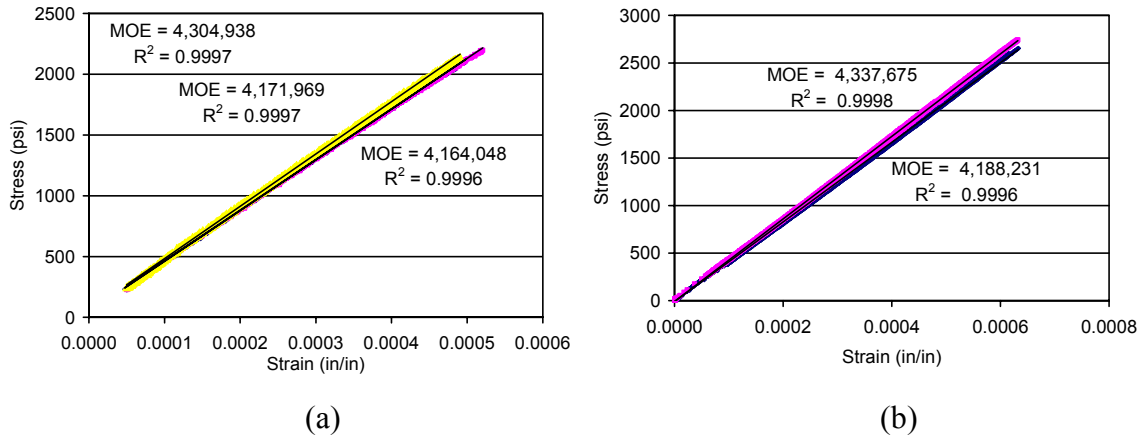


Figure 73. Modulus of elasticity charts for SYN topping. a) 28-day, b) 56-day.

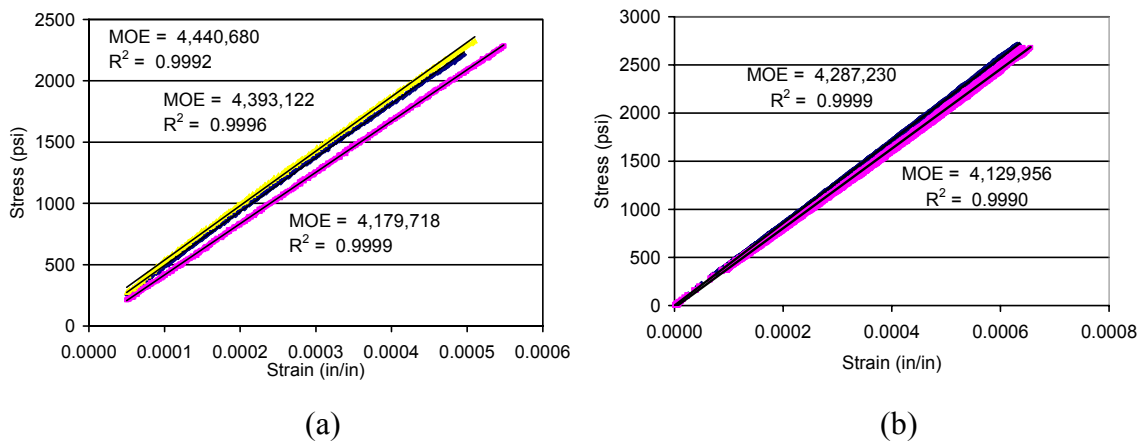


Figure 74. Modulus of elasticity charts for BND topping. a) 28-day, b) 56-day.

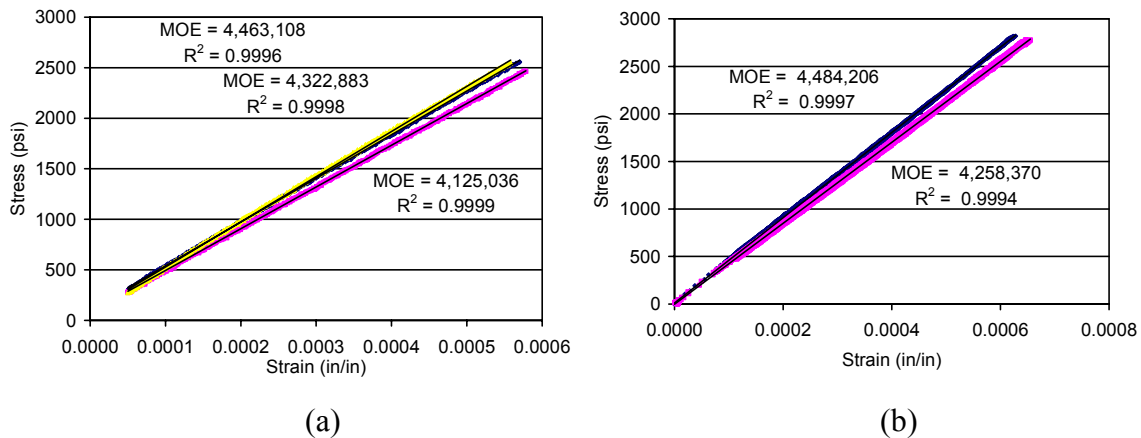
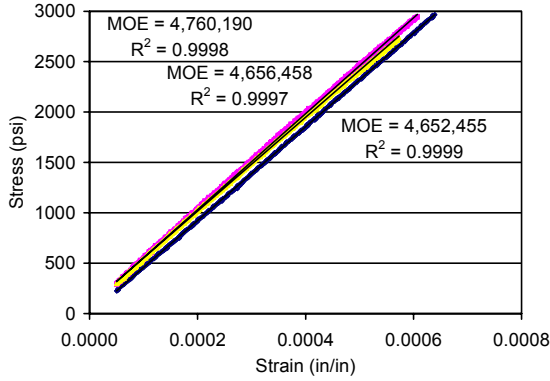
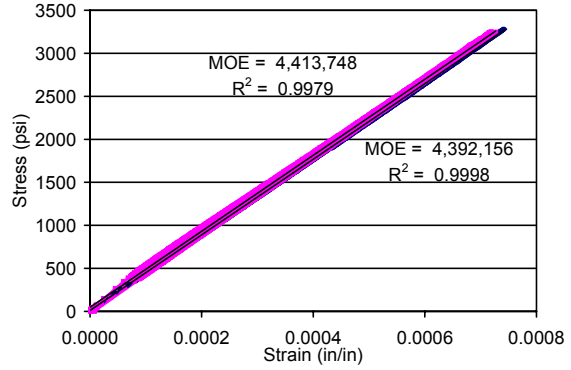


Figure 75. Modulus of elasticity charts for GRD topping. a) 28-day, b) 56-day.

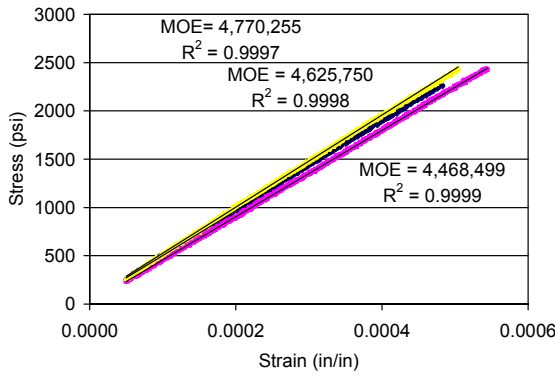


(a)

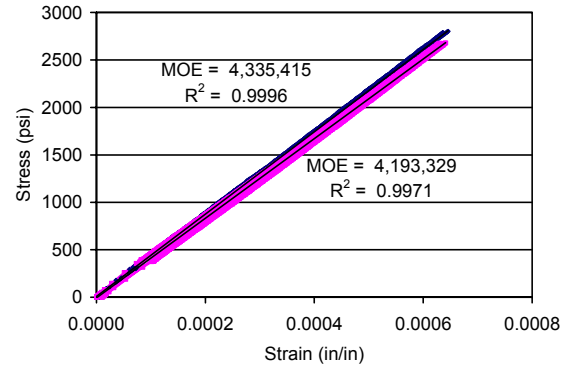


(b)

Figure 76. Modulus of elasticity charts for STL topping. a) 28-day, b) 56-day.

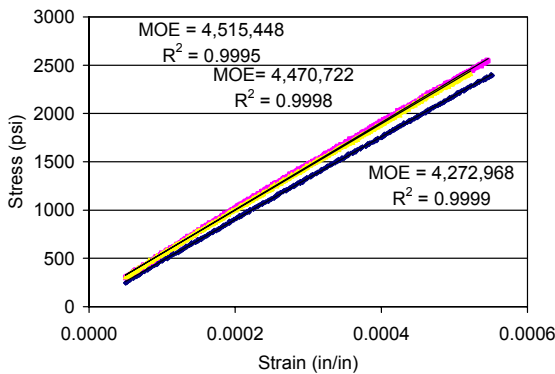


(a)

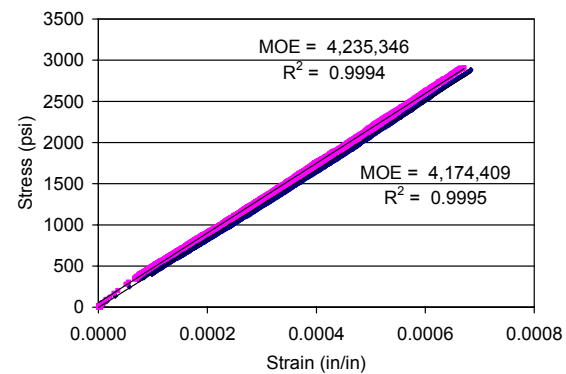


(b)

Figure 77. Modulus of elasticity charts for SRA topping. a) 28-day, b) 56-day.



(a)



(b)

Figure 78. Modulus of elasticity charts for CTL topping. a) 28-day, b) 56-day.

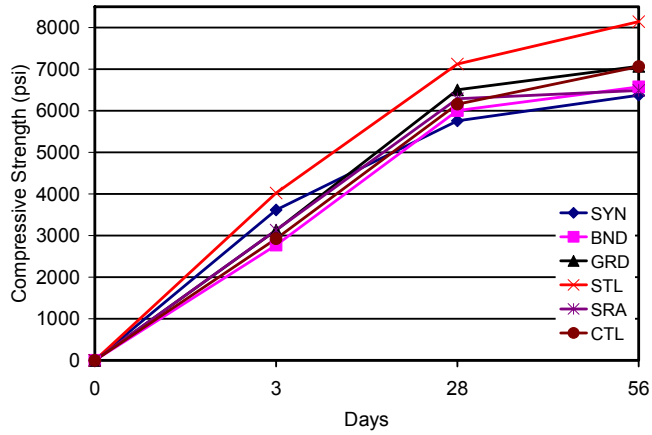


Figure 79. Compressive strength of cylinders at 3, 28, & 56-days.

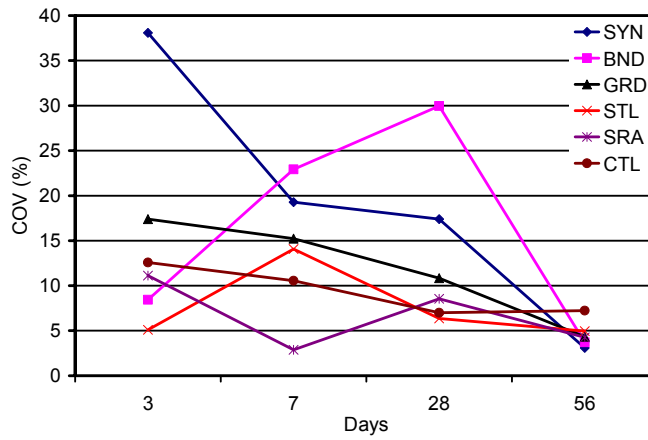


Figure 80. Coefficient of variation for load rate using pressure tension test.

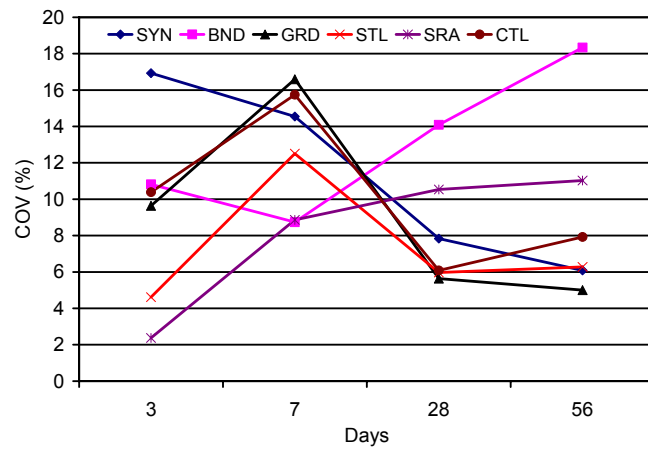


Figure 81. Coefficient of variation for strength using pressure tension test.

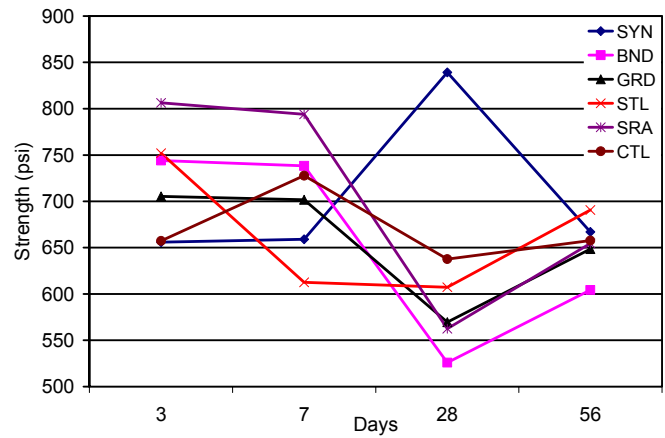


Figure 82. Tensile strength using pressure tension test.

APPENDIX D – Weather Data

Temperature and relative humidity data was collected from a weather station located approximately 2 miles away at the Tallahassee Regional Airport. It is operated by the National Climatic Data Center.

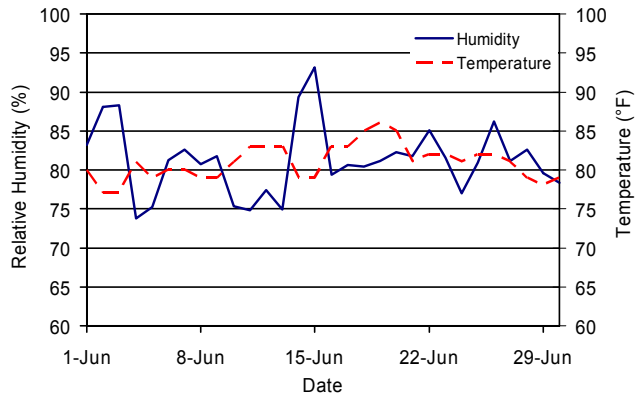


Figure 83. Humidity and temperature data for June 2004

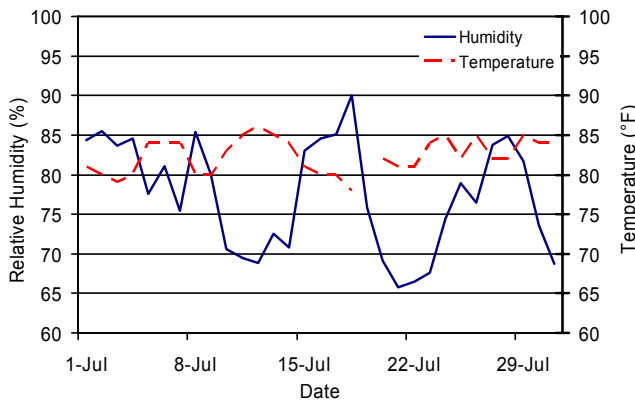


Figure 84. Humidity and temperature data for July 2004

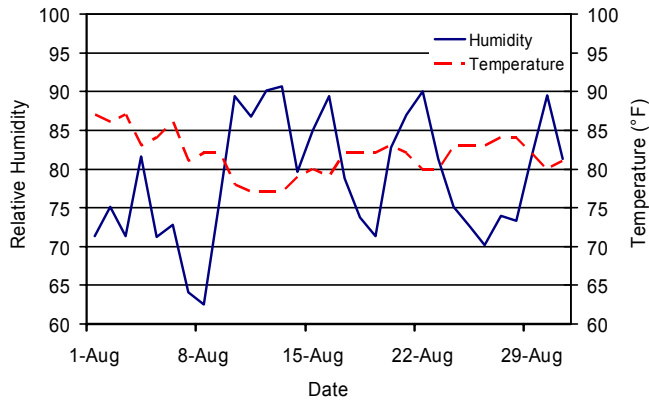


Figure 85. Humidity and temperature data for August 2004

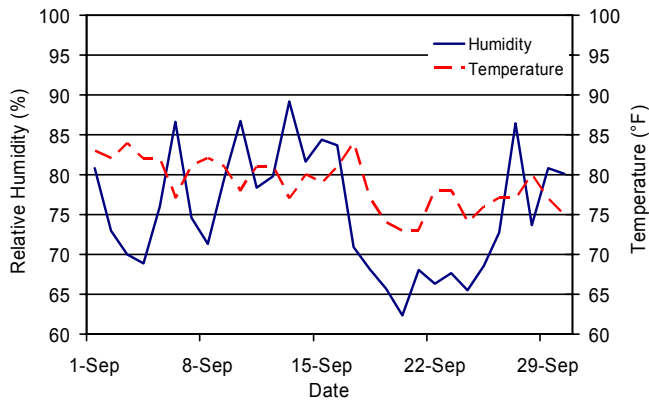


Figure 86. Humidity and temperature data for September 2004

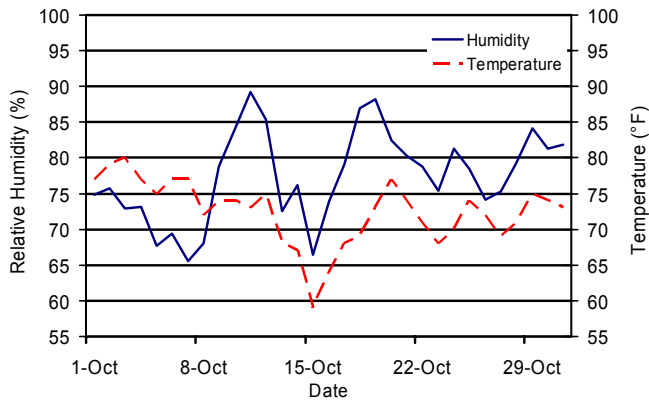


Figure 87. Humidity and temperature data for October 2004

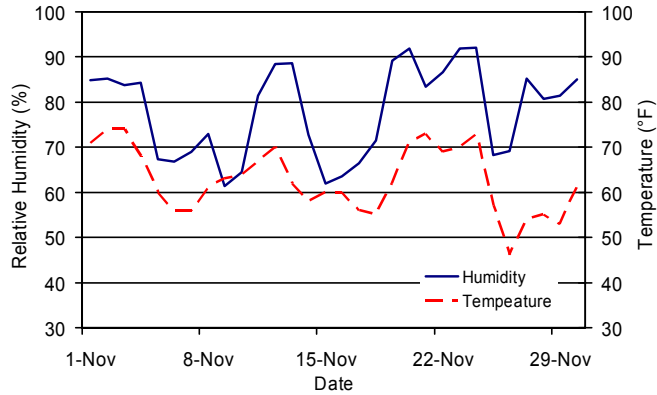


Figure 88. Humidity and temperature data for November 2004

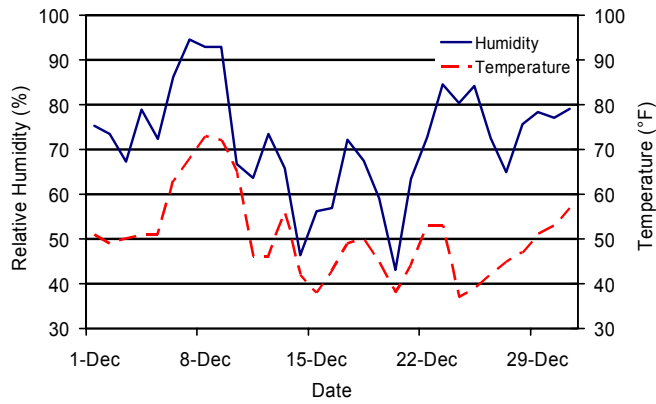


Figure 89. Humidity and temperature data for December 2004

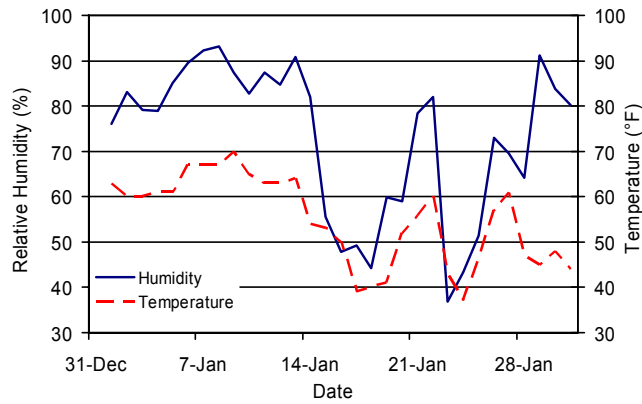


Figure 90. Humidity and temperature data for January 2004

APPENDIX E – Thermocouple Data

SYN

See Figure 34 and Figure 35 for location of thermocouples within topping.

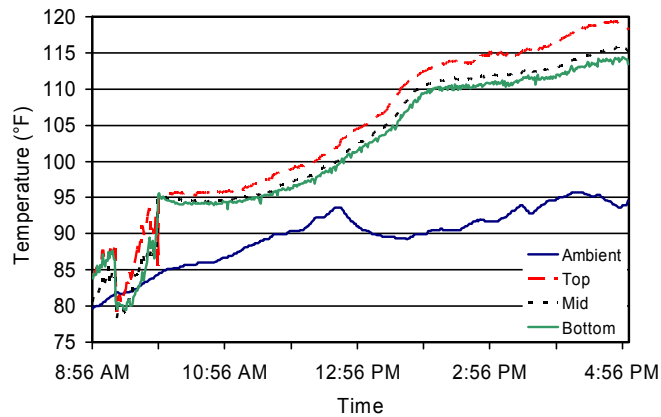


Figure 91. Curing temperatures for SYN-1

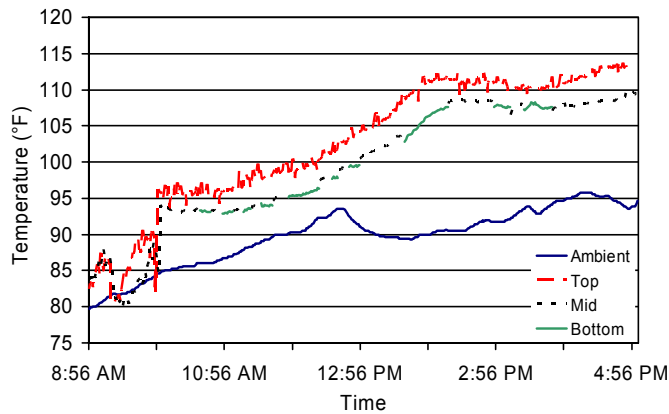


Figure 92. Curing temperatures for SYN-2

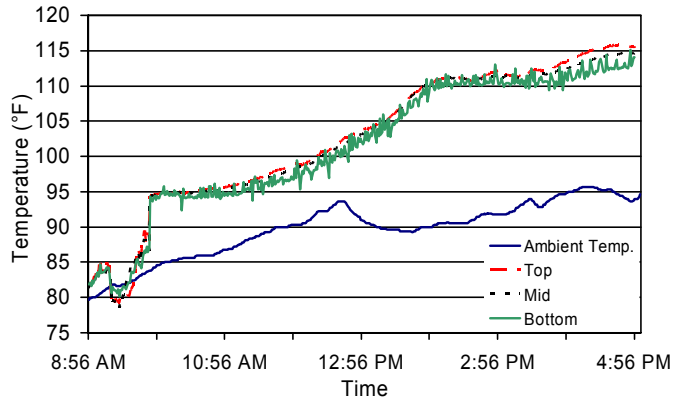


Figure 93. Curing temperatures for SYN-3

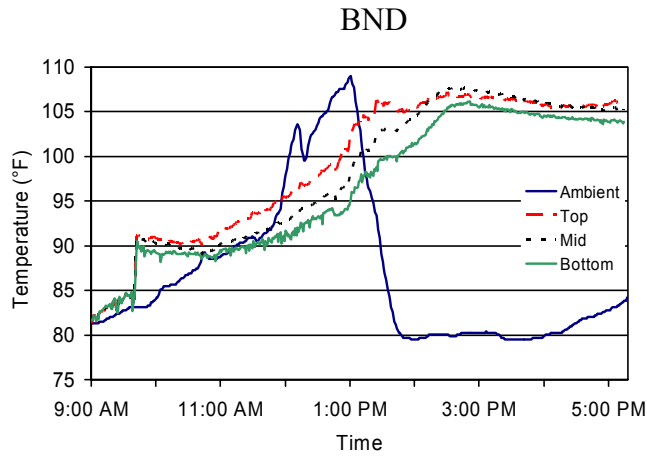


Figure 94. Curing temperatures for BND-1

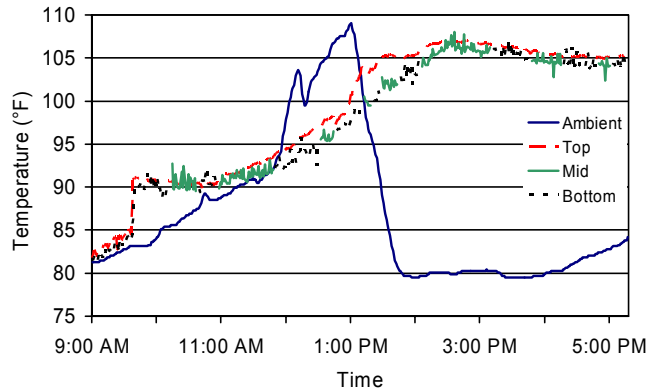


Figure 95. Curing temperatures for BND-2

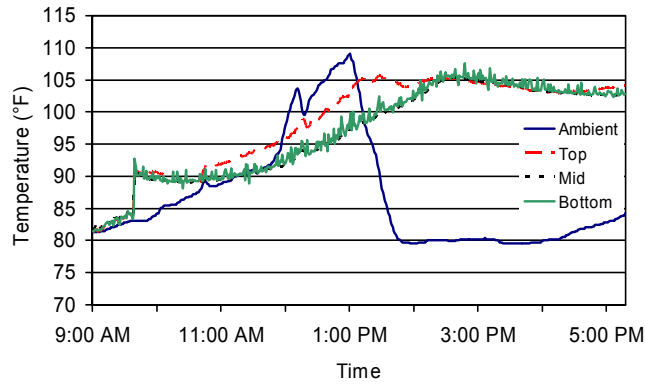


Figure 96. Curing temperatures for BND-3

STL

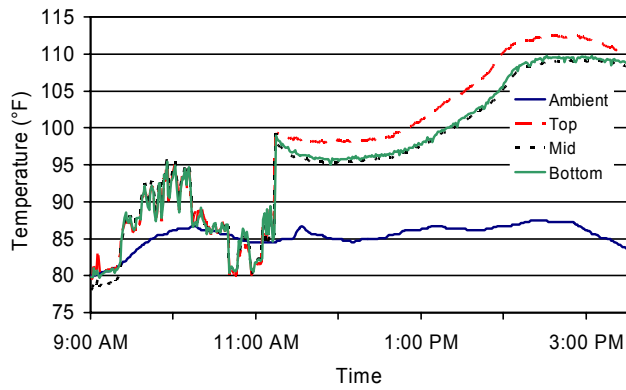


Figure 97. Curing temperatures for STL-1

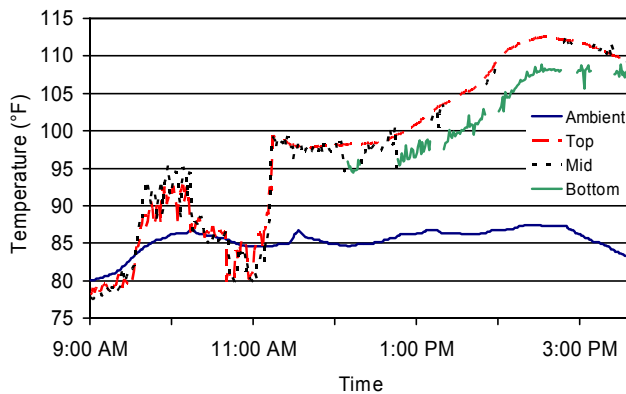


Figure 98. Curing temperatures for STL-2

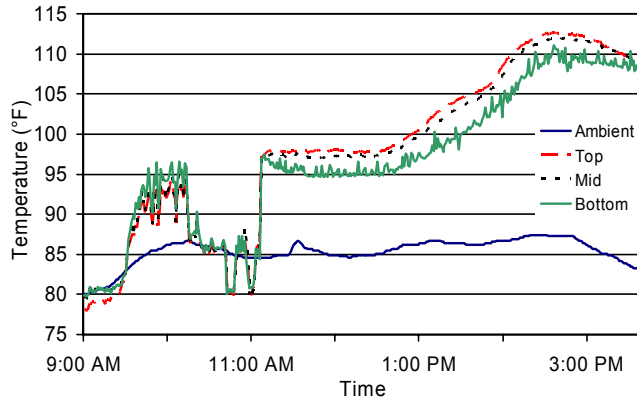


Figure 99. Curing temperatures for STL-3

SRA

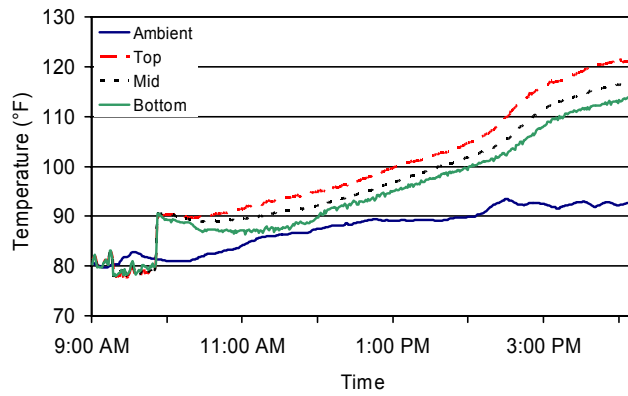


Figure 100. Curing temperatures for SRA-1

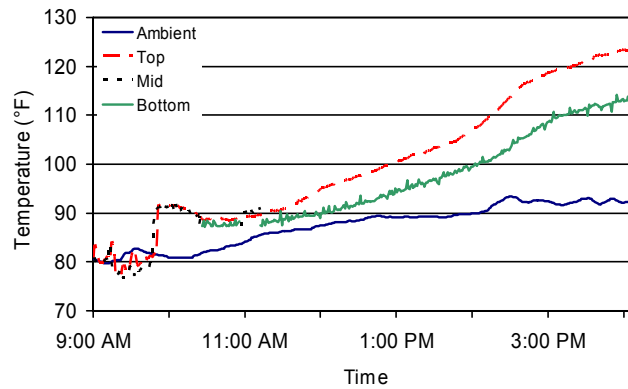


Figure 101. Curing temperatures for SRA-2

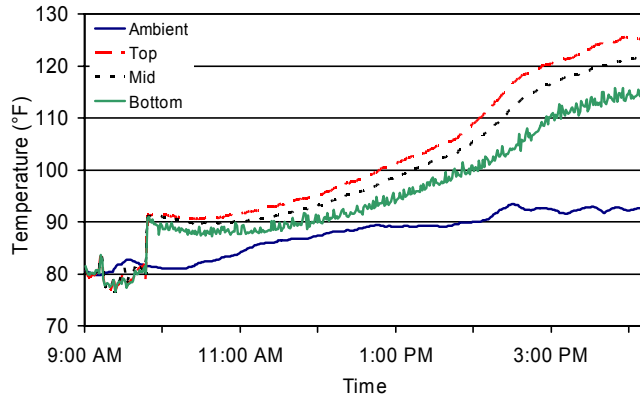


Figure 102. Curing temperatures for SRA-3

CTL

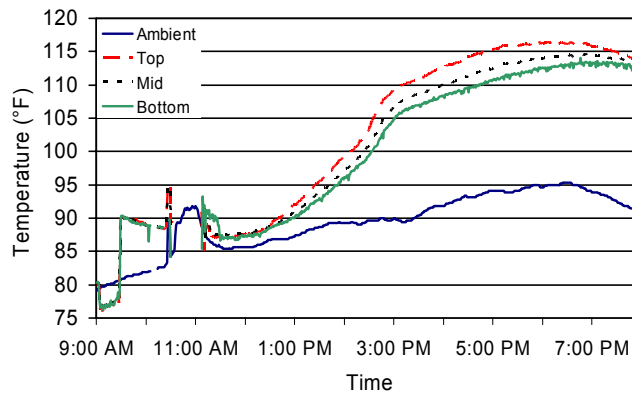


Figure 103. Curing temperatures for CTL-3

APPENDIX F – Construction Drawings

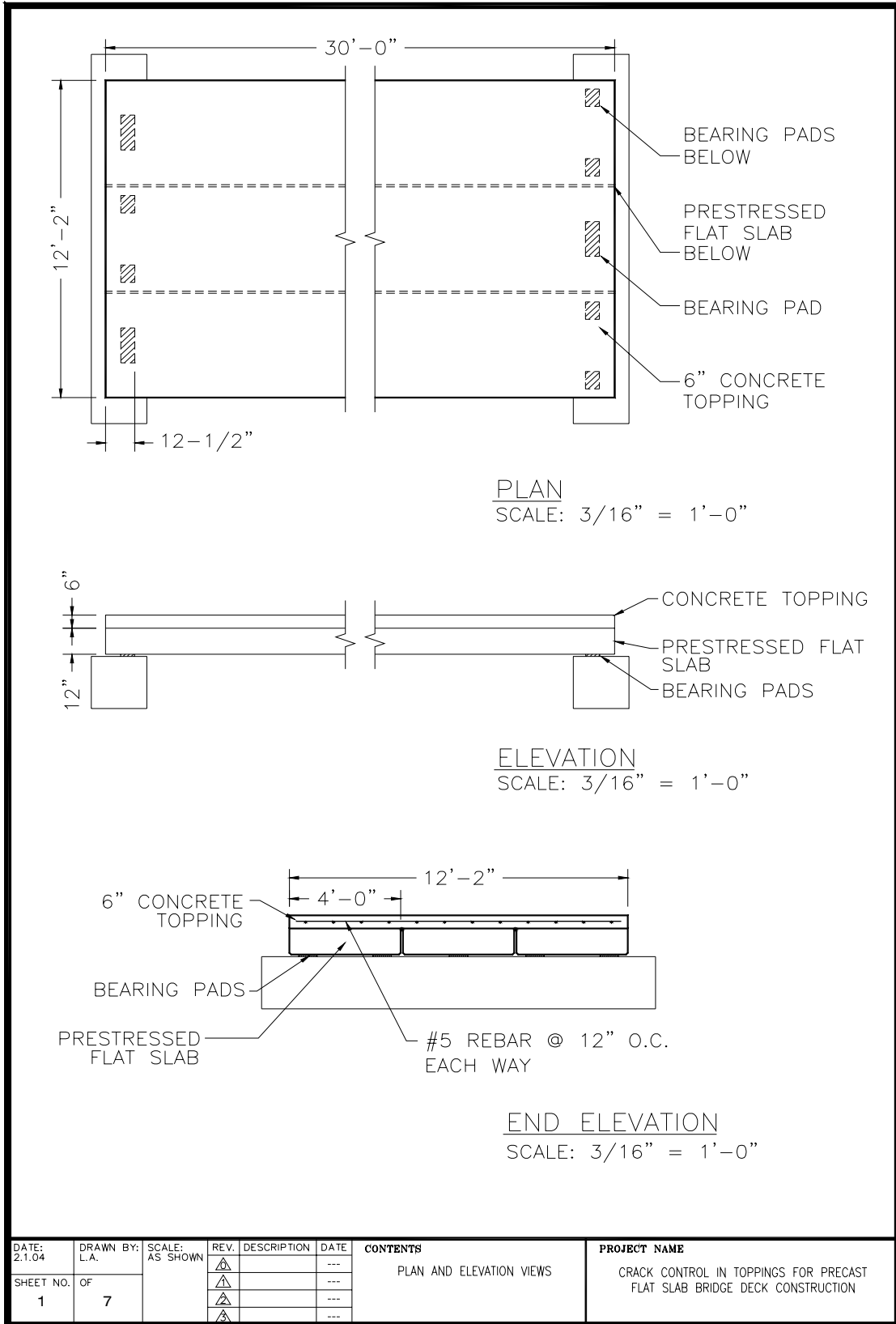


Figure 104. Plan and elevation view of specimen

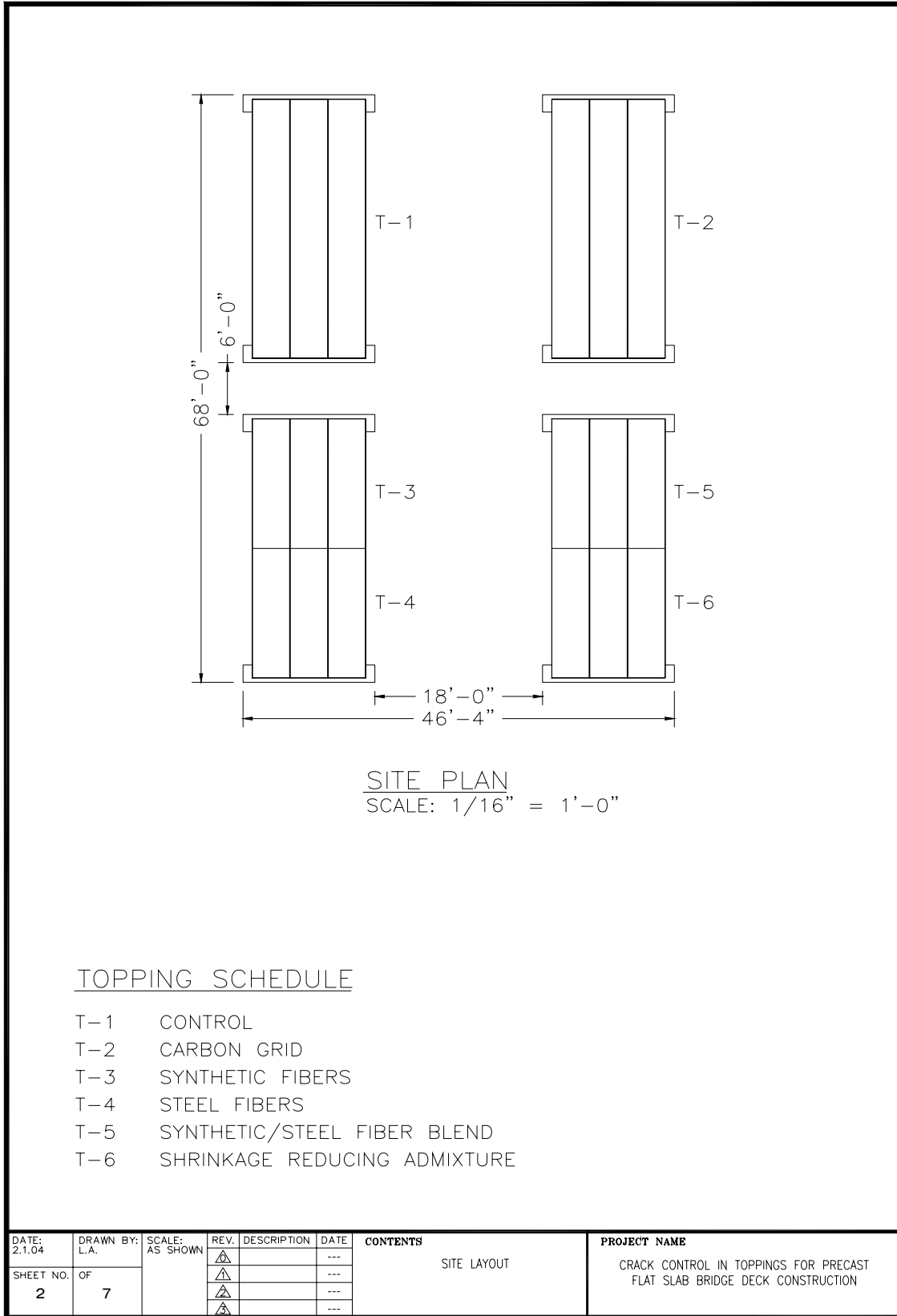


Figure 105. Site layout of specimens

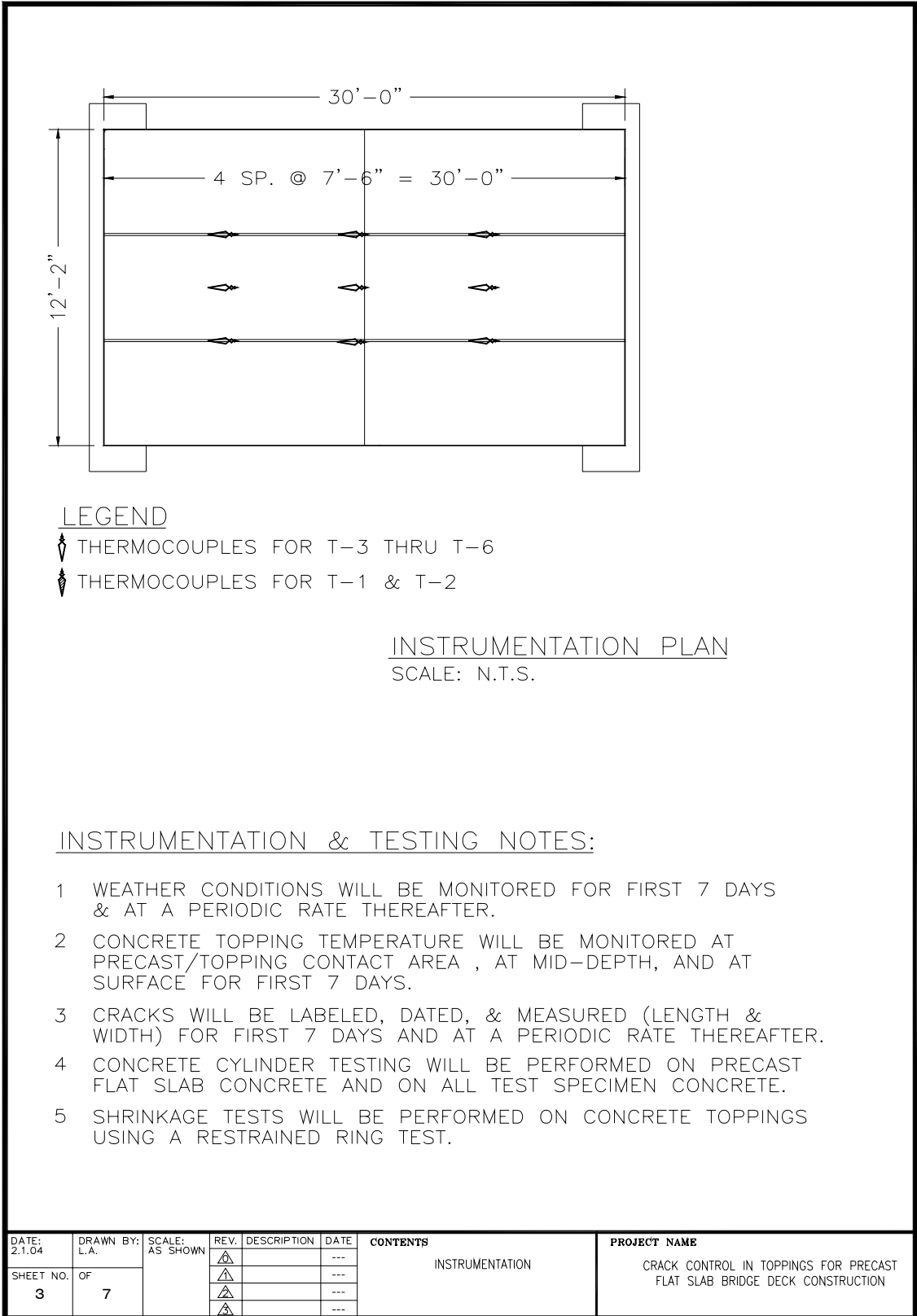


Figure 106. Instrumentation and testing notes

CONCRETE PLACEMENT & FINISHING NOTES:

NOTES TAKEN FROM FDOT'S 2004 EDITION STANDARD SPECIFICATIONS FOR ROAD & BRIDGE CONSTRUCTION, SECTION 350.

- 1 DISTRIBUTE CONCRETE ON THE FLAT SLABS TO SUCH DEPTH THAT, WHEN IT IS CONSOLIDATED AND FINISHED, THE SLAB THICKNESS REQUIRED BY THE PLANS WILL BE OBTAINED AT ALL POINTS AND THE SURFACE WILL AT NO POINT BE BELOW THE DEPTH SPECIFIED FOR THE FINISHED SURFACE.
- 2 DEPOSIT THE CONCRETE ON THE FLAT SLABS IN A MANNER THAT WILL REQUIRE AS LITTLE REHANDLING AS POSSIBLE.
- 3 IMMEDIATELY AFTER PLACING THE CONCRETE, STRIKE-OFF, CONSOLIDATE, AND FINISH IT TO PRODUCE A SMOOTH FINISHED PAVEMENT.
- 4 PERFORM THE SEQUENCE OF OPERATIONS AS FOLLOWS: STRIKE-OFF; CONSOLIDATION; SCREEDING; FLOATING; REMOVAL OF LAITANCE; STRAIGHTEDGING; AND FINAL SURFACE FINISH.
- 5 FOR PURPOSES OF THIS PROJECT, FINISHING MAY BE DONE BY HAND METHODS IF FINISHING MACHINES ARE NOT AVAILABLE.

STRIKE-OFF & SCREEDING: USE A SCREED THAT IS SUFFICIENTLY RIGID TO RETAIN ITS SHAPE AND IS AT LEAST 2 FEET LONGER THAN THE MAXIMUM WIDTH OF THE STRIP TO BE SCREEDED. MOVE THE SCREED FORWARD ON THE FORMS WITH A COMBINED LONGITUDINAL AND TRANSVERSE SHEARING MOTION. IF NECESSARY, REPEAT THIS UNTIL THE SURFACE IS OF UNIFORM TEXTURE, TRUE TO GRADE AND CROSS-SECTION, AND FREE FROM POROUS AREAS.

CONSOLIDATION: USE HAND-OPERATED SPUD-TYPE VIBRATORS TO CONSOLIDATE.

FLOATING: USE LONG-HANDLED FLOATS TO FLOAT THE CONCRETE. TAKE THE NECESSARY CARE TO AVOID DEPRESSIONS OR RIDGES DURING THIS OPERATION.

CONCRETE FORM WORK & CURING NOTES:

NOTES TAKEN FROM FDOT'S 2004 EDITION STANDARD SPECIFICATIONS FOR ROAD & BRIDGE CONSTRUCTION, SECTION 350.

- 1 AFTER COMPLETING THE FINISHING OPERATIONS AND AS SOON AS THE CONCRETE HAS HARDENED SUFFICIENTLY APPLY A FDOT APPROVED CURING COMPOUND.
- 2 APPLY A CURING COMPOUND TO THE SURFACE IN A SINGLE COAT, CONTINUOUS FILM, AT THE MINIMUM RATE OF 0.005 GAL/FT², BY A MECHANICAL SPRAYER.
- 3 FORM WORK MAY BE REMOVED UNTIL THE CONCRETE HAS SET FOR AT LEAST 12 HOURS. AFTER REMOVING THE FORMS, IMMEDIATELY CURE THE SIDES OF THE SLAB IN THE SAME MANNER AS THE SURFACE OF THE TOPPING.

DATE:	DRAWN BY:	SCALE:	REV.	DESCRIPTION	DATE	CONTENTS	PROJECT NAME
2.1.04	L.A.	AS SHOWN	△		---	NOTES	CRACK CONTROL IN TOPPINGS FOR PRECAST FLAT SLAB BRIDGE DECK CONSTRUCTION
SHEET NO.	OF		△		---		
4	7		△		---		
			△		---		

Figure 107. Concrete placement, finishing, and curing notes

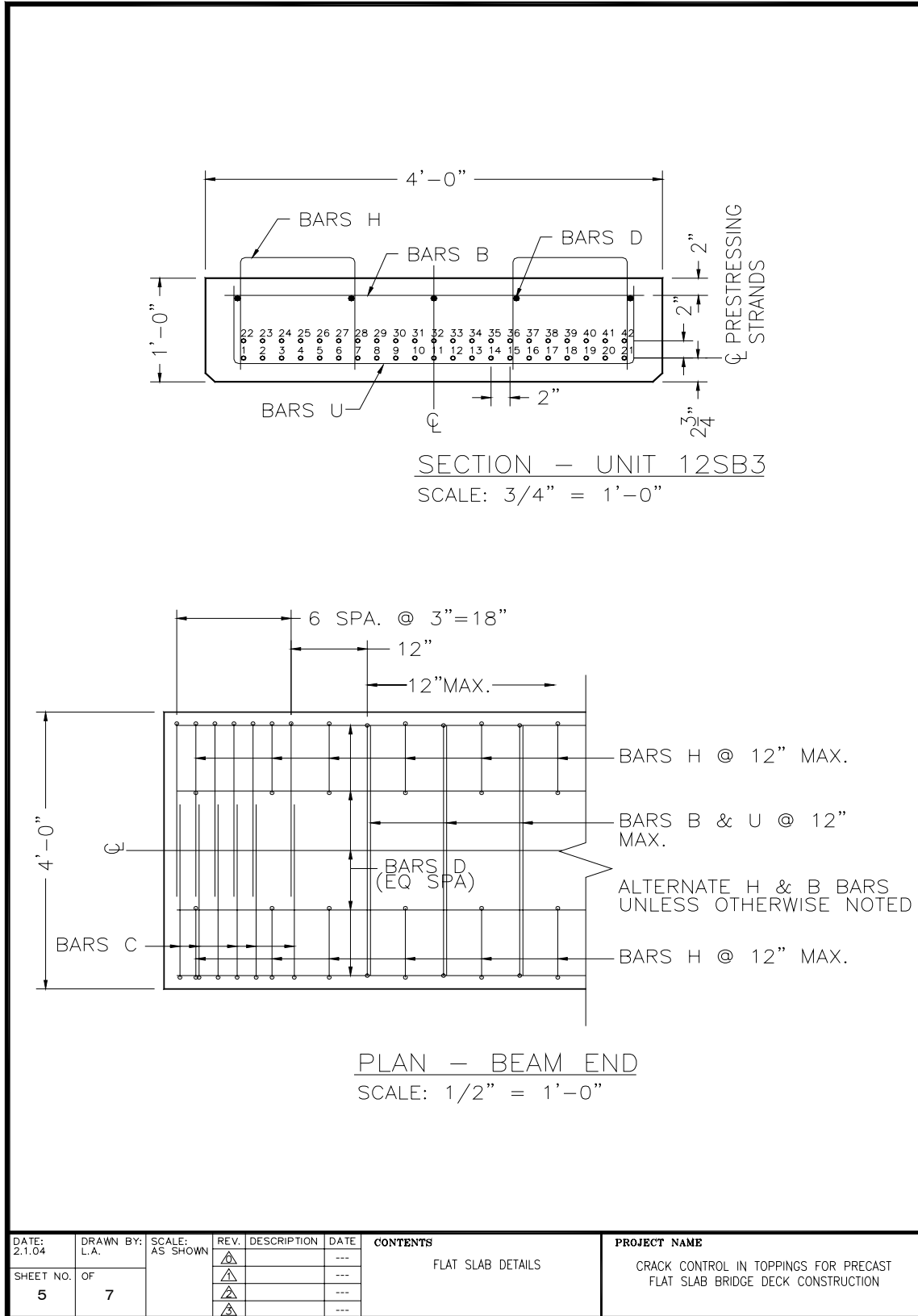


Figure 108. Flat slab detail drawings

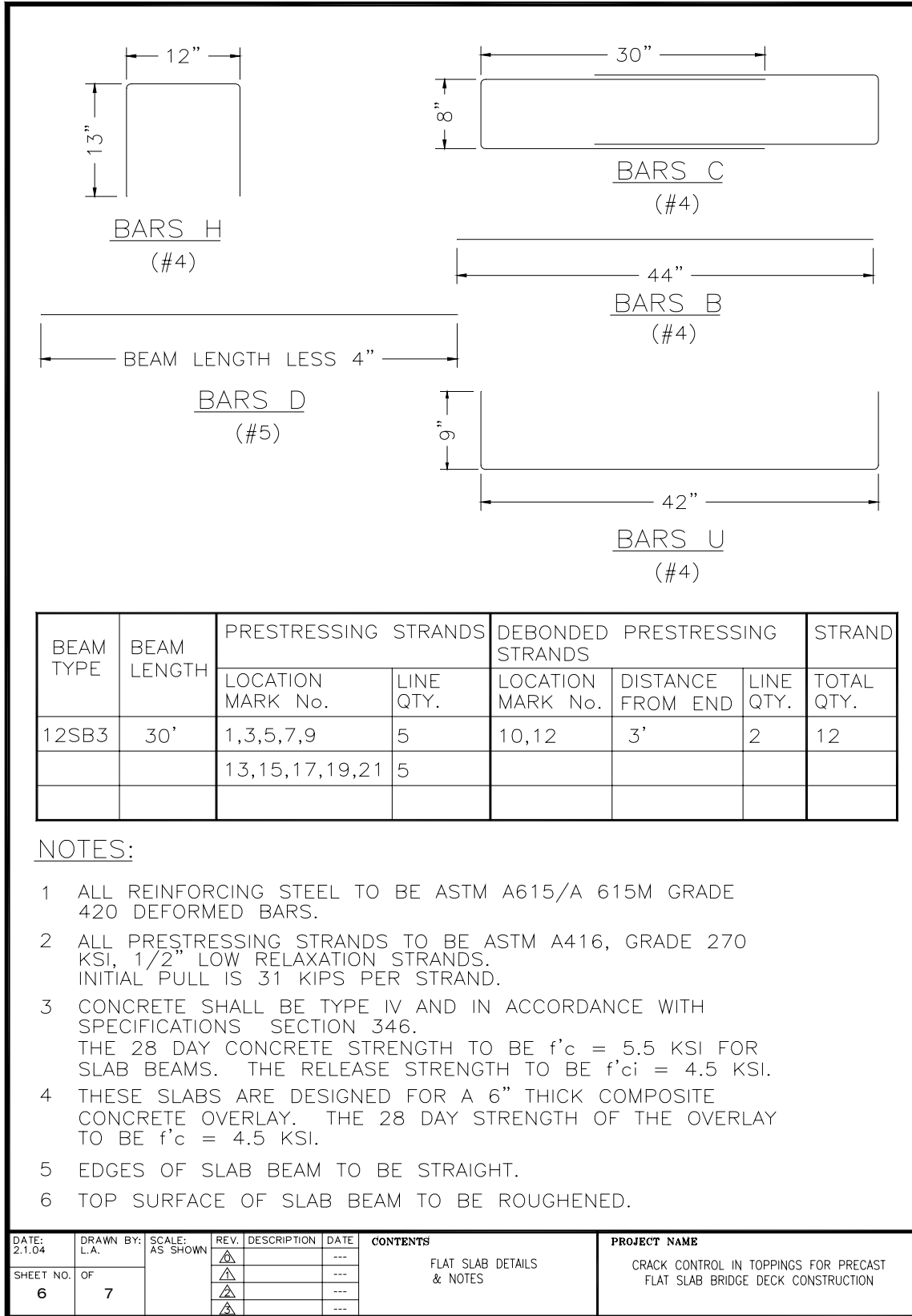


Figure 109. Flat slab reinforcement details

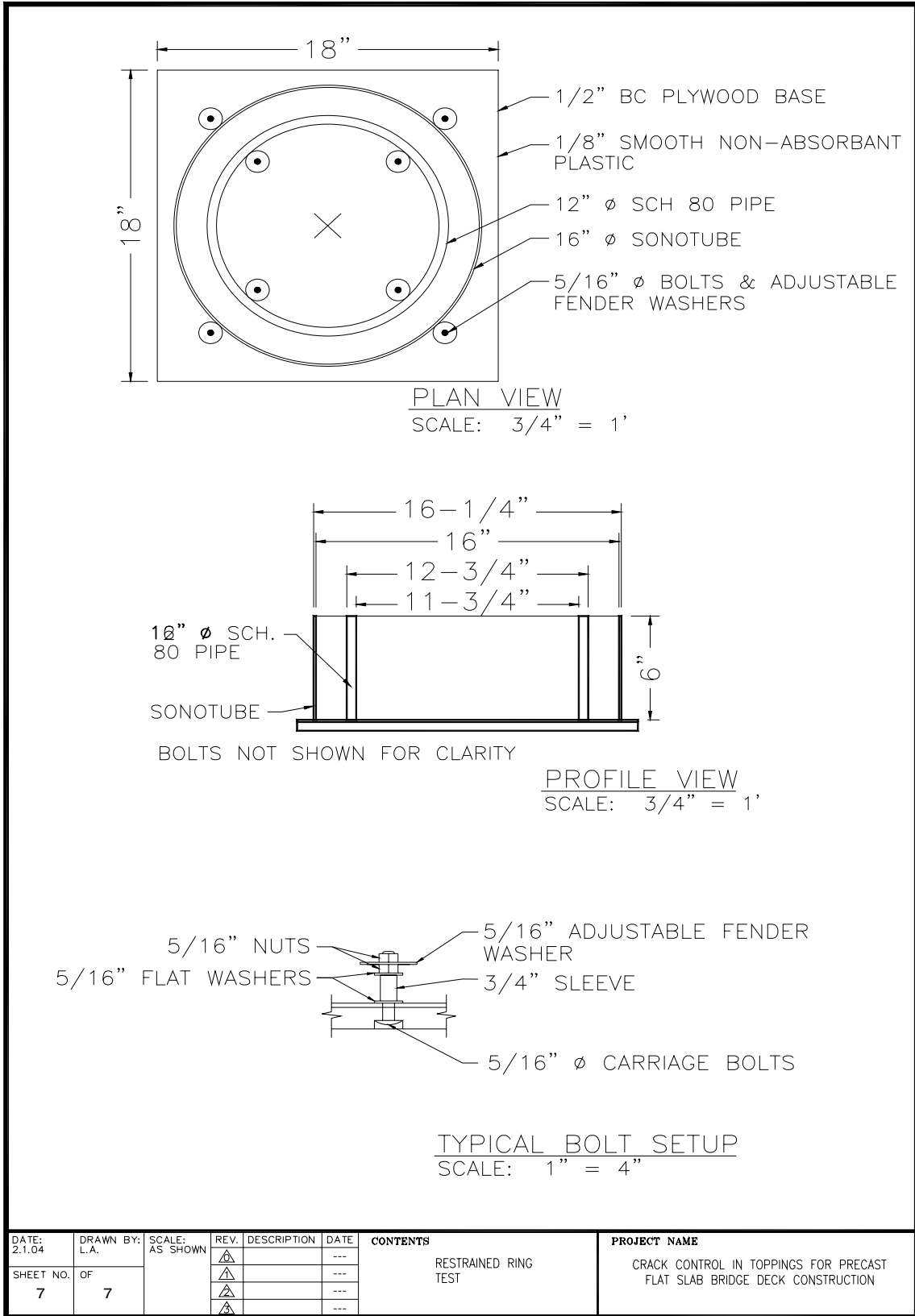


Figure 110. Restrained ring test fabrication drawing

APPENDIX G – Joint Depth Variation

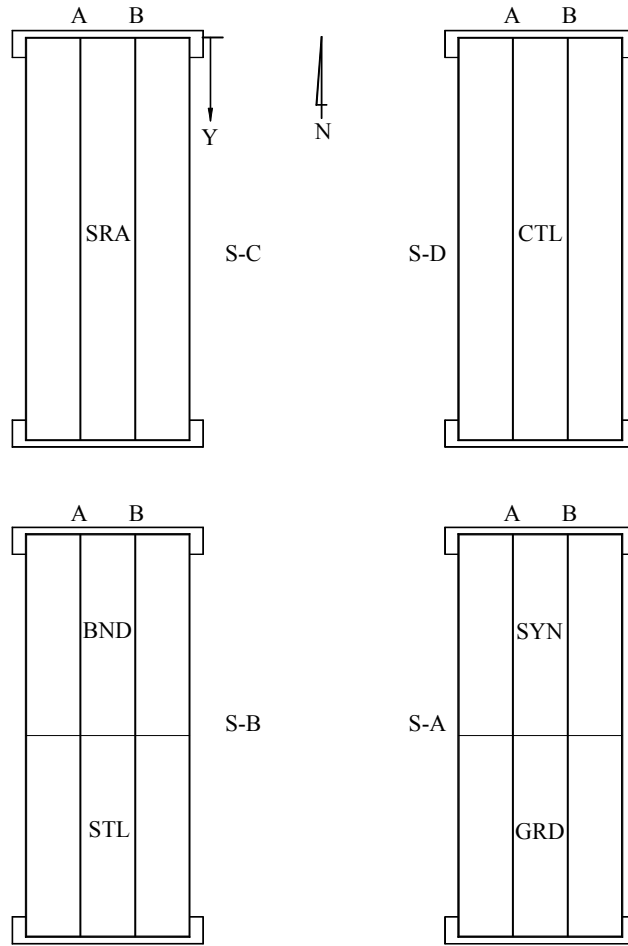


Figure 111. Topping depth reference

Table 36. Depth of topping over flat slab joint

Y (ft)	S-A		S-B		S-C		S-D	
	A	B	A	B	A	B	A	B
0	6	6	6.5	12	7	7	6.5	6.5
1	7	8	13.25	13	6.75	6.5	18	18
2	6	8	12.25	9	7.5	6.25	7.75	7.5
3	8.5	8.5	13	9	8.25	7	7	8
4	12	8.5	7.25	7.75	9.25	7.5	7	7.25
5	10	7.75	14.5	7.5	11	7	7	8.75
6	10	7.5	17.25	8.75	8.5	6.5	6.75	6.5
7	7	7	18	8	9.5	6	8.75	7.5
8	7.25	8	14	8	6.5	6	9	10.75
9	8.5	7.5	15	7.25	7.25	6	9.5	13.5
10	12	8.25	16	7.75	7.25	5.5	9.75	12.5
11	13.5	9.25	16	10.5	7	6.25	12	9.25
12	6.5	9.75	12.5	15	7.5	6.75	9.5	6.75
13	6.75	7.25	13.5	15	7.5	6	8.25	6.5
14	6	7.25	14	11	7	6	10.25	7
15	6.5	6.25	7	7	8.25	6	11.75	8.25
16	6.25	6.25	6.25	6.5	8.5	5.75	12	8.25
17	5.75	5.75	6.5	6.25	9.5	6	10.25	6
18	6.25	6	7.25	7.25	10.5	6.5	7.25	7.25
19	5.5	5.5	7.75	5.5	7.75	6	8	8.25
20	5.5	5.75	7.75	6.75	6.75	6	10.5	7.75
21	6.25	5.75	7.75	6.5	7	5.75	14.25	8
22	6	5.75	6.5	6.75	6.75	5.75	5.75	8
23	5.75	6.25	6.25	6.75	6.5	5.75	6.25	8.75
24	5.5	5.75	6.5	7	7	5.75	5.5	8.5
25	5.75	6	7	5.75	7.5	5.75	13.5	8.25
26	5.5	6	6.5	8.5	7	6.5	13.25	8.75
27	5.75	6.25	7.5	9.5	7.75	5.75	13.5	8.5
28	6	5.75	7.25	8	6.5	5.75	13	9.75
29	6.25	6	6.5	7.25	6.5	6	14	9
30	6.5	6	6.5	6.75	6.5	7	6	7